

Oligocene/early Miocene major E/W-shortening and NW-oriented sinistral slip with associated wrench-fault assemblage in the Oman Mountains related to oblique Arabia-India convergence

Andreas Scharf¹, Frank Mattern¹, Robert Bolhar², Ivan Callegari³, Paul Erik Mattern⁴, and Uwe Ring⁵

¹Sultan Qaboos University

²University of the Witwatersrand

³German University of Technology, Department of Applied Geosciences (AGEO)

⁴Freie Universität Berlin

⁵Department of Geological Sciences, Stockholm University

November 24, 2022

Abstract

Field survey, satellite image interpretation, geological map interpretation, literature review, GPlates reconstruction and LA-ICP-MS U-Pb dating of synkinematic calcites demonstrate that E/W-shortening in eastern Oman was significant and related to oblique convergence of Arabia and India from 32.5 to 20 Ma. Approximately N/S-oriented compressive structures, WNW to NNW-striking sinistral faults and E/W-oriented normal faults characterize a major shear zone in the eastern Oman Mountains (Hajar Shear Zone, HSZ) and its wrench-fault assemblage within an area spanning ~250 km x ~50 km. More than 10,000 mostly NW-striking lineaments as deduced from satellite image interpretation and numerous faults/folds indicate that strain of the HSZ is widely distributed but concentrated along WNW to NNW-striking major faults/fault zones at the SW margin of the Saih Hatat Dome. These faults/fault zones represent reactivated basement faults. GPlates reconstructions reveal that N-drifting India rotated 8° counter-clockwise with respect to fixed Arabia from 32.5 to 20 Ma, leading to ~100-135 km E/W-convergence between both plates (minimum value). This convergence created the sinistral HSZ with a displacement of a few to several tens of kilometers. Independently from the GPlates time constraints, two U-Pb ages of synkinematic calcites, crystallized along faults during HSZ movement, yield compatible ages of 30.08 ± 0.47 and 22.31 ± 2.15 Ma (2 standard error). E/W-shortening also affected the northern Oman Mountains, creating the N/S-oriented Hagab Thrust in the Musandam Peninsula and the Jabal Hafit Anticline.

Oligocene/early Miocene major E/W-shortening and NW-oriented sinistral slip with associated wrench-fault assemblage in the Oman Mountains related to oblique Arabia-India convergence

Andreas Scharf^a, Frank Mattern^b, Robert Bolhar^c, Ivan Callegari^d, Paul Mattern^e, Uwe Ring^f

^a Department of Earth Sciences, College of Science, Sultan Qaboos University, PC 123, Al-Khod, Muscat, Sultanate of Oman

^b School of Geosciences, University of the Witwatersrand, Braamfontein, 2001 South Africa

^c Department of Applied Geosciences, German University of Technology in Oman, PC 130, Halban, Sultanate of Oman

^d Institute of Geological Sciences, Freie Universität Berlin, 12249 Berlin, Germany

e Department of Geological Sciences, Stockholm University, 10691 Stockholm, Sweden

Corresponding author: Andreas Scharf

E-mail: scharfa@squ.edu.om

Abstract

Field survey, satellite image interpretation, geological map interpretation, literature review, GPlates reconstruction and LA-ICP-MS U-Pb dating of synkinematic calcites demonstrate that \sim E/W-shortening in eastern Oman was significant and related to oblique convergence of Arabia and India from 32.5 to 20 Ma. Approximately N/S-oriented compressive structures, WNW to NNW-striking sinistral faults and \sim E/W-oriented normal faults characterize a major shear zone in the eastern Oman Mountains (Hajar Shear Zone, HSZ) and its wrench-fault assemblage within an area spanning \sim 250 km x \sim 50 km. More than 10,000 mostly NW-striking lineaments as deduced from satellite image interpretation and numerous faults/folds indicate that strain of the HSZ is widely distributed but concentrated along WNW to NNW-striking major faults/fault zones at the SW margin of the Saih Hatat Dome. These faults/fault zones represent reactivated basement faults. GPlates reconstructions reveal that N-drifting India rotated 8° counter-clockwise with respect to fixed Arabia from 32.5 to 20 Ma, leading to \sim 100-135 km E/W-convergence between both plates (minimum value). This convergence created the sinistral HSZ with a displacement of a few to several tens of kilometers. Independently from the GPlates time constraints, two U-Pb ages of synkinematic calcites, crystallized along faults during HSZ movement, yield compatible ages of 30.08 ± 0.47 and 22.31 ± 2.15 Ma (2 standard error). E/W-shortening also affected the northern Oman Mountains, creating the \sim N/S-oriented Hagab Thrust in the Musandam Peninsula and the Jabal Hafit Anticline.

Plain Language Summary

Eastern Arabia was thrust by the well-known Semail Ophiolite and related deep-sea sedimentary rocks during the Late Cretaceous. Convergence was directed towards the SSW. Ongoing \sim N/S shortening between Arabia and Eurasia resulted in respective deformation within the Oman Mountains. However, field evidence indicates that \sim E/W-shortening affected the Oman Mountains, too. Detailed and comprehensive field survey, literature review, satellite image interpretation, map interpretation, GPlates reconstruction and absolute U-Pb dating of carbonates documents that E/W-shortening was significant in the Oman Mountains. E/W-shortening of 100-135 km was related to the counter-clockwise rotation of India with respect to Arabia at 32.5 to 20 Ma. In response to this shortening, a NW-striking sinistral shear zone with wrench-fault assemblage formed in the eastern Oman Mountains (i.e., N/S-compressive structures, E/W-extensional structures, WNW-striking sinistral Riedel faults, and SW-striking dextral anti-Riedel faults). This shear zone is the Hajar Shear Zone, which spans an area of 250 km by 50 km. Presumably NW-striking deeply rooted pre-existing faults facilitate shearing along the Hajar Shear Zone. E/W-shortening also affected the northern Oman Mountains and is responsible for deformation at the Hagab Thrust in Musandam and the Jabal Hafit Anticline at the Oman/UAE border.

Keywords

Post-obductional E/W-shortening; wrench-fault assemblage; reactivation of basement faults; strike-slip tectonics

1. Introduction

During the Late Cretaceous, northeastern Oman was overthrust from the NE by the iconic Semail Ophiolite, including tectonically underlying nappes of Neo-Tethyan sedimentary rocks (e.g., Glennie et al., 1974). N/S-shortening was recorded in the Oman Mountains during the Cenozoic due to the Arabia-Eurasia convergence (e.g., Fournier et al., 2006; Hansman et al., 2017; Levell et al., 2021). In addition, the Oman Mountains, especially their southeastern part, underwent post-mid-Eocene \sim E/W-shortening (e.g., Mann et al., 1990; Wyns et al., 1992; Fournier et al., 2006). This study focuses on timing and cause of this shortening.

Numerous N/S-striking post-mid-Eocene compressional structures of the eastern Oman Mountains are documented in maps and other publications (Table 1). However, these structures have never been examined in detail with respect to a common genetic context. Furthermore, major ~N/S-striking compressional structures of Oligocene to early-mid-Miocene age also occur on the western flank of the northern Oman Mountains (prominent ~N/S-oriented Hagab Thrust in the Musandam Peninsula and the NNW/SSE-trending Jabal Hafit Anticline; Fig. 1; Table 1). Besides ~N/S-oriented compressional features, abundant relevant post-mid-Eocene sinistral ~NW-striking faults are common in the eastern Oman Mountains, too.

At a local scale, Mann et al. (1990) recognized open N-trending folds in the Rusayl Embayment (Fig. 1), affecting mid-Eocene rocks. They related these folds to exhumation and gravitational collapse of the nearby Saih Hatat and Jabal Akhdar domes (Fig. 1), causing extensional transport to the NW from Saih Hatat Dome and to the NE from the Jabal Akhdar Dome. The converging rock masses produced N-trending folds. For the Rusayl Embayment, this would be a suitable geometric explanation. However, similarly aged N-trending compressive structures also exist beyond the Rusayl Embayment (i.e., Hagab Thrust, Jabal Hafit, Qalhat Fault; Fig. 1), where the formation of such structures must have a different cause.

At a large regional scale, Fournier et al. (2006) identified two compressional events in the Oman Mountains, which started during the late Oligocene or early Miocene with E/W to NE/SW-directed shortening (Fig. 2). They did not identify the actual causes of the deformation but pointed out that the origin of E/W to NE/SW-shortening is “not entirely clear and could result from the interaction between the Arabian and Indian plates”. Gaina et al. (2015) suggested minor E/W-shortening between Arabia and India from 40 Ma to the present (their Fig. 7). The strike of NW-striking faults varies in the eastern Oman Mountains, ranging from WNW to NNW. For simplification, we will refer to them as “NW-striking”. Such faults are known from the Rusayl Embayment in the NW, the southern margin of the Saih Hatat Dome, the Salma Plateau, the inverted Abat Basin and the Jabal Ja’alan area in the SE (Figs. 2 and 3; Table 1).

Table 1. Documented N/S to NW/SE-oriented post-obductional compressive structures and sinistral NW-striking faults of the Oman Mountains with focus on the eastern Oman Mountains. Listed in appearance from the NW (Musandam Peninsula) to the SE (Jabal Ja’alan/Batain area).

	N/S to NW/SE compressive structures	Age	Reference
1	Hagab Thrust	Oligocene to early Miocene	Searle et al., 2014
2	Jabal Hafit Anticline	Late Oligocene to early-middle Miocene	Hansman & Ring, 2018
3	Suneinah area	Late Oligocene to Middle Miocene?	Boote et al., 1990; Fournier et al., 2006
4	Rusayl Embayment	Post-mid-Eocene	Villey et al., 1986a, Fournier et al., 2006, Kajima et al., 2012a, 2012b, 2013, Scharf et al., 2016
5	Rusayl Embayment-offshore Sea of Oman	Late Eocene	Levell et al., 2021
6	Jabal Nakhl	Cenozoic	Rabu et al., 1986
7	Muscat area	Post-mid-Eocene?	Fournier et al., 2006, Searle et al., 2019, Hansman et al., 2021
8	Fanja area	Cenozoic	Villey et al., 1986b, Coffield (1990)
9	Saih Hatat Dome	Cenozoic	Le Métour et al., 1986a, 1986b
10	Eastern Saih Hatat	Cenozoic	Miller et al., 2002
11	Qalhat Fault and nearby other faults	Post-mid-Eocene, Miocene	Wyns et al., 2021, Fournier et al., 2006
12	Inversion of Abat Basin	Miocene	Wyns et al., 1992, Fournier et al., 2006

	N/S to NW/SE compressive structures	Age	Reference
13	Near Jabal Ja'alan	Post-mid-Eocene	Roger et al., 1991
14	Jabal Ja'alan	Post-mid-Eocene	Filbrandt et al., 1990
	NW-striking sinistral faults	Age	Reference
1	Rusayl Embayment (transpressive)	Post-mid-Eocene	Scharf et al., 2016
2	Rusayl Embayment (transtensional)	Post-mid-Eocene	Mattern et al., 2018c
3	Wadi Mansah Fault Zone (transtensional)	Post-mid-Eocene	Bailey et al., 2019 Scharf et al., 2019a
4	Wadi Amdeh Fault	Unknown	Mattern et al., 2020a
5	Issmaiya Fault Zone (transtensional)	Post-mid-Eocene	Callegari et al., 2020
6	Coastal Parallel Shear Zone (transpressional)	Post-mid-Eocene	Moraetis et al., 2018
7	Ja'alan Fault (transpressional)	Post-mid-Eocene	Filbrandt et al., 1990 Roger et al., 1991

It is surprising that the above-mentioned structures have never been scrutinized in detail in a mutual causal context. Likewise, some ~N/S-oriented compressive structures and ~NW-oriented sinistral faults are documented and were mapped in detail or occur along prominent roadcuts but have been largely neglected by geoscientific attention. We shed light on these known structures, which extend across the entire Oman Mountains (~700 km in length; Fig. 1).

This study aims to review previously documented structures and combine available knowledge (Table 1) with other mainly ~N/S-compressional and sinistral NW-striking structures in the field (Table 2) between the eastern Batinah Coastal Plain in the west to the Batain area in the East (Figs. 1-3). A focus will be placed on whether these structures are (1) of the same age, (2) belong to the same deformation plan, (3) can be linked with structures in the northern Oman Mountains, (4) evaluate possible geodynamic causes, including unrecognized plate tectonic process. To achieve above goals, existing literature was reviewed, existing geological maps were (re)interpreted, a comprehensive satellite image analysis and extensive field mapping was carried out, LA-ICP-MS U-Pb dating of synkinematic calcites was conducted, and plate configurations were reconstructed using the GPlates software.

2. Geological setting

Eastern Arabia was affected by the Late Paleozoic Pangean Neo-Tethys rifting, forming ~NW-striking extensional basement faults (e.g., Béchenec et al., 1990; Blendinger et al., 1990; Chauvet et al., 2009). Subsequent to rifting, Arabia remained largely a passive margin during the Permian to mid-Cretaceous (e.g., Glennie et al., 1974; Searle, 2007). This resulted in deposition of mostly shallow-marine, shelfal sedimentary rocks on the Arabian platform (Hajar Supergroup; e.g., Glennie et al., 1973, 1974; Searle, 2007). These rocks were overthrust by Neo-Tethys-derived allochthonous Hawasina-Basin and trench-facies rocks from the NE (~1-2 km in thickness) and the Semail Ophiolite during the Late Cretaceous (~10-15 km in thickness; e.g., Glennie et al., 1973, 1974; Béchenec et al., 1992; Nicolas et al., 2000; Blechschmidt et al., 2004; Searle, 2007), forming the Oman Mountains. At the base of the ophiolite, a metamorphic sole formed coeval with the formation of the ophiolite (Rioux et al., 2016).

Post-obductional successions in the Muscat-Seeb area (Figs. 3 and 4) consist of the <860-m-thick late Campanian to Maastrichtian Al-Khod (or Qahlah) Formation, containing alternating fluvial, coastal and deltaic shales, sandstones and conglomerates (e.g., Nolan et al., 1990; Abbasi et al., 2014; Pickford, 2017). The Al-Khod Formation is unconformably overlain by the 250-to-300-m-thick late Paleocene to early Eocene shallow-marine limestone of the Jafayn Formation (e.g., Nolan et al., 1990; Mattern and Bernecker, 2019). The Jafayn Formation is conformably overlain by the ~150-m-thick Rusayl Formation, consisting of marl, shallow marine limestone and sandstone of lower Eocene age (e.g., Nolan et al., 1990; Mattern et al., 2021). The Rusayl Formation is conformably topped by the Seeb Formation. The latter measures ~600 m in thickness, consists of middle to upper Eocene shallow-marine limestone (e.g., Nolan et al., 1990; Hersi & Al-Harthi,

2010). The Oligocene MAM or Ma'ahm Beds Formation, consisting of reefal limestone, rests unconformably on the Seeb Formation (Hersi and Al-Harthi, 2010). The thickness of this formation is not known, owing to the poor exposure but assumed by us to measure ~100 m. The latest Oligocene to probably Pliocene ~170-m-thick Barzaman Formation rests stratigraphically on top of the MAM Reefs Formation (Mattern et al., 2020b). The lithology of this formation is highly variable, ranging from conglomerates to sand- and claystones and limestones reflecting terrestrial and marine deposition, intense weathering and erosion of the Oman Mountains during arid to pluvial episodes (Mattern et al., 2020b). Further details on the geology and tectonics of the eastern Oman Mountains are provided in Scharf et al. (2021a, 2021b).

Immediately after and/or slightly coeval with the emplacement of the ophiolite, major exhumation and top-to-the-NE shearing occurred in the Saih Hatat Dome, and some gentle exhumation with top-to-the NE shearing in the Jabal Akhdar Dome (e.g., Nolan et al., 1990; Breton et al., 2004; Fournier et al., 2006; Saddiqi et al., 2006; Al-Wardi and Butler, 2007; Searle, 2007; Agard et al., 2010; Hansman et al., 2017, 2021; Grobe et al., 2018, 2019; Scharf et al., 2019b; Figs. 1 and 4). Further convergence of Arabia and Eurasia led to major doming of the Jabal Akhdar and some mild doming/surface uplift in the Saih Hatat during the late Eocene to Oligocene (~43-30 Ma; e.g., Hansman et al., 2017, 2018; Grobe et al., 2018, 2019; Corradetti et al., 2019). Convergence was NE/SW-directed (e.g., Fournier et al., 2006; Fig. 5).

Extensional tectonics associated with doming at the flanks resulted from gravitational collapse (e.g., Hanna, 1990; Mann et al., 1990; Mattern & Scharf, 2018; Scharf et al., 2019a). Extension at the northern margin of the two domes was facilitated along the Frontal Range Fault (Mattern & Scharf, 2018; Figs. 2-4). The area between the northern Jabal Akhdar and Saih Hatat domes in the Muscat-Seeb area was deformed during extension (Rusayl Embayment; Fig. 3). Extension in the Rusayl Embayment was NE/SW-directed during the latest Cretaceous to early Eocene (Tectonic Stage 1) and NE/SW and NW/SE-directed (Tectonic Stage 2A and 2B) during the late Lutetian to possibly Miocene (Fournier et al., 2006; Scharf et al., 2020b; Figs. 4 and 5).

The geology and tectonics of the Batain area differs from that of the Oman Mountains. The Batain area is characterized by mostly deep-sea sediments derived from the Batain Basin whose fill was thrust to the WNW onto Arabia during the course of the obduction of the Masirah Ophiolite at the Cretaceous/Cenozoic boundary (e.g., Mountain & Prell, 1990; Shackleton & Ries, 1990; Schreurs & Immenhauser, 1999; Fig. 1). Emplacement of the Masirah Ophiolite and Batain nappes followed deposition of the upper Maastrichtian flysch-type Fayah Formation on the oceanic lithosphere of the Batain Basin (Immenhauser, 1996).

After the emplacement of the Masirah Ophiolite, the Batain area underwent extensional and compressional deformation (Schreurs & Immenhauser, 1999). The earlier extension is characterized by NNE-SSW and E/W-orientated conjugated extensional faults within Cenozoic sedimentary rocks (Fig. 5). Extension is probably linked to Cenozoic reactivation of the Cretaceous Masirah Graben, which is located beneath the Batain area (Beauchamp et al., 1995; Fig. 1). Deformation in the Batain area may correlate with extension in the Gulf of Aden starting during the late Eocene (e.g., Hempton, 1987). Basanite/alkaline intrusions in the Batain area of late Eocene age may be associated with this extension (e.g., Peters et al., 2001).

Extension was followed by Miocene-Pliocene compression, which affected late Paleocene to early Miocene rocks (Schreurs & Immenhauser, 1999). A ~NE/SW to ~E/W-oriented shortening interval produced NW/SE to N/S-oriented open folds (Roger et al., 1991). The Miocene Tahwah and Sur formations are intensely folded near the Qalhat Fault (Wyns et al., 1992). In the footwall of the Qalhat Fault, the uppermost beds of the Miocene Sur and Salmiyah formations cut across lower beds of the same formations, forming an angular unconformity (Wyns et al., 1992). The Miocene Salmiyah Formation is folded within an open N/S-trending syncline (Wyns et al., 1992).

Uplift and inversion in the Jabal Ja'alan area is post-mid-Eocene in age (Fournier et al., 2006). Uplift is associated with N/S-trending asymmetric anticlines and occurred during E/W-compression (Filbrandt et al., 1990). All these field observations indicate that the area near the Qalhat Fault underwent ~E/W-shortening from the Miocene to the present.

The transition between the Oman Mountains and the Batain area is broadly localized along the Qalhat Fault (Filbrandt et al., 1990; Figs. 1, 2). This major N/S-striking fault has a long-lasting history and may have originated during Pan-African terrane accretion, similar to the Semail Gap Fault Zone at the eastern margin of the Jabal Akhdar Dome (Romine et al., 2004; Scharf et al., 2019a; Mattern & Scharf, 2019; Weidle et al., 2021; Fig. 2). During the Phanerozoic, the Qalhat Fault was likely reactivated several times in different ways (Fournier et al., 2006). During the early Cenozoic, the transtensional Qalhat Fault bounded the Abat Basin and the future Salma Plateau to the West, with the Salma Plateau being uplifted the Abat Basin inverted during the Miocene (e.g., Wyns et al., 1992; Fournier et al., 2006). Details on the stratigraphy of the Abat Basin and the Salma Plateau are provided in Fournier et al. (2006) and Figure 4. The rocks west of the Qalhat Fault (Tiwi Platform or Salma Plateau) mostly consist of late Paleocene to mid-Eocene shallow-marine limestone, now uplifted to ~2000 m of elevation. This area is still uplifting, as indicated by a historical earthquake at Qalhat and uplifted marine terraces (e.g., Wyns et al., 1992; Fournier et al., 2006; Mattern et al., 2018a; Moraetis et al., 2018; Ermertz et al., 2020; Hoffmann et al., 2020). In contrast, no or only little Quaternary tectonic activity has been reported from the Central Oman Mountains (Scharf et al., 2019a; Moraetis et al., 2020). Mid-Eocene to Oligocene shallow-marine rocks east of the Qalhat Fault are not currently being uplifted and represent the footwall of the Qalhat Fault (Wyns et al., 1992).

In the Northern Oman Mountains, the Oligocene to early Miocene Hagab Thrust is a prominent N/S-striking compressional feature, interpreted to be associated with the Arabia/Eurasia convergence (Searle et al., 2014), although the thrust is highly obliquely oriented relative to the WNW-ESE-striking convergence zone. Further to the South, at the Oman/UAE border, the sizable NNW/SSE-oriented anticline of Jabal Hafit occurs (Fig. 1). This anticline grew during the late Oligocene to early-middle Miocene and is related to WSW-directed shortening (Hansman & Ring, 2018).

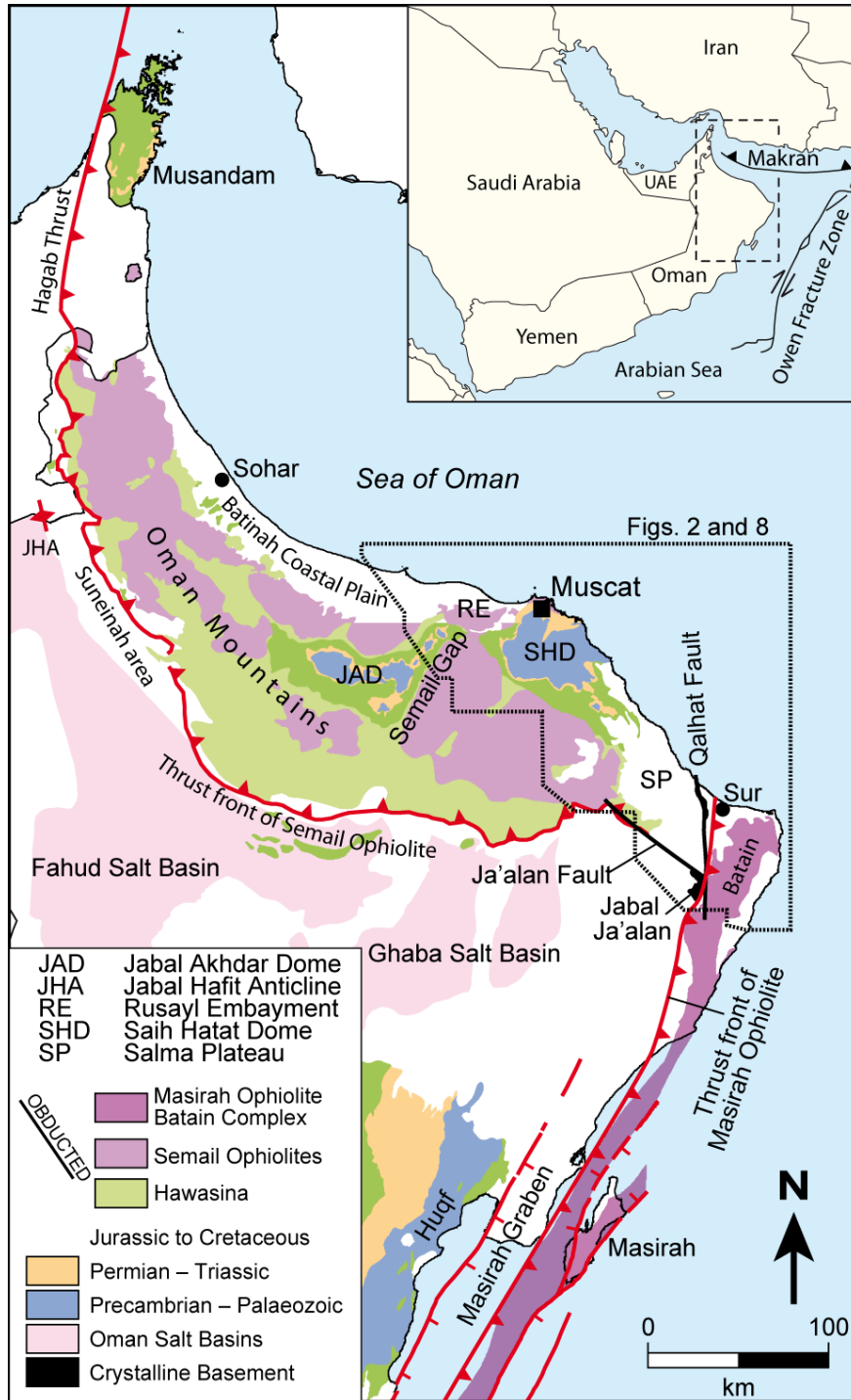


Figure 1. Geological map of the Oman Mountains after Schreurs and Immenhauser (1999) and Forbes et al. (2010). Black, dotted line indicates the outline of Figures 2 and 31. Overview image shows the larger study area with the Makran Subduction Zone and the Owen Fracture Zone, the present-day plate boundary between Arabia and India (Rodriguez et al. (2014).

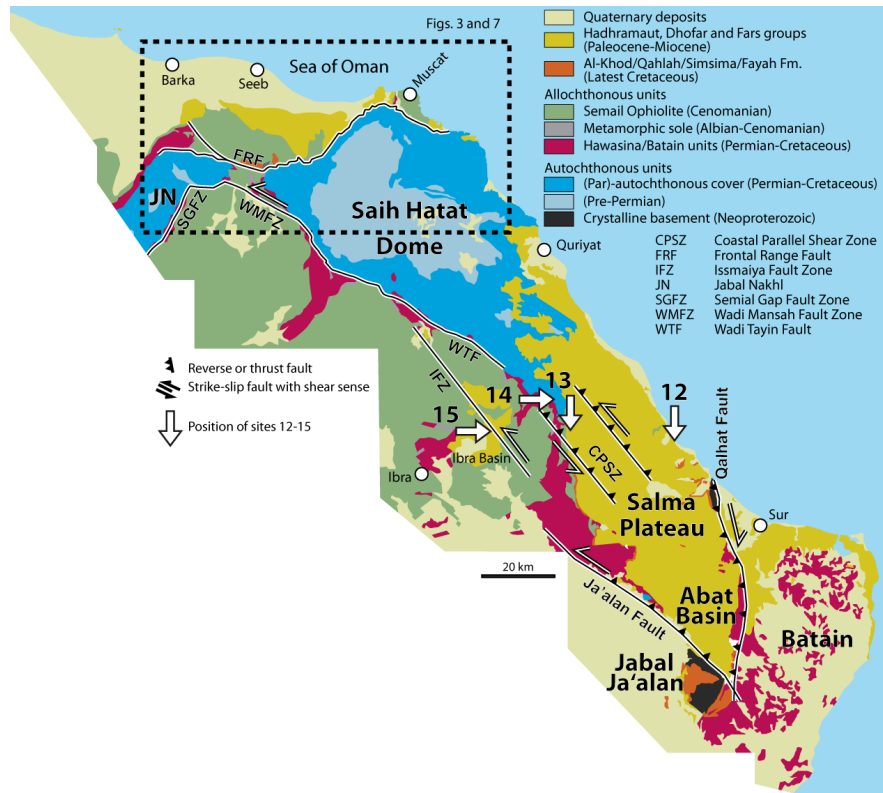


Figure 2. Geological map of the greater Saih Hatat to Batain area, simplified after Béchenec et al. (1986), Le Métour et al. (1986a, 1986b), Rabu et al. (1986), Villey et al. (1986a, 1986b), Roger et al. (1991), Wyns et al. (1992) and Peters et al. (2001, 2005). Box with black, dotted line outlines Figure 3. The Jabal Nakhl (JN) is the northern part of the Jabal Akhdar Dome.

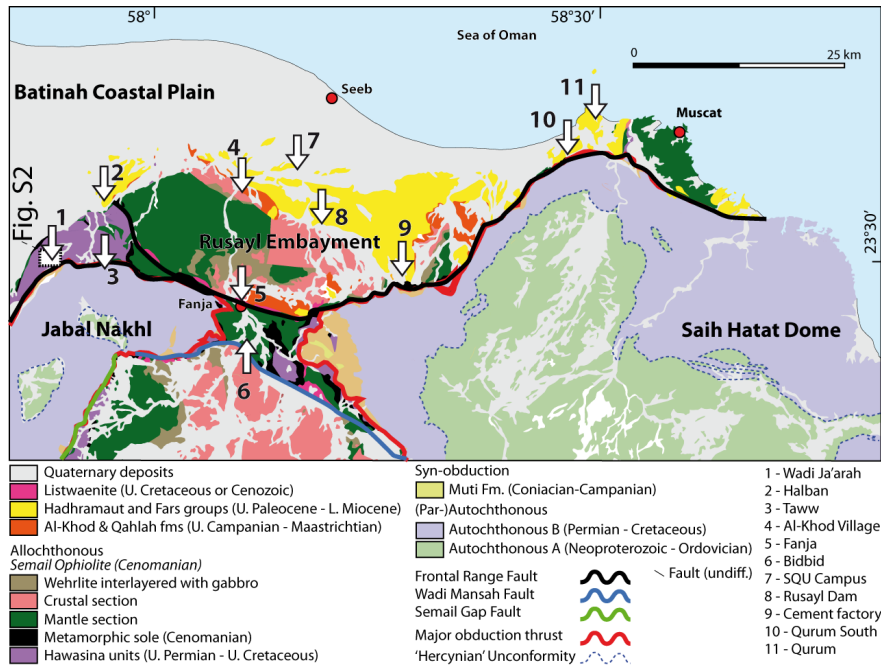


Figure 3. Geological map of the Muscat-Seeb area after Scharf et al. (2021c). Numbers 1-11 correspond to the sample sites of the structural measurements (Table 2; Supplementary Material S2).

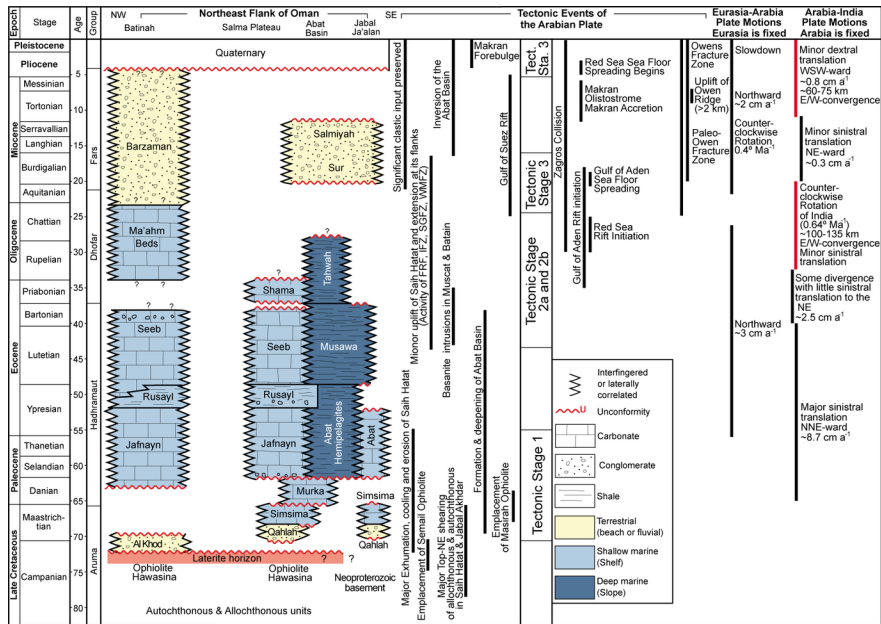


Figure 4. Simplified stratigraphic column of the post-obduction formations from the SE Batinah Coastal Plain to Jabal Ja'alán/Batain area, modified after Hansman et al. (2017) and Ninkabou et al. (2021). Stratigraphic column after Nolan et al. (1990), Fournier et al. (2006) and Mattern et al. (2020b). Age of major top-NE shearing (Grobe et al., 2018), emplacement of Semail Ophiolite (Searle, 2007), major exhumation and cooling of Saih Hatat (Hansman et al., 2017, 2021), minor uplift and extension of flank of

Saih Hatat (Hansman et al., 2017; Scharf et al., 2020; FRF – Frontal Range Fault; IFZ – Issmaiya Fault Zone; SGFZ – Semail Gap Fault Zone; WMFZ – Wadi Mansah Fault Zone), formation and deepening of Abat Basin (Fournier et al., 2006), Masirah Ophiolite (Schreurs & Immenhauser, 1999), Basinite intrusions (Gnos & Peters, 2003; Scharf et al., 2020), Tectonic stages 1-3 (Fournier et al., 2006; Fig. 2), Gulf of Aden (Leroy et al., 2013), Zagros collision (Fakhari et al., 2008; Gavillot et al., 2010; Agard et al., 2011; Mouthereau et al., 2012), Makran subduction and olistostrome (Platt et al., 1988; Schlüter et al., 2002; Burg et al., 2008), Owen Fracture Zone (Fournier et al., 2011; Rodriguez et al., 2014), Red Sea (Ghebreab, 1998; Augustin et al., 2014), Makran Forebulge (Rodgers and Gunatilaka, 2002), Arabia-Eurasia plate motion (McQuarrie et al., 2003), Arabia-India plate motion (own data, based on GPlate, see section 4.4). Red bars indicate time for E/W-shortening in eastern Arabia.

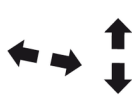
Southeastern Oman Mountains		Batain area	
Time	Stress directions	Stress directions	Time
Tectonic Stage 1 Late Cretaceous to early Eocene extension Fournier et al. (2006)			Latest Maastrichtian to Paleocene Schreurs and Immenhauser (1999)
Tectonic Stage 2A Late Lutetian to Miocene extension - stage A			Late Eocene Conjugated sets of normal faults (NNE-SSW and E-W directed) Peters et al. (2001)
Tectonic Stage 2B Late Lutetian to Miocene extension - stage B Fournier et al. (2006) Scharf et al. (2020)			
Tectonic Stage 3 Late Oligocene to early Miocene shortening E-W to NE-SW			Early Miocene, Fournier et al. (2006) to late Miocene-Pliocene folding Schreurs and Immenhauser (1999)
Pliocene N-S shortening Fournier et al. (2006)			Post-mid-Eocene E/W-compression near Jabal Ja'alan Filbrandt et al. (1990)

Figure 5. Stress directions in the southeastern Oman Mountains and the Batain area. Time of Tectonic Stage 2 of Fournier et al. (2006) was adjusted using data of Scharf et al. (2020).

3. Methods

3.1. Kinematic analyses

Kinematic analyses of brittle fault planes in the field were performed, following Petit (1987) and Angelier (1994). All structural measurements are expressed as dip direction/dip angle for planar elements and plunge direction/plunge angle for linear features.

3.2. Remote sensing data interpretation

Satellite images to identify sub-vertical linear structures were analyzed. These structures were digitalized using the geographical information system (GIS). Linear features on a satellite image are commonly poly-genetic planar elements (fractures, faults, strike-parallel features of resistant strata etc.). For simplification, we term such features on the satellite image as “lineaments“, although they are planar elements. The entire study area (~250 km by 50 km) was analyzed using world satellite imageries at different scales. Linear objects are interpreted as straight segments of valleys or geomorphological alignments related to brittle deformation of rock masses.

The interpretation of remote sensing data, combined with published geological maps of the study area (Béchenec et al., 1986; Villey et al., 1986a, 1986b; Le Métour et al., 1986b; Rabu et al., 1986; Wyns et

al., 1992; Roger et al., 1991; Peters et al., 2001, 2005) provided the basis for a brittle deformation model of our study area. More than 10,000 lineaments have been analyzed. The length of these linear features ranges between 100 m and 20 km. The results are summarized with respective rose diagrams for different sectors and for the entire working area, using the GIS extension tool of Jenness (2014).

Comparison of the linear features with geological maps confirms displacement at several places. Remote sensing data interpretation was conducted to see whether the linear features represent geological structures. The interpretation was carried out using the GIS tools (PolarPlots v.1.0.253 of Jenness, 2014) for ArcMap (v. 10.2, Esri ) for the analysis of satellite imageries for northeastern Oman. The imagery features provided by Esri are WV03_VNIR satellite imagery with resolution of 0.31 m, accuracy of 10.2%, and source Digital Globe.

3.3. LA-SF-ICP-MS U-Pb dating

U-Th-Pb analyses were carried out in the Earthlab at the University of the Witwatersrand. The analytical protocol is similar to Ring and Bolhar (2020) (Supplementary Material S1).

Graphic presentation and calculation of lower intercept ages on a Tera-Wasserburg diagram were carried out using the software ISOPLOT-R (Vermeesch, 2018). Uncertainties of individual and mean/regressed ages are 2 SE (standard error, absolute). Intercept ages were based on individual dates and internal errors (not propagated). Propagated errors on U/Pb ratios can be estimated to be 1.25 times the internal errors for a similar analytical setup as adopted here (Woodhead & Petrus, 2019). Depth-resolution within each analysis is enabled by using a primary carbonate standard (WC-1; Roberts et al., 2017), coupled with downhole-fractionation correction; this further allowed to identify (and exclude) regions of high common Pb, and also to separate time intervals with distinctly variable U/Pb during ablations, sometimes resulting in more than one date for each spot (Woodhead & Petrus, 2019), reflecting age heterogeneity or variable common Pb within the carbonate.

LA-ICPMS data for standards are reported in tables S2 and S3. Sixty-six analyses of Duff Brown carbonate (ID-MC-ICP-MS age: 64.04 ± 0.67 ; 60.5 ± 4.6 ; 66.3 ± 3.9 Ma; 2 SE) produce a lower intercept age of 66.16 ± 0.5 Ma (MSWD=13; n=66), in excellent agreement with published values (Hill et al., 2016). Fifty-five analyses of the Richard's Spur speleothem provide an age of 299.96 ± 2.36 Ma (MSWD=3; n=55). This age is higher than the accepted ID-TIMS age of 289.2 ± 0.7 Ma (Woodhead et al., 2010) by 3.4 % (relative to accepted value). U-Pb ages for carbonates can be older for LA-based datasets when compared to isotope dilution (ID)-based datasets, possibly reflecting inadequate correction of common Pb in the gas blank (Woodhead & Petrus, 2019), or systematic differences in ablation behavior between carbonates types (speleothems versus micritic carbonates; Nuriel et al., 2017). One in-house standard ("Rio calcite") provides an accurate age of 56.25 ± 0.20 Ma (MSWD=4.7, n=39; C. Lana pers. Comm.). Two unknown samples yield an age of 30.08 ± 0.47 and 22.31 ± 2.15 Ma (Table S4). Values of MSWD (2.4 and 5.3) are comparable to, or slightly higher than, the range quoted for U-Pb LA-ICP-MS carbonate ages of 2-4 (Woodhead and Petrus, 2019). Three other samples collected from the thrust at site 7a did not produce ages due to low U concentrations and very limited dispersion (Table S5).

3.4. GPlates reconstruction

The relative motions of Arabia and India during the Cenozoic were analyzed by the software GPlates (www.gplates.org). GPlates is based on a large database, including coastlines and seafloor magnetic anomalies (Matthews et al., 2011, 2016; Müller et al., 2016). In our study, Arabia is considered fixed while the relative translation and rotation of India was observed, allowing for estimation of changing distances between India and the eastern margin of Arabia through time.

4. Results

4.1. Field observations

The Oman Mountains from the eastern Batinah Coastal Plain to the Sur area (Fig. 1), encompass several

Eocene to Miocene NW-striking sinistral transtensional and transpressional faults, including (1) the “Tertiary Ridge” of Al-Khod Village (Scharf et al., 2016), (2) the Sunub Fault Zone (Mattern et al., 2018c), (3) the Wadi Mansah Fault Zone (Bailey et al., 2019; Scharf et al., 2019a), (4) the Issmaiya Fault Zone (Callegari et al., 2020), (5) the Ja’alan Fault (Filbrandt et al., 1990; Rogers et al., 1991), and (6) the Coastal Parallel Shear Zone (Wyns et al., 1992; Moraetis et al., 2018).

Eleven field sites in the Muscat-Seeb area were investigated, exhibiting N/S-striking compressional features and/or NW-striking sinistral faults (Figs. 2 and 3). Sites 1, 2, 3, 6, 10 and 11 are within and sites 4, 5, 7, 8 and 9 are outside the Rusayl Embayment (Fig. 3). Two NW-striking sinistral faults and one N-striking fold were studied at and near the Salma Plateau (Fig. 2; site 12-14). A NW strike-slip fault, E/W normal fault, N/S folds and thrusts were investigated in the Ibra Basin (site 15). The structures and their locations are shown in figures 1-3 and summarized in tables 2 and S1. Detailed outcrop descriptions are documented in the Supplementary Material (S2).

Table 2. Summary of field observations. More field details are presented in Table S1 and section S2. Sites are depicted in the Figures 2 and 3 and listed from the NW to the SE.

Sites	Location	Latitude	Longitude	Structure	Orientation
1	Wadi Ja’arah	23°2904	57°5500	Sinistral shear zone	WNW-striking
2	Halban	23°3317	57°5821	Open syncline Dextral fault	Sub-horizontal fold axis, trending SW-striking
3	Taww	23°2919	57°5814	Sinistral shear zone	E/W-striking
4	Al-Khod Village	23°3349	58°0709	Reverse Fault	266/67
5	Fanja	23°2728	58°0700	Strike-slip shear zone	007/84
6	Bidbid	23°2450	58°0702	Sinistral shear zones	WNW to NW-striking
7a	SQU Campus	23°3524	58°0940	Synsedimentary thrust	083/27
7b	SQU Campus	23°3516	58°1033	Sinistral fault	052/77
8	Rusayl Dam	23°3154	58°1207	Open folds	Gently plunging fold axes to the
9	Cement factory	23°2845	58°1757	Open syncline	Gently plunging fold axis to the
10	Qurum South	23°3600	58°2858	Open anticline	Gently plunging fold axis toward
11	Qurum	23°3700	58°3036	Thrust Open anticline	270/30 Sub-horizontal fold axis, trending
12	Tiwi	22°4656	59°1655	Sinistral positive flower structure	244/77
13	Salma Plateau	22°4930	59°0059	Sinistral faults Open anticline	026/65 and 037/59 Gently plunging fold axis to the
14	Wadi Al Khabbah	22°5019	58°5854	Sinistral fault	WNW-striking
15	Ibra Basin	22°0442	58°4448	Strike-slip fault Thrusts Normal fault Open anticline and syncline	NW-striking N/S-striking E/W-striking Sub-horizontal fold axes, trending

4.2. Remote sensing analysis

Linear elements of the study area are projected on a satellite image, based on Remote Sensing data analysis (Fig. 6). Approximately 10,000 linear features were identified within the eastern Oman Mountains and the Batain area (Fig. 6). The investigated area was divided into eight sub-areas following a regional tectonic subdivision (Fig. 6; 1 – Jabal Nakhl; 2 – Rusayl Embayment; 3 – Fanja Saddle; 4 – Saih Hatat Dome; 5 – Salma Plateau; 6 – Wadi Mansah Fault Zone/ Wadi Tayin Fault/ Issmaiya Fault Zone/ Ja’alan Fault; 7 – Qalhat Fault; 8 – Batain area). All sub-areas reveal a similar lineament orientation pattern. Most of the lineaments trend WNW to NW (Fig. 6). Some of the lineaments are E/W and NE/SW-oriented ($\sim 055-235^\circ$). The latter orientation is more common in the Batain area.

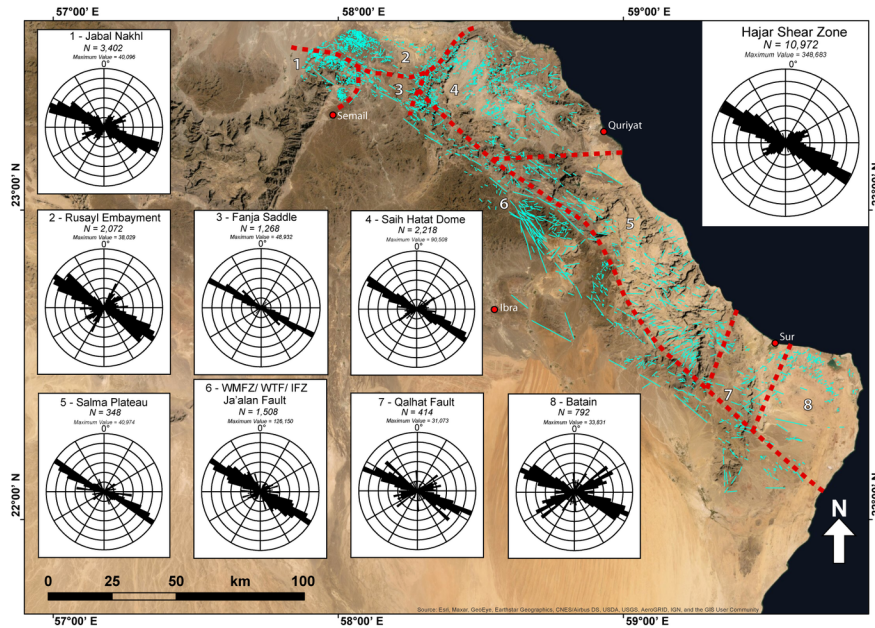


Figure 6. Satellite image analyses of the study area from west of the Rusayl Embayment to the Batain area. The study area is divided into eight sub-areas to potentially reveal local/regional variations in orientation of the lineamentary features (areas 1-8, separated by the red dashed lines). The orientations of the lineaments (light blue lines) from the satellite image are plotted in the rose diagrams (Jenness, 2014), with a bin size of 5°. All measurements are plotted in the rose diagram at the upper right. N=number of measured linear features; Maximum Values is the total length (in meters) of all measured lineaments.

4.3 Map analysis

This section summarizes previously mapped \sim N/S-oriented compressive structures, \sim E/W-oriented normal faults and \sim NW-striking sinistral faults within eastern Oman (Figs. 7 and 8; Table 1). These structures affect mostly Paleocene/mid-Eocene sedimentary rocks but also some Miocene rocks, especially near the Qalhat Fault. Besides the mappable features, Wyns et al. (1992) measured sub-horizontal stylolite axes within Cenozoic carbonates, including those of the Oligocene Shama Formation near the Qalhat Fault. Stylolite axes are oriented ENE-WSE and interpret as axes of maximum compression during the Miocene (Wyns et al., 1992).

4.3.1. Folds

N/S to NW/SE-oriented folds within the post-obductional formation in the Muscat-Seeb area and the Permian rocks of the Saih Hatat Dome have been reported by Le Métour et al. (1986a), Villey et al. (1986a, 1986b), Mann et al. (1990), Miller et al. (2002), Kajima et al. (2012a, 2021b, 2021c), Scharf et al. (2016), Searle et al. (2019), Hansman et al. (2021) and Levell et al. (2021), and are summarized in Table 1. Traces of fold axes are shown in Figure 7. The respective folds deform stratigraphic units up to the mid-Eocene limestone of the Seeb Formation. Mapped folds are open to tight and display sub-vertical fold axial planes. Fold axes plunge gently towards the north to NW or are sub-horizontally. The interlimb angle of individual folds within the Rusayl Embayment varies. Towards the South, the same fold elements (synclines/anticlines) are tighter than in the North, where the folds open (Mann et al., 1990). Interlimb angles are homogeneous along individual folds outside the Rusayl Embayment.

Ninkabou et al. (2021) and Levell et al. (2021) presented seismic and well data from offshore northeastern Oman. A pre-late Eocene NNE-trending major fold has been spotted by Levell et al. (2021). This fold occurs in the NNE-ward projected extension of the Jabal Akhdar/Jabal Nakhl. Further \sim N/S-trending folds extend

from the Rusayl Embayment into the Sea of Oman and near Muscat. Rabu et al. (1986) and Coffield et al. (1990) mapped several Cenozoic \sim N/S to NNW/SSE-trending faults in the Fanja area between the Jabal Akhdar and Saih Hatat domes as well as along the Frontal Range Fault and the Wadi Mansah Fault (Fig. 7).

Approximately N/S-oriented open to tight folds have been mapped within Paleocene to Miocene formations near Quriyat, in the Salma Plateau and Batain area (Le Métour et al., 1986a, 1986b; Roger et al., 1991; Wyns et al. 1992; Peters et al., 2001). Further \sim N/S-oriented open asymmetric folds and monoclines deformed Maastrichtian to Eocene rocks at Jabal Ja'alan (Filbrandt et al., 1990). The traces of some of these folds are depicted in Figure 8.

4.3.2 Faults

Fournier et al. (2006) mapped sets of conjugate strike-slip faults within the Jafnayn Formation in the Muscat area (Figs. 7 and 8). Dextral and sinistral faults strike NE/SW and E/W, respectively (Fournier et al., 2006). The computed maximum horizontal stress trends ENE/WSW (between N54°E and N85°E; Fournier et al., 2006).

A segment of the Paleogene rocks, including the Jafnayn, Rusayl and Seeb formations at the “Tertiary Ridge” at Al Khod Village represents a WNW-striking transpressive sinistral shear zone with \sim N/S-oriented compressive structures (folds and reverse faults) and \sim E/W-striking normal faults (Scharf et al., 2016). The horizontal shorting direction was ENE/WSW (Scharf et al., 2016).

In the Sunub area of the Rusayl Embayment and near the Frontal Range Fault, the well-exposed WNW-striking sinistral transtensional Sunub Shear Zone associated with \sim E/W-striking normal faults exists. It has been interpreted as a negative flower structure with a shale dike (Mattern et al., 2018c).

The southwestern margin of the Saih Hatat Dome and the Fanja area is characterized by the Wadi Mansah Fault Zone (Bailey et al., 2019; Scharf et al., 2019a). This major extensional shear zone has a throw of [?]7 km and a sinistral shear component. It has been interpreted as active during doming of the Jabal Akhdar and Saih Hatat domes during the late Eocene to Miocene (Scharf et al., 2019a). The southeastern extend of the Wadi Mansah Fault Zone is parallel to the margin of the Saih Hatat Dome and merges with the extensional Wadi Tayin Fault of Searle (2007). The latter has a throw of \sim 2 km (Searle, 2007). Numerous \sim WNW-striking faults in the Fanja area affected autochthonous and allochthonous rocks (Stanger, 1985).

Within the Semail Ophiolite, parallelly orientated to the Wadi Mansah Fault Zone and near the Wadi Tayin Fault, a further sinistral transtensional fault zone is present – the Issmaiya Fault Zone (Callegari et al., 2020). This \sim NW-striking shear zone is \sim 30 km long and \sim 3 km wide. Activity along this fault zone occurred first during the Maastrichtian to early Eocene and then following the mid-Eocene (Callegari et al., 2020).

The Salma Plateau, including mid-Eocene limestones, has been affected by numerous faults of the NW-striking sinistral transpressive Coastal Parallel Shear Zone (Wyns et al., 1992; Moraetis et al., 2018). Sinistral slip was determined by Roger et al. (1991) and Wyns et al. (1992).

In the southeastern prolongation of the Issmaiya Fault Zone, the NW-striking Ja'alan Fault is exposed (Roger et al., 1991; Wyns et al., 1992; Fig. 8). This fault is a present-day major reverse fault with a sinistral component (Filbrandt et al., 1990; Wyns et al., 1992). The throw amounts to a few kilometers. The Ja'alan Fault marks the southwestern limit of the Salma Plateau (Fig. 2).

The \sim N/S-striking Qalhat Fault is located near Sur and defines the eastern margin of the Salma Plateau (Fig. 2). The throw along the major fault amounts to a few to several kilometers, where the Neoproterozoic crystalline basement was thrust onto Oligocene/Miocene sedimentary rocks (Wyns et al., 1992). Adjacent to the Qalhat Fault are several \sim N/S-oriented folds (Roger et al., 2001). The rocks east of the Qalhat Fault were not uplifted, while the same Cenozoic rocks to the West have been uplifted to an elevation of >2000 m.

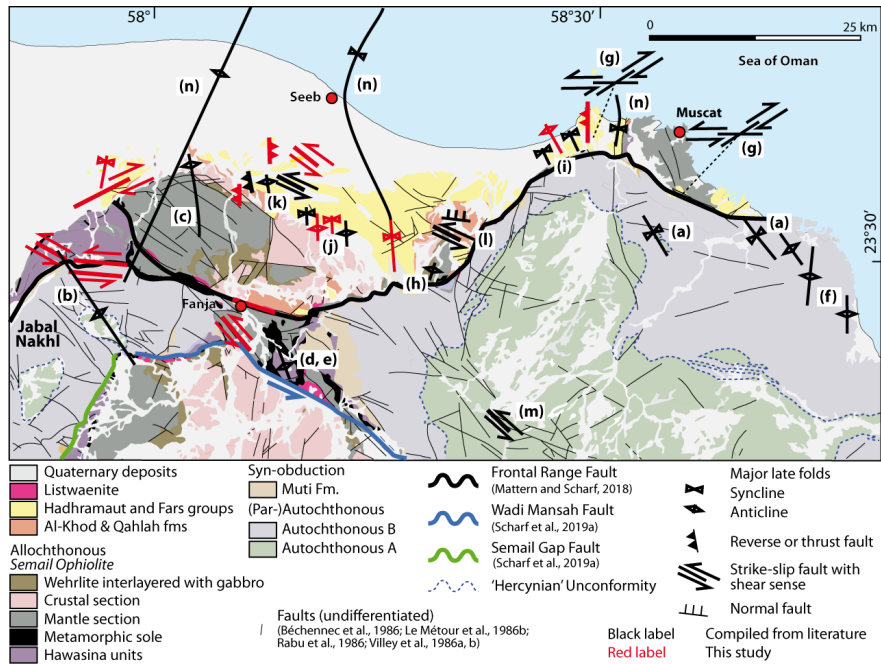


Figure 7. Structural map of the Muscat-Seeb area of Figure 4. Most of the black folds/faults are of post-mid-Eocene age; (a) – Le Métour et al. (1986a, 1986b); (b) – Rabu et al. (1986); (c) – Villey et al. (1986a); (d) – Villey et al. (1986b); (e) – Coffield (1990); (f) – Miller et al. (2002); (g) – Fournier et al. (2006); (h) – Kajima et al. (2012a); (i) – Kajima et al. (2012b); (j) – Kajima et al. (2012c); (k) – Scharf et al. (2016); (l) – Mattern et al. (2018c); (m) – Mattern et al. (2020a); (n) – Levell et al. (2021). Thin black lines represent undifferentiated faults, taken from Béchenec et al. (1986), Villey et al. (1986a, 1986b), Le Métour et al. (1986b) and Rabu et al. (1986). The age of these faults is unknown. Note that the large NNE-oriented anticline as continuation of the Jabal Akhdar/Jabal Nakhl is late Eocene in age, based on seismic data (Levell et al., 2021).

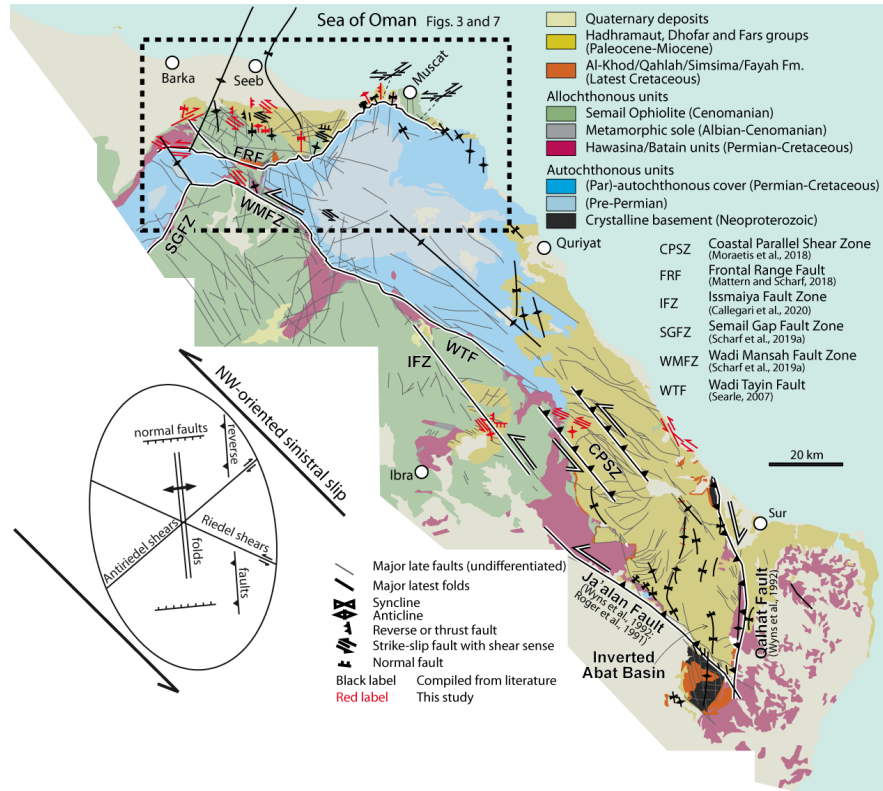


Figure 8. Structural map of eastern Oman, depicting post-mid-Eocene structures. Compiled after Béchenec et al. (1986), Villey et al. (1986a, 1986b), Le Métour et al. (1986a, 1986b), Rabu et al. (1986), Wyns et al. (1992), Roger et al. (1991), Peters et al. (2001, 2005), Moraetis et al. (2018), Callegari et al. (2020) and Levell et al. (2021). The age of the undifferentiated faults is unknown. The Harding Strain Ellipse (Harding, 1974) indicates a wrench-fault assemblage geometry for NW-striking sinistral slip. Note that most mapped structures conform to this geometry!

4.4. U-Pb dating of carbonates

Synkinematic carbonates from faults were analyzed with the U-Pb in-situ LA-ICPMS method (e.g., Woodhead & Petrus, 2019; Carminati et al., 2020; Ring & Bolhar, 2020; Roberts et al., 2020). Out of five carbonate samples only two synkinematic carbonates produced reliable and precise U-Pb LA-ICPMS ages (sample Baz 2 and HAB 1). Analytical data are presented in Figure 9 and reported in tables 3 and S2. Sample Baz 2 was collected from a sinistral fault from the Sultan Qaboos University Campus (site 7b) and yields an U-Pb age of 22.31 ± 2.15 Ma (2 SE). Sample HAB 1 consists of synkinematic calcite from a dextral fault of Halban (site 2), yielding an U-Pb age of 30.08 ± 0.47 Ma (2 SE).

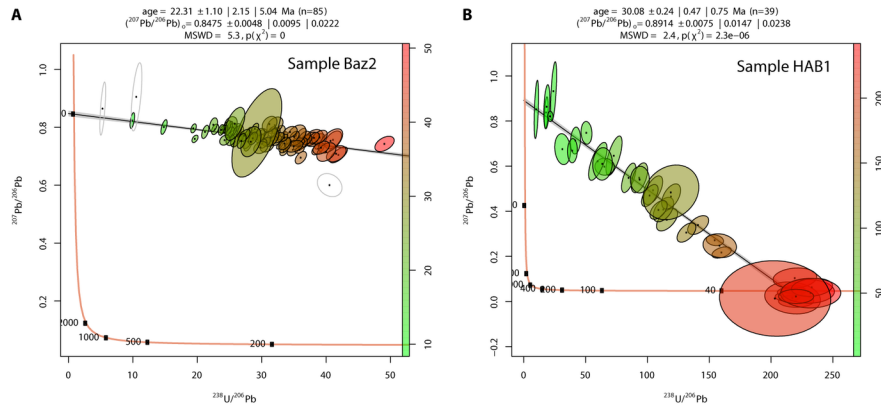


Figure 9. Tera-Wasserburg disagrams showing U-Pb age data (error ellipse=2 SE) for sample Baz 2 and HAB1 (A and B). Gray areas around discordia represent 2 SE uncertainty of linear regression. Analytical precision (age, initial $^{207}\text{Pb}/^{206}\text{Pb}$) is indicated as analytical uncertainty (first value, 1 sigma), “studentized 100(1- α)% confidence interval for t using the appropriate number of degrees of freedom” (second value) and “approximate 100(1- α)% confidence interval for t with over-dispersion, calculated as $z=y[?]\text{MSWD}$ ” (value 3). MSWD =mean squared weighted deviations, n =numbers of spot analyses. The U-Pb data ellipses are color-coded according to their $^{238}\text{U}/^{206}\text{Pb}$ value, displayed in the individual color scales at the right margin of the diagrams. Data points plotting to the left of the concordia were excluded from age regression; some outliers were also excluded, which plotted off the main regression line, without altering the original age estimate, but improving precision and MSWD values. Graphic presentation and age calculation utilized IsolpotR (Vermeesch, 2018).

Table 3. Sample details with U-Pb age results

Sample	Lat	Long	Lithology/structure
Baz 2	23°35'16"	58°10'33"	Carbonates and siliciclastics of the Barzaman Fm. / Calcified sinistral strike-slip fault (s
HAB 1	23°33'17"	57°58'21"	Carbonates of the Jafnayn Fm. / Calcified dextral strike-slip fault with cataclasite (site

4.5 GPlate reconstructions

Relative plate motions induce corresponding regional strain into plates near the plate boundary (Ledouzey, 1986; Heidbach et al., 2007; Zoback & Zoback, 2007). Eastern Oman is located near the present-day Arabia-India plate boundary, i.e., near the Owen Fracture Zone (Fournier et al., 2008; DeMets et al., 2010; Fig. 1).

The ~N/S to NW/SE-oriented Eocene to Miocene compressive structures deformed sedimentary rocks likely due to ~E/W to NE/SW-directed shortening. A suitable geodynamic cause for this shortening is the convergence history between the Arabian and Indian plates as suggested by Fournier et al. (2006) and Gaina et al. (2015). The latter authors suggested minor E/W-shortening between the Arabian and Indian plates from 40 Ma to the present (their Fig. 7). We analyzed the plate configurations of Arabia and India during the Cenozoic using the GPlates software to develop the causal relationship.

In all our reconstructions, Arabia is anchored (fixed). We describe the distance of India (near the present-day location of Karachi at 24°50N/66°40E) and the western tip of the 64 Ma isochron, as part of the Indian Plate, with respect to Arabia (East of Sur: 22°2930N/59°49E; Figs. 10-12). We calculated/measured the E/W-component of distance of the two fix points between India and Arabia at different times (distance between Karachi and Sur, and distance between western tip of the 64 Ma isochron and Sur).

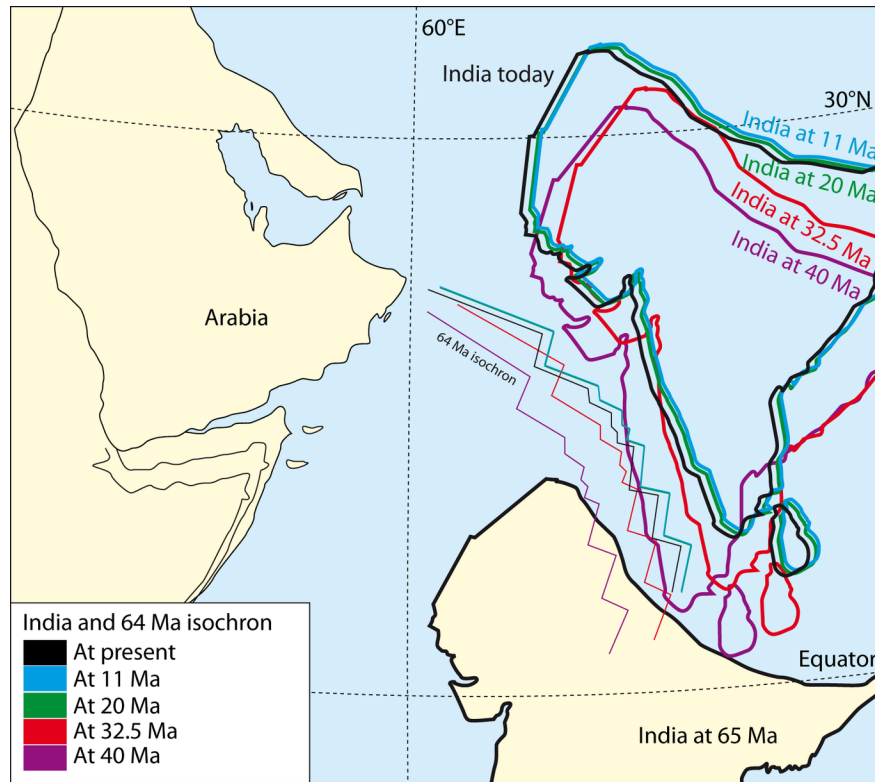


Figure 10. Cenozoic plate reconstruction between Arabia (fixed) and India, based on GPlates (version 2.2.0) with a 3D orthographic projection. Eurasia at the present stage is not depicted.

4.5.1 65 to 32.5 Ma

Left-lateral translation was the main relative motion between the Arabian and Indian plates between the beginning of the Cenozoic and ~ 40 Ma. At 65 and 40 Ma, the reference points at the Indian Plate were set at $3^{\circ}59'24''N/61^{\circ}10'12''E$ and $22^{\circ}29'30''N/59^{\circ}49'E$, respectively. Thus, India moved ~ 2165 km towards the NNE between 65 and 40 Ma (average velocity of 86.6 mm/a) with respect to fixed Arabia (Fig. 10).

Between 40 to 32.5 Ma, both plates underwent some divergence with left-lateral translation (~ 185 km translation of India towards the NE; ~ 24.67 mm/a; between 40 and 32.5 Ma; Fig. 10). The Indian reference point was set at $23^{\circ}13'48''N/68^{\circ}42'E$ at 32.5 Ma (Fig. 10). Thus, the relative motion between Arabia and India did not cause any shortening in Oman from 65 to 32.5 Ma.

4.5.2 32.5 Ma to present

Between ~ 32.5 and 20 Ma, both plates experienced ~ 100 to 135 km $\sim E/W$ -directed convergence owing to a minor \sim northward motion and coeval anticlockwise rotation of India (8° ; $\sim 0.64^{\circ}/Ma$) with respect to Arabia (~ 228 km of rotation and translation of India to the NW; ~ 18.2 mm/a; between 32.5 and 20 Ma; Fig. 11). The Indian reference point was set at $24^{\circ}54'N/67^{\circ}21'E$ at 20 Ma (Fig. 11).

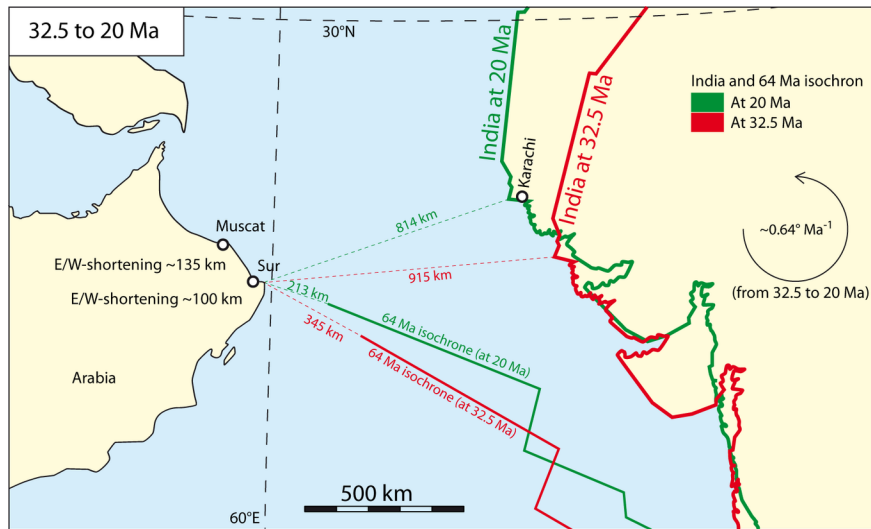


Figure 11. Plate reconstruction between Arabia and India between 32.5 and 20 Ma, using GPlates (version 2.2.0) with a 3D orthographic projection. Note that India rotated counterclockwise, resulting in oblique convergence between both plates! The component of E/W-shortening between both plates amounted to ~100-135 km.

After 20 Ma convergence stopped as counterclockwise rotation of India ceased, and both plates experienced minor left-lateral motion until 11 Ma with some divergence between both plates (~27 km translation of India toward the NE; ~2.7 mm/a; between 20 and 11 Ma). The Indian reference point was at 25°0748N/67°2436E at 11 Ma.

From ~11 Ma to the present, India translated relatively towards the WSW, resulting in right-lateral motion and ~ENE/WSW-convergence between Arabia and India (~83 km translation of India towards the WSW; ~7.5 mm/a; between 11 Ma and today; Fig. 12).

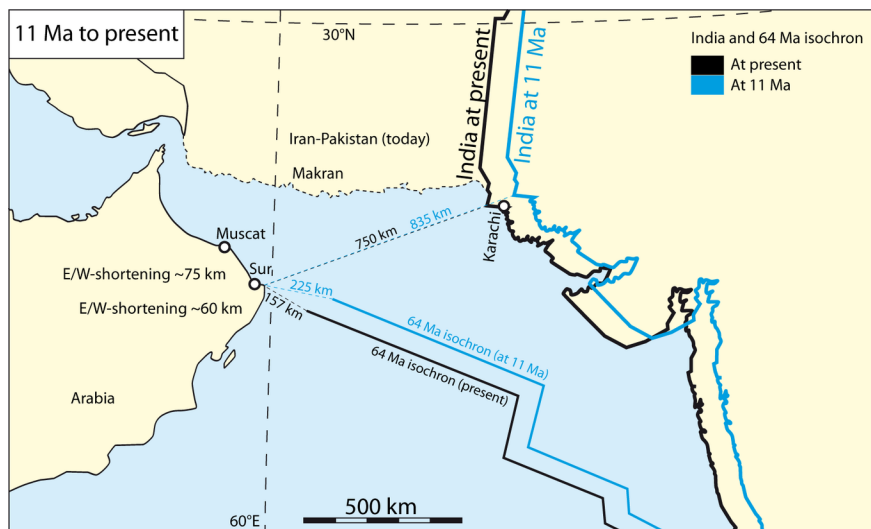


Figure 12. Plate reconstruction of Arabia and India between 11 Ma and today, using GPlates (version 2.2.0) with a 3D orthographic projection. Note that India translates towards the west-southwest, resulting

in convergence and dextral motion at the plate boundary! The amount of E/W-shortening between both plates ranges between ~60 and ~75 km. Shortening/convergence is ongoing.

The time slots from ~32.5 to 20 Ma and from 11 Ma to the present indicate a relative ~E/W-directed convergence and shortening between the Arabian and Indian plates (Figs. 11 and 12). The E/W-directed shortening between the Arabian (near Sur) and Indian plates (near Karachi and the western end of the 64 Ma isochrone) amounted to ~100-135 km from ~32.5 to 20 Ma (Fig. 11) and ~60-75 km from 11 Ma to present-day (Fig. 12), resulting in convergence rates of ~10-12 mm/a and 5-7 mm/a, respectively.

5. Interpretation and discussion

5.1 Wrench-fault assemblage and satellite image analysis

Field analysis of 15 sites (Supplementary Material S2) and map interpretations indicate that all formations/units (except the Quaternary deposits) in northeastern Oman were affected by NW-striking sinistral faults, associated with ~WNW-striking sinistral Riedel faults, ~N/S to ~NW/SE-oriented compressive structures (i.e., folds, reverse faults, thrusts) and ~E/W-oriented normal faults. At Site 2 (Halban), a SW-striking dextral fault has been mapped. This dextral fault is interpreted as an anti-Riedel fault (antithetic to the main fault). All these structures combined indicate a wrench-fault assemblage of an overall NW-striking major sinistral shear zone (see Harding Strain Ellipse in Fig. 8).

Most of the >10,000 identified lineamentary features within the study area are WNW/ESE to NW/SE-oriented (Fig. 6). The orientation of the lineamentary features differs outside the study area (i.e., along the eastern margin of the Jabal Akhdar Dome and adjacent ophiolite rocks, with a mostly NNE/SSW-orientation; Scharf et al., 2019a). The general orientation of lineamentary features within different sub-areas of the study area does not change significantly (Fig. 6). Thus, most of the identified linear features formed during the same deformation/shearing event.

The WNW-oriented linear features are interpreted as sinistral Riedel faults with respect to the ~NW-striking main fault, while ~E/W-striking features are probably normal faults (see Harding Strain Ellipse of Fig. 8). The ~NE/SW-oriented lineaments are mostly found in the Batain area (Fig. 6). Only the Batain area was affected by ~WNW-directed obduction of the Masirah Ophiolite. Thus, we conclude that these features are related to the thrusting of the Masirah Ophiolite (i.e., these features present largely thrusts of the Masirah fold-and-thrust belt).

5.2 The Hajar Shear Zone

Wrench-fault assemblage (~NW-striking sinistral faults, ~N/S-oriented compressive structures, ~E/W-oriented extensional structures, ~WNW-striking sinistral fault – Riedel faults and ~SW-oriented dextral faults – anti-Riedel faults) and the WNW to NW-oriented lineamentary features are distributed over a wide area with a minimum length and width of ~250 km and ~50 km, respectively, from the eastern Batinah Coastal Plain to the Batain area (Fig. 8). This entire zone underwent NW-directed sinistral shear and E/W-shortening after the mid-Eocene. We reference this zone as “Hajar Shear Zone” (HSZ). Some parts along the HSZ are active, indicating ongoing ~E/W-shortening (e.g., seismicity near the Qalhat Fault and uplifting marine terraces; Fig. 1). Numerous faults, compressive and extensional structures are present within this area, indicating widely distributed strain. However, most of the sinistral shear is concentrated along major faults, probably because they reactivated older structures. These include a segment of the Frontal Range Fault near Fanja, the Wadi Mansah Fault Zone, possibly the Wadi Tayin Fault, the Issmaiya Fault Zone, the Coastal Parallel Shear Zone and the Ja’alan Fault (Fig. 8). In our model, we connect/link all these faults to one major sinistral fault zone, along which most of the shearing of the HSZ has been accommodated.

In the southeast, Quaternary deposits cover large parts of the Batain region, which makes it challenging to trace/map the continuation of the HSZ. The width of the HSZ could exceed 50 km because rocks to the SW of the Wadi Mansah/Issmaiya/Ja’alan faults display widely distributed WNW to NW-oriented sinistral

faults, too (Fig. 8). However, most of this area consists of the Semail Ophiolite, where shearing is difficult to detect and date.

5.3. Time-constraining the deformation

5.3.1 Interval I

Ages of several structures within the HSZ have been constrained by different geological approaches to be Oligocene or younger. Most of the \sim N/S-oriented structures (faults and folds) deformed late to mid-Eocene formations but also some Oligocene/Miocene formations in the Rusayl Embayment and Sur area. Thus, \sim E/W-shortening must be younger than mid-Eocene.

Sinistral WNW to W-striking faults at Wadi Ja'arah, Taww and Fanja (sites 1, 2 and 5) cut all structures including top-to-the NE extensional structures (e.g., compare Al-Wardi and Butler, 2007; Grobe et al., 2018; Mattern and Scharf, 2018). Furthermore, sinistral strike-slip faults are vertical or sub-vertical and were not tilted during the main doming interval of the Jabal Akhdar, which lasted from the late Eocene to Oligocene (Hansman et al., 2017; compare Levell et al., 2021 for offshore folding). We suggest that these NW-striking sinistral faults are part of the HSZ with the \sim E/W to WNW-striking sinistral faults representing Riedel faults (synthetic faults). Strike-slip faults at Taww post-date Jabal Akhdar doming and top-to-the-NNE extensional shearing and, thus, occurred during the Oligocene or later.

At Fanja, the strike-slip faults cut all extensional structures of the southern Fanja Half Graben. The first extensional interval at this half graben lasted from the latest Cretaceous to early Paleogene (Tectonic Stage 1 of Fournier et al., 2006) and the second interval was post-mid-Eocene (probably Oligocene; Tectonic Stage 2 of Fournier et al., 2006; Fig. 5). Therefore, strike-slip faults at Fanja are also Oligocene or younger in age.

The sinistral fault at the southwestern margin of the Saih Hatat Dome, at Wadi Al Khabbah (site 14; Fig. S22) displaces autochthonous Jurassic and Cretaceous rocks, which were tilted during the late Eocene to Oligocene doming of the Saih Hatat (Hansman et al., 2017). Thus, this WNW-striking fault must be Oligocene or younger, too.

A key outcrop is the syndepositional thrust at the Sultan Qaboos University Campus (site 7a; Fig. S13). This thrust occurs within the Upper Oligocene to Lower Miocene section of the Barzaman Formation (age based on foraminifer genera; Mattern et al., 2020b), attesting that \sim E/W-directed shortening was active during the latest Oligocene to Early Miocene. This designated age agrees with computed paleostress information derived from fault slip data by Fournier et al. (2006), indicating that E/W-compression occurred during the early Miocene.

A similar and slightly younger (Miocene) age for \sim E/W-shortening has inferred by Fournier et al. (2006) and Schreurs and Immenhauser (1999) for the Batain/Sur area (Fig. 5). Filbrandt et al. (1990) assigned a post-mid-Eocene age to \sim E/W-shortening in the Jabal Ja'alan area. The inversion of the Abat Basin started during the late Burdigalian (compare Wyns et al., 1992).

GPlates reconstructions document \sim E/W-shortening between Arabia and India. Interval I is related to the counterclockwise rotation of India between 32.5 and 20 Ma (Rupelian to Burdigalian; Cohen et al., 2013). This deformation created the HSZ and its wrench-fault assemblage. Owing to coeval counterclockwise rotation of India and northward motion of India, the direction of shortening also rotated counterclockwise from \sim E/W to \sim ENE/WSW. This rotation and the coeval northward movement of India resulted in non-coaxial deformation (simple shear) at northeastern Oman.

Furthermore, U-Pb dating of synkinematic calcite proves a latest Oligocene/earliest Miocene age for sinistral deformation in the Barzaman Formation (22.31 ± 2.15 Ma; site 7b; Fig. S14). The age of 22.31 Ma corresponds to the Aquitanian (Cohen et al., 2013). This age indicates that deformation ensued during deposition of the Barzaman Formation, consistent with the age of the synsedimentary thrust at site 7a (Fig. S13).

A further precise U-Pb age for carbonate was obtained from the Halban area (30.08 ± 0.47 Ma; site 2; Fig. S3-6). This early Oligocene age (Rupelian; Cohen et al., 2013) dates dextral motion along a \sim SW-striking

anti-Riedel Fault of the HSZ and within the Jafnayn and Rusayl formations.

The independently obtained age constraints for \sim E/W-shortening from map interpretation, cross-cutting relationships, syndepositional thrusting, GPlates reconstruction and U-Pb dating of synkinematic carbonate, demonstrate shortening along the HSZ between 32.5 and 20 Ma and define our Interval I.

5.3.2 Interval II

GPlates reconstructions indicate that no E/W-shortening between the Arabian and Indian plates occurred between 20 to 11 Ma. Further convergence with an E/W-shortening component started at 11 Ma (early Tortonian, Cohen et al., 2013) and lasting until present-day associated with \sim 60-75 km of shortening (Interval II). This ongoing shortening interval may have reactivated the Qahlah Fault (recent seismicity), is responsible for activities at the transpressional Coastal Parallel Shear Zone, inverted the Abat Basin and uplifted marine terraces NW of the Qalhat Fault (Fig. 13). However, further structural work and dating are needed confirm the GPlates results.

5.4 Amount of deformation in eastern Arabia and the HSZ

According to GPlates reconstructions, the E/W-convergence between the Arabian and Indian plates amounts to \sim 100-135 km from 32.5-20 Ma. Thus, the combined amount of shortening of all described structures from Musandam to the Batain area cannot exceed this amount, assuming that the pre-Oligocene and present-day coastline of eastern Oman were at the same position and of the same shape as today.

The amount of Oligocene to early Miocene westward translation along the Hagab Thrust measures >15 km (Searle, 1988). The Oligocene/early Miocene shortening along Jabal Hafit Anticline and the Suneinah area has not been quantified but is assumed by us to amount to a few tens of kilometers (compare Boote et al., 1990; Hansman & Ring, 2018).

The amount of sinistral shearing (lateral displacement during Interval I) along the HSZ and \sim E/W-shortening is unknown, due to a lack of markers. Numerous small structures occur within the HSZ (folds, thrusts, reverse faults, normal faults and strike-slip faults), and these structures are widely distributed throughout our study area of \sim 250 km by \sim 50 km. Folds are mostly open and range in size from several meters to kilometers in wave length. Mapped faults have a displacement of a few kilometers. We acknowledge that not all structures within this large area were measured and mapped.

A conservative estimate for sinistral shearing and \sim E/W-shortening within the HSZ amounts to a few to several tens of kilometers. Some unknown amount of sinistral shearing and \sim E/W-shortening may have been absorbed (1) in the non-mapped areas of the HSZ (Batain Coastal Plain and Batain area), (2) within the Arabian Plate, i.e., the Central and Northern Oman Mountains, (3) the Omani margin offshore Batain (compare Rodriguez et al., 2014; 2016), (4) the former plate boundary of Arabia and India and (5) within the Indian Plate.

The amount of \sim ENE/WSE-oriented shortening within eastern Oman (Interval II) remains unknown due to a lack of markers. The amount of plate convergence between India and Arabia is \sim 85 km since 11 Ma, resulting in 60-75 km of E/W-shortening (Fig. 12). The amount of dextral motion between the Arabian and Indian plates for the last 11 Ma (\sim 7.5 mm/a; based on GPlates) exceeds the reported present-day dextral motion at the Owen Fracture Zone of 3 ± 0.4 mm/a (Fournier et al., 2008; DeMets et al., 2010). Thus, other active faults/plastic deformation/uplift may have absorbed the difference in plate motion (i.e., \sim 4.5 mm/a). Potential “absorbing structures” are the Owen Ridge with an uplift of >2 km (Rodriguez et al., 2014), the active Qalhat Fault and the uplifting marine terraces of the coastal Salma Plateau (e.g., Wyns et al., 1992; Mattern et al., 2018a; Moraetis et al., 2018).

5.5. Tectonic implications

Eastern Arabia contains \sim NW-striking basement faults, which formed during the Pangean/Neo-Tethys rifting. One of these faults or fault zones is below the HSZ at the southwestern margin of the Saih Hatat Dome.

It is likely that this structure was reactivated during the Oligocene/early Miocene \sim E/W-convergence between Arabia and India. Thus, the pre-existing basement structure plays a major role in the localization of the HSZ, especially the localization and concentration of sinistral slip and absorption of \sim E/W-shortening-related strain along the aligned Wadi Mansah, Wadi Tayin, Issmaiya and Ja'alan faults (Figs. 2 and 13).

GPlates modeling of motion between the Arabian and India plates shows that India rotated counterclockwise from \sim 32.5 to 20 Ma by \sim 8° with coeval northward motion of India; Fig. 11). Consequently, the direction of shortening during this stage rotated counterclockwise, too, resulting in simple shear deformation in eastern Oman and activity along the HSZ (Interval I). The overall \sim E/W-convergence/shortening between the Arabian and Indian plates amounts to a minimum of \sim 100-135 km.

The eastern Arabian Plate was affected by this deformation, evident by the wrench-fault assemblage associated with the HSZ (Figs. 8 and 13A). The amount of sinistral slip along the HSZ, including its associated wrench-fault assemblage, is not well constrained but could amount to a few to several tens of kilometers. Thus, the easternmost tip of continental Arabia was located further to the east by a few to several tens of kilometers prior to the Oligocene than today (Fig. 13). This interpretation is supported by the outline of the present-day shelf break (i.e., \sim 200 m water depth). The shelf break of eastern Oman may have been more or less straight before the Oligocene (Fig. 13A) and must have changed during the Oligocene due to left-lateral shearing. Correspondingly, the present-day shelf break changes direction. It kinks or veers to the North in the Batain area (Fig. 13). Most of this directional change occurs in the realm of the HSZ (Fig. 13). A former pre-Oligocene straight shelf break implies that easternmost Oman was left-laterally sheared for a few to several tens of kilometers (Fig. 13). Factoring in this aspect E/W-shortening during Interval I must have amounted to more than the estimated \sim 100-135 km of E/W-convergence/shortening, because GPlates uses the present-day contour of the shelf break which is post-deformational.

In addition, the present-day Qalhat Fault strikes NNW at its northern end, while it is oriented \sim N/S to NNE/SSW further to the South at Jabal Ja'alan (Fig. 2). This directional change is gradual. The latter orientation is similar to that of other major faults within the Oman Mountains such as the Semail Gap Fault Zone (Fig. 8; Weidle et al., 2021). We suggest that during sinistral shearing, the former \sim N/S to NNE/SSW-oriented Qalhat Fault was passively rotated or dragged in a counter-clockwise way to a NNE-strike at its northern end. A consequence of shortening and left-lateral shearing is that the Saih Hatat and Jabal Akhdar domes may have been further apart from one another in map view prior to shearing. In addition, we conclude that the \sim N/S to NW/SE-striking compressive structures in the northern Oman Mountains (e.g., Hagab Thrust, Jabal Hafit Anticline) also formed during Oligocene/early Miocene Arabia/India-shortening. This interpretation is supported by the orientation and age of these structures. The \sim N/S-oriented compressive structures unlikely formed during the NNE/SSW-directed Arabia/Eurasia-convergence as previously interpreted (e.g., Boote et al., 1990; Searle et al., 2014), because this convergence would have produced differently oriented compressional structures.

If Interval II is accepted as factual, the sinistral faults were not reactivated during Interval I because the direction of shortening (\sim ENE/WSW) is at a high angle to the orientation of the NW-striking HSZ. Shortening during Interval II rather produced conjugate strike-slip faults, which are indicative for pure shear deformation (e.g., Fournier et al., 2006). Thus, Interval II deformation likely overprinted elements of the wrench-fault assemblage of the HSZ such as the compressive structures at the Coastal Parallel Shear Zone, responsible for Neogene to Quaternary uplift of marine terraces between Quriyat and Sur, Neogene inversion of the Abat Basin and active tectonics at the Qalhat Fault (Fig. 13).

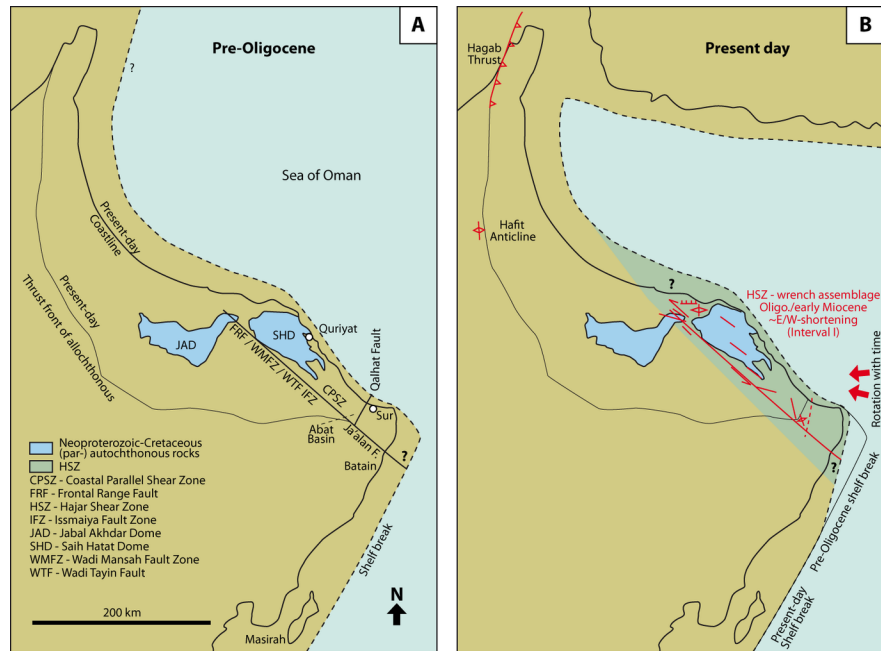


Figure 13. Outline of eastern Arabia before (A) and after (B) activity of the HSZ. Most likely, a pre-existing ~NW-striking fault zone exists below the HSZ, especially where the aligned Wadi Mansah Fault Zone, Wadi Tayin Fault, Issmaiya Fault Zone and Ja'alan Fault occur. This fault zone was reactivated during the Oligocene/early Miocene (Interval I). Outline of present-day shelf break (~200 m water depth) using Google Earth. Left-lateral shearing along the HSZ with wrench-fault assemblage is widely distributed and passively rotated/dragged structures, such as the Qalhat Fault, the shelf break and the Saih Hatat Dome.

6. Conclusions

Structural field investigations, map analyses, satellite imagery analyses, syndepositional thrusting, GPlates reconstructions and absolute U-Pb dating of synkinematic calcite reveal that eastern Oman was affected by widely distributed NW-oriented sinistral motion within and along the Hajar Shear Zone, which is associated with a wrench-fault assemblage. Shearing affected an area of ~250 km by ~50 km, lasted from ~32.5 to 20 Ma (Rupelian to Burdigalian) and amounted to a few to several tens of kilometers displacement. Most shearing was absorbed along ~250 km long major fault zones from the Batinah Coastal Plain (Jabal Nakhl area), via the Fanja Saddle (Frontal Range Fault and Wadi Mansah Fault Zone), along the southwestern margin of the Saih Hatat Dome (Wadi Mansah Fault Zone, Wadi Tayin Fault, Issmaiya Fault Zone, Coastal Parallel Shear Zone, Ja'alan Fault) to the Batain area. It is likely that below these shear zones reactivated pre-existing faults exist, that may have formed during the Pangean Neo-Tethys rifting or earlier events.

Collected data indicates that pre-existing basement structures were likely reactivated during times of suitably oriented stress fields. Thus, such deep-seated structures are responsible for deformation/uplift at passive margins such as the one in eastern Oman.

The deformation pattern of the Hajar Shear Zone can be correlated with ~N/S-oriented compressional structures in the northern Oman Mountains (Hagab Thrust, Jabal Haft Anticline). Thus, these structures formed during the ~E/W-directed Arabia/India-convergence and are not related to ~NNE/SSW-directed Arabia-Eurasia shortening. Convergence between Arabia and India is responsible for a minimum of ~100-130 km E/W-shortening in the Oman Mountains during the Oligocene and early Miocene.

The Oman Mountains were affected by largely coeval Oligocene/early Miocene convergence of Arabia-India (E/W) and Arabia-Eurasia (NNE/SSW). Previously, most mid-Cenozoic structures were believed to have

formed in response to the Arabia/Eurasia-convergence. Our results document that many of these structures have developed due to the Arabia/India convergence. Thus, E/W-shortening in the Oman Mountains and eastern Arabia played a more important role than previously considered.

A further conclusion related to the ongoing ~WSW/ENE-convergence between Arabia and India is that respective deformation may have occurred at or near the Arabia-India plate boundary. Frequently reported earthquakes in the Sea of Oman and active tectonics/uplift in the Sur/Quriyat area may be due to this shortening.

Acknowledgements

Fieldwork was carried out from 2016-2021 with the continued support of the Sultan Qaboos University. We acknowledge the field assistance of Katharina Scharf and Gianluca Frijia. We furthermore thank Hamdan Al-Zidi and Bader Al-Waili (both Sultan Qaboos University) for preparation of rock samples for the U-Pb dating. R. Bolhar acknowledges financial support to establish the LA-SF-ICP-MS facility at the School of Geosciences, University of the Witwatersrand, through a NRF-NEP grant (UID 105674). The Editor xxx and the two reviewers xxx and xxx greatly improved the manuscript.

References

- Abbasi, I.A., Hersi, O.S., & Al-Harthy, A. (2014). Late Cretaceous conglomerates of the Qalhah formation, north Oman. In: Rollinson, H.R., Searle, M.P., Abbasi, I.A., Al-Lazki, A.I., Al-Kindy, M.H. (Eds.), *Tectonic evolution of the Oman Mountains*. Geological Society, London, Special Publication, vol. 392(1), pp. 325-341, doi: 10.1144/SP392.17.
- Agard, P., Searle, M.P., Alsop, G., & Dubacq, B. (2010). Crustal stacking and expulsion tectonics during continental subduction: P-T deformation constraints from Oman. *Tectonics* 29, 1-19, doi: 10.1029/2010TC002669.
- Agard, P., Omrani, J., Jolivet, L., Whitechurch, H., Vrielynck, B., Spakman, W., Monié, P., Meyer, B., & Wortel, R. (2011). Zagros orogeny: a subduction-dominated process. *Geological Magazine* 148(5-6). 692-725.
- Al-Wardi, M., & Butler, R.W.H. (2007). Constrictional extensional tectonics in the northern Oman mountains, its role in culmination development and the exhumation of the subducted Arabian continental margin. In: Ries, A.C., Butler, R.W.H., Graham, R.H. (Eds.), *Deformation of the Continental Crust: The Legacy of Mike Coward*. Geological Society, London, Special Publications, vol. 272, pp. 187-202.
- Angelier, J. (1994). Fault slip analysis and paleostress reconstruction. In, P.L. Hancock (Ed.), *Continental Deformation*, pp. 53-100. Oxford, Pergamon Press.
- Augustin, N., Devey, C.W., van der Zwan, F.M., Feldens, P., Tominaga, M., Bantan, R.A., & Kwasnitschka, T. (2014). The rifting to spreading transition in the Red Sea. *Earth and Planetary Science Letters* 395, 217-239, doi: 10.1016/j.epsl.2014.03.047.
- Bailey, C.M., Hurtado, C., Scharf, A., & Mattern, F. (2019). Structural controls on listwaenite genesis in the Semail Ophiolite, Northern Oman. EGU 2019-5794, Vienna, Austria.
- Beauchamp, W.H., Ries, A.C., Coward, M.P., & Miles, J.A. (1995). Masirah Graben, Oman: A Hidden Cretaceous Rift Basin? *AAPG Bulletin* 79(6), 864-879.
- Beavington-Penney, S.J., Wright, V.P., & Racey, A. (2006). The Middle Eocene Seeb Formation of Oman: An Investigation of Acyclicity, Stratigraphic Completeness, and Accumulation Rates in Shallow Marine Carbonate Settings. *Journal of Sedimentary Research* 76(10), 1137-1161, doi: 10.2110/jsr.2006.109.
- Béchenec, F., Beurrier, M., Hutin, G., & Rabu, D. (1986). Geological map of Barka, sheet NF 40-3B, scale 1:100,000, Explanatory notes: Directorate General of Minerals, Oman Ministry of Petroleum and Minerals.
- Béchenec, F., Le Métour, J., Rabu, D., Bourdillon-de-Grissac, C., de Wever, P., Beurrier, M., & Villey, M. (1990). The Hawasina Nappes; Stratigraphy, paleogeography and structural evolution of a fragment of

the South-Tethyan passive continental margin. In: Robertson, A.H.F., Searle, M.P., Ries, A.C. (Eds.), *The Geology and Tectonics of the Oman Region*. Geological Society London Special Publication, vol. 49, pp. 213-223.

Béchenec, F., Roger, J., Le Métour, J., & Wyns, R. (1992). Geological map of Seeb, sheet NF 40-03, scale 1:250,000, with Explanatory Notes: Directorate General of Minerals, Oman Ministry of Petroleum and Minerals.

Blebschmidt, I., Dumitrica, P., Matter, A., Krystyn, L., & Peters, T. (2004). Stratigraphic architecture of the northern Oman continental margin – Mesozoic Hamrat Duru Group Hawasina Complex, Oman. *GeoArabia* 9(2), 81-132.

Blendinger, W., van Vliet, A.T., & Hughes Clarke, M.W. (1990). Updoming, rifting and continental margin development during the Late Paleozoic in northern Oman. In: Robertson, A.H.F., Searle, M.P., Ries, A.C. (Eds.), *The Geology and Tectonics of the Oman Region*. Geological Society of London, Special Publication, vol. 49, pp. 27-37.

Boote, D.R.D., Mou, D., & Waite, R.I. (1990). Structural evolution of the Suneinah Foreland, Central Oman Mountains. In: Robertson, A.H.F., Searle, M.P., Ries, A.C. (Eds.), *The Geology and Tectonics of the Oman Region*. Geological Society of London, Special Publication, vol. 49, pp. 397-418.

Breton, J.-P., Béchenec, F., Le Métour, J., Moen-Maurel, L., & Razin, P. (2004). Eoalpine (Cretaceous) evolution of the Oman Tethyan continental margin: insights from a structural field study in Jabal Akhdar (Oman Mountains). *GeoArabia* 9(2), 41-58.

Burg, J.P., Bernoulli, D., Smit, J., Dolati, A., & Bahroudi, A. (2008). A giant catastrophic mud-and-debris flow in the Miocene Makran. *Terra Nova* 20, 188-193, doi: 10.1111/j.1365-3221.2008.00804.x.

Callegari, I., Braaten, A., Scharf, A., Mattern, F., Holzbecher, E., Al Kharusi, A., & Al Hajri, A. (2020). Evidence of postobductional, brittle and transtensional deformation: the lineamentary Issmaiya Fault Zone – insights from kinematic analyses and remote sensing data interpretation (Semail Ophiolite near Ibra, Oman Mts., Sultanate of Oman). *EGU 2020-12472*, Vienna, Austria.

Carminati, E., Aldega, L., Smeraglia, L., Scharf, A., Mattern, F., Albert, R., & Gerdes, A. (2020). Tectonic Evolution of the Northern Oman Mountains, Parts of the Strait of Hormuz Syntaxis: New Structural and Paleothermal analyses and U-Pb Dating of Synkinematic Calcite. *Tectonics* 39, e2019TC005936, doi: 10.1029/2019TC005936.

Chauvet, F., Dumont, T., & Basile, C. (2009). Structures and timing of Permian rifting in the central Oman Mountains (Saih Hatat). *Tectonophysics* 475, 563-574, doi: 10.1016/j.tecto.2009.07.008.

Cohen, K.M., Finney, S.C., Gibbard, P.L., & Fan, J.-X. (2013) (updated 2016-04). The ICS International Chronostratigraphic Chart. *Episodes* 36, 199-204.

Coffield, D.Q. (1990). Structures associated with nappe emplacement and culmination collapse in the Central Oman Mountains. In: Robertson, A.H.F., Searle, M.P., Ries, A.C. (Eds.), *The Geology and Tectonics of the Oman Region*. Geological Society of London, Special Publication, vol. 49, pp. 447-458.

Corradetti, A., Spina, V., Tavani, S., Ringenbach, J.C., Sabbatino, M., Razin, P., Laurant, O., Bricchau, S., & Mazzoli, S. (2019). Late-stage tectonic evolution of the Al-Hajar Mountains, Oman: new constraints from Palaeogene sedimentary units and low-temperature thermochronometry. *Geological Magazine*, 1-14, doi: 10.1017/S0016756819001250.

DeMets, C., Gordon, R.G., & Argus, D.F. (2010). Geologically current plate motions. *Geophysical Journal International* 182, 1-80, doi: 10.1111/j.1365-246X.2009.04491.x.

Ermertz, A.M., Kázmér, M., Adolphs, S.K., Falkenroth, M., & Hoffmann, G. (2019). Geoarchaeological evidence for the decline of the Medieval City of Qalhat, Oman. *Open Quaternary* 5(8), 1-14, doi: 10.5334/oq.56.

- Fakhari, M.D., Axen, G.J., Horton, B.K., Hassanzadeh, J., & Amini, A. (2008). Revised age of proximal deposits in the Zagros Foreland Basin and implications for Cenozoic evolution of the high Zagros. *Tectonophysics* 451, 170-185, doi: 10.1016/j.tecto.2007.11.064.
- Filbrandt, J.B., Nolan, S.C., & Ries, A.C. (1990). Late Cretaceous and early Tertiary evolution of Jabal Ja'alan and adjacent areas, NE Oman. In: Robertson, A.H.F., Searle, M.P., Ries, A.C. (Eds.), *The Geology and Tectonics of the Oman Region*. Geological Society of London, Special Publication, vol. 49, pp. 697-714.
- Forbes, G.A., Jansen, H.S.M., & Schreurs, J. (2010). Lexicon of Oman subsurface stratigraphy. Reference guide to the stratigraphy of Oman's Hydrocarbon basins. *GeoArabia*, Special Publication 5 by Gulf Petro Link, p. 373.
- Fournier, M., Lepvrier, C., Razin, P., & Jolivet, L. (2006). Late Cretaceous to Paleogene Post-obduction extension and subsequent Neogene compression in the Oman Mountains. *GeoArabia* 11(4), 17-40.
- Fournier, M., Chamot-Rooke, N., Petit, C., Fabbri, O., Huchon, P., Maillot, B., & Lepvrier, C. (2008). In situ evidence for dextral active motion at the Arabia-India plate boundary. *Nature geoscience* 1, 54-58, doi: 10.1038/ngeo.2007.24.
- Fournier, M., Chamot-Rooke, N., Rodriguez, M., Huchon, P., Petit, C., Beslier, M.O., & Zaragosi, S. (2011). Owen fracture zone: The Arabia-India plate boundary unveiled. *Earth and Planetary Science Letters* 302, 247-252, doi: 10.1016/j.epsl.2010.12.027.
- Gaina, C., van Hinsbergen, D.J.J., & Spakman, W. (2015). Tectonic interactions between India and Arabia since the Jurassic reconstructed from marine geophysics, ophiolite geology, and seismic tomography. *Tectonics* 34(5), 875-906, doi: 10.1002/2014TC003780.
- Gavillot, Y., Axen, G.J., Stockli, D.F., Horton, B.K., & Fakhari, M.D. (2010). Timing of thrust activity in the high Zagros fold-thrust belt, Iran, from (U-Th)/He thermochronometry. *Tectonics* 29, TC4025, doi: 10.1029/2009TC002484.
- Ghebreab, W. (1998). Tectonics of the red Sea region reassessed. *Earth-Science Reviews* 45(1-2), 1-44, doi: 10.1016/S0012-8252(98)00036-1.
- Glennie, K.W., Boeuf, M.G.A., Hughes Clarke, M.W., Moody-Stuart, M., Pilaar, W.F.H., & Reinhardt, B.M. (1973). Late Cretaceous nappes in Oman Mountains and their geological evolution. *American Association of Petroleum Geologists Bulletin* 57, 5-27.
- Glennie, K.W., Boeuf, M.G.A., Hughes Clarke, M.W., Moody-Stuart, M., Pilaar, W., & Reinhardt, B.M. (1974). Geology of the Oman Mountains. *Koninklijk Nederlands Geologisch en Mijnbouwkundig Genootschap, Transactions* 31(1), p. 423.
- Gnos, R., & Peters, T. (2003). Mantle xenolith-bearing Maastrichtian to Tertiary alkaline magmatism in Oman. *Geochemistry, Geophysics, Geosystems* 4(9), doi: 10.1029/2001GC000229.
- Grobe, A., Virgo, S., von Hagke, C., Urai, J.L., & Littke, R. (2018). Multiphase structural evolution of a continental margin during obduction orogeny: Insights from the Jebel Akhdar Dome, Oman Mountains. *Tectonics* 37(3), 888-913, doi: 10.1002/2016TC004442.
- Grobe, A., von Hagke, C., Littke, R., Dunkl, I., Wübbeler, F., Muechez, P., & Urai, J.L. (2019). Tectono-thermal evolution of Oman's Mesozoic passive continental margin under the obducting Semail Ophiolite: a case study of Jebel Akhdar, Oman. *Solid Earth* 10, 149-175, doi: 10.5194/se-10-149-2019.
- Hanna, S.S. (1990). The Alpine deformation of the central Oman Mountains. In: Robertson, A.H.F., Searle, M.P., Ries, A.C. (Eds.), *The Geology and Tectonics of the Oman Region*. Geological Society of London, Special Publication, vol. 49, pp. 341-359.
- Hansman, R.J., & Ring, U. (2018). Jabal Hafit anticline (UAE and Oman) formed by décollement folding followed by trishear fault-propagation folding. *Journal of Structural Geology* 117, 168-185, doi:

10.1016/j.jsg.2018.09.014.

Hansman, R.J., Ring, U., Thomson, S.N., den Brock, B., & Stübner, K. (2017). Late Eocene uplift of the Al Hajar Mountains, Oman, supported by stratigraphic and low-temperature thermochronology. *Tectonics* 36(12), 3081-3109, doi: 10.1002/2017TC004672.

Hansman, R.J., Albert, R., Gerdes, A., & Ring, U. (2018). Absolute ages of multiple generations of brittle structures by U-Pb dating of calcite. *Geology* 46(3), 207-210, doi: 10.1130/G39822.1.

Hansman, R.J., Ring, U., Scharf, A., Glodny, J., & Wan, B. (2021). Structural architecture and Late Cretaceous exhumation history of the Saih Hataat Dome (Oman), a review based on existing data and semi-restorable cross-sections. *Earth-Science Review*, 103595, doi: 10.1016/j.earscrv.2021.103595.

Harding, T.P. (1974). Petroleum traps associated with wrench faults. *AAPG bulletin* 58(7), 1290-1304.

Heidbach, O., Reinecker, J., Tingay, M., Müller, B., Sperner, B., Fuchs, K., & Wenzel, F. (2007). Plate boundary forces are not enough: Second- and third-order stress patterns highlighted in the World Stress Map database. *Tectonics* 26, TC6014, doi: 10.1029/2007TC002133.

Hempton, M.R. (1987). Constraints on Arabian Plate motion and extensional history of the Red Sea. *Tectonics* 6(6), 687-705.

Hersi, O.S., & Al-Harathi, A. (2010). Lithofacies attributes of a Transgressive Carbonate System: The Middle Eocene Seeb Formation, Al Khoudh area, Muscat, Oman. *Sultan Qaboos University Journal for Science* 15, 41-54.

Hill, C.A., Polyak, V.J., Asmerom, Y., & Provencio, P.P. (2016). Constraints on a Late Cretaceous uplift, denudation, and incision of the Grand Canyon region, southwestern Colorado Plateau, USA, from U-Pb dating of a lacustrine limestone. *Tectonics* 35, 896-906, doi: 10.1002/2016TC004166.

Hoffmann, G., Schneider, B., Mechernich, S., Falkenroth, M., Dunai, T., & Preusser, F. (2020). Quaternary uplift along a passive continental margin (Oman, Indian Ocean). *Geomorphology* 350, 106870, doi: 10.1016/j.geomorph.2019.106870.

Immenhauser, A. (1996). Cretaceous sedimentary rocks on the Masirah Ophiolite (Sultanate of Oman); evidence for an unusual bathymetric history. *Journal of the Geological Society of London* 153, 539-551.

Jenness, J. (2014). *Polar plots and circular statistics: Extension for ArcGIS*. Jenness Enterprises.

Kajima, M., & Ishii, G. (2012a). Geological map of Al Ansab, sheet NF 40-3C4/C, scale 1:25,000, with Explanatory notes: Directorate General of Minerals, Oman Ministry of Commerce and Industry.

Kajima, M., Ishii, G., Otake, M., & Goto, M. (2012b). Geological map of Al Khuwayr, sheet NF 40-3C4/D, scale 1:25,000, with Explanatory notes: Directorate General of Minerals, Oman Ministry of Commerce and Industry.

Kajima, M., Ishii, G., & Goto, M. (2012c). Geological map of Ar Rusayl, sheet NF 40-3C3/C, scale 1:25,000, with Explanatory notes: Directorate General of Minerals, Oman Ministry of Commerce and Industry.

Le Métour, J., Villey, M., & de Gramont, X. (1986a). Geological map of Masqat, sheet NF 40-4A, scale 1:100,000, Explanatory notes: Directorate General of Minerals, Oman Ministry of Petroleum and Minerals.

Le Métour, J., Villey, M., & de Gramont, X. (1986b). Geological map of Quryat, sheet NF 40-4D, scale 1:100,000, Explanatory notes: Directorate General of Minerals, Oman Ministry of Petroleum and Minerals.

Leroy, S., Razin, P., Autin, J., Bache, F., d'Acremont, E., Watremez, L., Robinet, J., Baurion, C., Denèle, Y., Bellahsen, N., & Lucazeau, F. (2013). From rifting to oceanic spreading in the Gulf of Aden: A synthesis. In K. Al Hosni, F., Roure, R., Ellison, S. Lokier (Eds.), *Lithosphere Dynamics and Sedimentary Basins: The Arabian Plate and Analogues*, pp. 385-427. Berlin, Heidelberg: Springer Berlin Heidelberg, doi: 10.1007/978-3-642-30609-9_20.

Levell, B., Searle, M., White, A., Kedar, L., Droste, H., & van Steenwinkel, M. (2021). Geological and seismic evidence for the tectonic evolution of the NE Oman continental margin and Gulf of Oman. *Geosphere* 17, doi: 10.1130/GEO02376.1.

Mann, A., Hanna, S.S., & Nolan, S.C. (1990). The post-Campanian tectonic evolution of the Central Oman Mountains: Tertiary extension of the Eastern Arabian Margin. In: Robertson, A.H.F., Searle, M.P., Ries, A.C. (Eds.), *The Geology and Tectonics of the Oman Region*. Geological Society of London, Special Publication, vol. 49, pp. 285-305.

Mattern, F., & Bernecker, M. (2019). A shallow marine clinof orm system in limestones (Paleocene to Eocene Jafnayn Formation, Oman): geometry, microfacies, environment and processes. *Carbonates and Evaporites* 34, 101-113, doi: 10.1007/s13146-018-0444-z.

Mattern, F., & Scharf, A. (2018). Postobductional extension along and within the Frontal Range of the Eastern Oman Mountains. *Journal of Asian Earth Sciences* 154, 369-385, doi: 10.1016/j.jseae.2017.12.031.

Mattern, F., & Scharf, A. (2019). Transition from the Hajir Formation to the Muaydin Formation: a facies change coinciding with extensional, syndepositional faulting (Ediacaran, Jabal Akhdar, Central Oman Mountains). *Journal of African Earth Sciences* 152, 237-244, doi: 10.1016/j.jafrearsci.2019.02.016.

Mattern, F., Moraetis, D., Abbasi, I., Al-Shukaili, B., Scharf, A., Claereboudt, M., Looker, E., Al-Haddabi, N., & Pracejus, B. (2018a). Coastal dynamics of uplifted and emerged Late Pleistocene near-shore coral patch reefs at Fins (eastern coastal Oman, Gulf of Oman). *Journal of African Earth Sciences* 138, 192-200, doi: 10.1016/j.afrearsci.2017.11.018.

Mattern, F., Scharf, A., & Al-Amri, S.H.K. (2018b). East-west directed Cenozoic compression in the Muscat area (NE Oman): timing and causes. 10th Gulf Seismic Forum, seismology and Earthquake Studies in the Arabian Plate Region, 19th-22th March 2018, Muscat, Oman.

Mattern, F., Scharf, A., Al-Sarmi, M., Pracejus, B., Al-Hinaai, A., & Al-Mamari, A. (2018c). Compaction history of Upper Cretaceous shale and related tectonic framework, Arabian Plate, Eastern Oman Mountains. *Arabian Journal of Geosciences* 11(16), 444, doi: 10.1007/s12517-018-3781-2.

Mattern, F., Scharf, A., Pu-Jun, W., Callegari, I., Abbasi, I., Al-Wahaibi, S., Pracejus, B., & Scharf, K. (2020a). Deformation of the Cambro-Ordovician Amdeh Formation (members 1 and 2): characteristics, origins and stratigraphic significance (Wadi Amdeh, Saih Hatat Dome, Oman Mountains). *Geosciences* 10, 48, doi: 10.3390/geosciences10020048.

Mattern, F., Al-Sayigh, A., Farfour, M., Scharf, A., Al-Amri, S., & Al-Omairi, J. (2020b) Microfacies, Biostratigraphy, Depositional Environment, Seismic Refraction and Correlation of Coralline Limestones of the Barzaman Formation (Oligocene-Pliocene? Al-Khod, Muscat Area, Oman). *Sultan Qaboos University Journal for Science* 25(2), 85-99, doi: 10.24200/squjs.vol25iss2pp85-99.

Mattern, F., Scharf, A., Al-Sarmi, M., Al-Sayigh, A., Al-Maktoumi, M., Al-Omairi, N., & Al-Rawahi, T. (2021). Lithostratigraphy, microfacies and paleogeography of the shallow marine Middle Limestone Member of the Lower Eocene Rusayl Formation, Oman: relationship to the Early Eocene Climatic Optimum, sea-level changes and regional uplift. *Journal of African Earth Sciences* 184, 104312, doi: 10.1016/j.jafrearsci.2021.104312.

Matthews, K.J., Müller, R.D., Wessel, P., & Whittaker, J.M. (2011). The tectonic fabric of the ocean basins. *Journal of Geophysical Research*, doi: 10.1029/2011/JB008413.

Matthews, K.J., Maloney, K.T., Zahirovic, S., Williams, S.E., Seton, M., & Müller, R.D. (2016). Global plate boundary evolution and kinematics since the late Paleozoic. *Global and Planetary Change*, doi: 10.1016/j.gloplacha.2016.10.002.

McQuarrie, N., Stock, J.M., Verdel, C., & Wernicke, B.P. (2003). Cenozoic evolution of Neotethys and implications for the casues of plate motions. *Geophysical Research Letters* 30(20), 2036, doi:

10.1029/2003GL017992.

Miller, J.M., Gray, D.R., & Gregory, R.T. (2002). Geometry and significance of internal windows and regional isoclinal folds in northeast Saih Hatat, Sultanate of Oman. *Journal of Structural Geology* 24, 359-386, doi: 10.1016/S0191-8141(01)00061-X.

Moraetis, D., Mattern, F., Scharf, A., Frijia, G., Kusky, T.M., Yuan, Y., & Hussain, I.L. (2018). Neogene to Quaternary uplift history along the passive margin of the northeastern Arabian Peninsula eastern Hajar Mountains, Oman. *Quaternary Research* 90(2), 418-434, doi: 10.1017/qua.2018.51.

Moraetis, D., Scharf, A., Mattern, F., Pavlopoulos, K., & Foreman, S. (2020). Quaternary thrusting in the Central Oman Mountains – novel observations and causes: insights from OSL dating and kinematic fault analyses. *Geosciences* 10, 166, doi: 10.3390/geoscience10050166.

Mountain, G.S., & Prell, W.L. (1990). A multiphase plate tectonic history of the southeast continental margin of Oman. In: Robertson, A.H.F., Searle, M.P., Ries, A.C. (Eds.), *The Geology and Tectonics of the Oman Region*. Geological Society of London, Special Publication, vol. 49, pp. 725-743.

Mouthereau, F., Lacombe, O., & Vergés, J. (2012). Building the Zagros collisional Orogen: Timing, strain distribution and the dynamics of Arabia/Eurasia plate convergence. *Tectonophysics* 532-535, 27-60.

Müller, R.D., Seton, M., Zahirovic, S., Williams, S.E., Matthews, K.J., Wright, N.M., Shephard, G.E., Maloney, K.T., Barnett-Moore, N., Hosseinpour, M., Bower, D.J., & Cannon, J. (2016). Ocean Basin Evolution and Global-Scale Plate Reorganization Events Since Pangea Breakup. *Annual Review of Earth and Planetary Sciences* 44, pp. 107, doi: 10.1146/annurev-earth-060115-012211.

Nicolas, A., Boudier, F., Ildefonse, B., & Ball, E. (2000). Accretion of Oman and United Arab Emirates ophiolite – Discussion of a new structural map. *Marine Geophysical Researches* 21, 147-179.

Ninkabou, D., Agard, P., Nielsen, C., Smit, J., Gorini, C., Rodriguez, M., Haq, B., Chamot-Rooke, N., Weidle, C., & Ducassou, C. (2021). Structure of the Offshore Obducted Oman Margin: Emplacement of Semail Ophiolite and Role of Tectonic Inheritance. *Journal of Geophysical Research: Solid Earth* 126, e2020JB020187, doi: 10.1029/2020JB020187.

Nolan, S.C., Skelton, P.W., Clissold, B.P., & Smewing, J.D. (1990). Maastrichtian to Early Tertiary stratigraphy and paleogeography of the Central and Northern Oman Mountains: In: Robertson, A.H.F., Searle, M.P., Ries, A.C. (Eds.), *The Geology and Tectonics of the Oman Region*. Geological Society of London, Special Publication, vol. 49, pp. 307-325.

Nuriel, P., Weinberger, R., Kylander-clark, A.R.C., Hacker, B.R., & Craddock, J.P. (2017). The onset of the Dead Sea transform based on calcite age-strain analyses. *Geology* 45, 587-590.

Peters, T., Al Battashy, M., Bläsi, H., Hauser, M., Immenhauser, A., Moser, L., & Al Rajhi, A. (2001). Geological map of Sur and Al Ashkharah, sheets NF 40-8F and NF 40-12C, scale: 1:100,000, with Explanatory notes: Directorate General of Minerals, Oman Ministry of Commerce and Industry.

Peters, T., Blechschmidt, I., Krystyn, L., Dumitrica, P., Mercolli, I., El Amin, O., & Al Towaya, A. (2005). Geological map of Ibra with Explanatory notes, sheet NF 40-08A, scale 1:100,000. Directorate General of Minerals, Ministry of Commerce and Industry of Oman.

Petit, J.P. (1987). Criteria for the sense of movement on fault surfaces in brittle rocks. *Journal of Structural Geology* 9(5-6), 597-608, doi: 10.1016/0191-8141(87)90145-3.

Pickford, M. (2017). Late Cretaceous Lanistes (Mollusca, Gastropoda) from Al-Khodh, Oman. *Al Hajar* 23, 15-27.

Platt, J.P., Leggett, J.K., & Alam, S. (1988). Slip vectors and fault mechanics in the Makran accretionary wedge, Southwest Pakistan. *Journal of Geophysical Research* 93(4), 7955, doi: 10.1029/JB093iB07p07955.

Rabu, D., Béchenec, F., Beurrier, M., & Hutin, G. (1986). Geological map of Nakhl, sheet NF40-3E, scale: 1:100,000, with Explanatory Notes: Directorate General of Minerals, Oman Ministry of Petroleum and Minerals.

Ring, U., & Bolhar, R. (2020). Tilting, uplift, volcanism and disintegration of the Southern German block. *Tectonophysics* 228611, doi: 10.1016/j.tecto.2020.228611.

Rioux, M., Garber, J., Bauer, A., Bowring, S., Searle, M.P., Kelemen, P., & Hacker, B. (2016). Synchronous formation of the metamorphic sole and igneous crust of the Semail ophiolite: New constraints on the tectonic evolution during ophiolite formation from high-precision U-Pb zircon geochronology. *Earth and Planetary Science Letters* 451, 185-195, doi: 10.1016/j.epsl.2016.06.051.

Roberts, N. M., Rasbury, E. T., Parrish, R. R., Smith, C. J., Horstwood, M. S., & Condon, D. J. (2017). A calcite reference material for LA-ICP-MS U-Pb geochronology. *Geochemistry, Geophysics, Geosystems*, 18(7), 2807-2814.

Roberts, N.M.W., Drost, K., Horstwood, M.S.A., Condon, D.J., Chew, D., Drake, H., Milodowski, A.E., McLean, N.M., Smye, A.J., Walker, R.J., Haslam, R., Hodson, K., Imber, J., Beaudoin, N., & Lee, J.K. (2020). Laser ablation inductively coupled plasma mass spectrometry (LA-ICP-MS) U-Pb carbonate geochronology: strategies, progress, and limitations. *Geochronology* 2, 33-61, doi: 10.5194/gchron-2-33-2020.

Rodgers, D.W., & Gunatilaka, A. (2002). Bajada formation by monsoonal erosion of a subaerial forebulge, Sultanate of Oman. *Sedimentary Geology* 154(3-4), 127-146.

Rodriguez, M., Chamot-Rooke, N., Huchon, P., Fournier, M., & Delescluse, M. (2014). The Owen ridge uplift in the Arabian Sea: Implications for the sedimentary record of Indian monsoon in late Miocene. *Earth and Planetary Science Letters* 394, 1-12, doi: 10.1016/j.epsl.2014.03.011.

Rodriguez, M., Huchon, P., Chamot-Rooke, N., Fournier, M., Delescluse, M., & François, T. (2016). Tracking the paleogene India-Arabia plate boundary. *Marine and Petroleum Geology* 72, 336-358, doi: 10.1016/j.marpetgeo.2016.02.019.

Roger, J. Béchenec, F., Janjou, D., Le Métour, J., Wyns, R., & Beurrier, M. (1991). Geological map of Ja'alan, sheet NF 40-08E, scale:100,000, with Explanatory Notes: Directorate General of Minerals, Oman Ministry of Petroleum and Minerals.

Romine et al. (2004). North Oman Haima-Huqf Tectonostratigraphic Study, SRK Confidential Report to PDO, July 2004.

Saddiqi, O., Michard, A., Goffé, B., Poupeau, G., & Oberhänsli, R. (2006). Fission-track thermochronology of the Oman Mountains continental widows, and current problems of tectonic interpretation. *Bulletin de la Société Géologique de France* 177(3), 127-134, doi: 10.2113/gssgfbull.177.3.127.

Scharf, A., Mattern, F., & Al Sadi, S. (2016). Kinematics of Post-obduction Deformation of the Tertiary Ridge at Al-Khod Village (Muscat Area, Oman). *Sultan Qaboos University Journal for Science* 21(1), 26-40.

Scharf, A., Mattern, F., Moraetis, D., Callegari, I., & Weidle, C. (2019a). Postobductional Kinematic Evolution and Geomorphology of a Major Regional Structure – The Semail Gap Fault Zone (Oman Mountains). *Tectonics* 38(8), 2756-2778, doi: 10.1029/2019TC005588.

Scharf, A., Mattern, F., & Pracejus, B. (2019b). Two new microscopic ductile kinematic indicators from the Oman Mountains. *Journal of Structural Geology* 119, 107-117, doi: 10.1016/j.jsg.2018.12.006.

Scharf, A., Sudo, M., Pracejus, B., Mattern, F., Callegari, I., Bauer, W., & Scharf, K. (2020b). Late Lutetian (Eocene) mafic intrusion into shallow marine platform deposits north of the Oman Mountains (Rusayl Embayment) and its tectonic significance. *Journal of African Earth Sciences* 170, 103941, doi: 10.1016/j.jafrearsci.2020.103941.

- Scharf, A., Mattern, F., Al-Wardi, M., Frijia, G., Moraetis, D., Pracejus, B., Bauer, W., & Callegari, I. (2021a). Tectonostratigraphy of the eastern part of the Oman Mountains. *Geological Society, London, Memoirs*, M54(1), 11-47, doi: 10.1144/M54.2.
- Scharf, A., Mattern, F., Al-Wardi, M., Frijia, G., Moraetis, D., Pracejus, B., Bauer, W., & Callegari, I. (2021b). Tectonic evolution of the Oman Mountains. *Geological Society, London, Memoirs*, M54(1), 67-103, doi: 10.1144/M54.5.
- Scharf, A., Mattern, F., Al-Wardi, M., Frijia, G., Moraetis, D., Pracejus, B., Bauer, W., & Callegari, I. (2021c). Appendices to: The geology and tectonics of the Jabal Akhdar and Saih Hatat domes, Oman Mountains. *Geological Society, London, Memoirs*, M54(1), 113-115, doi: 10.1144/M54.7.
- Schlüter, H.U., Prexl, A., Gaedicke, C., Roeser, H., Reichert, C., Meyer, H., & von Daniels, C. (2002). The Makran accretionary wedge: Sediment thicknesses and ages and the origin of mud volcanoes. *Marine Geology* 185(3-4), 219-232, doi: 10.1016/S0025-3227(02)00192-5.
- Schreurs, G., & Immenhauser, A. (1999). West-northwest directed obduction of the Batain Group on the eastern Oman continental margin at the Cretaceous-Tertiary boundary. *Tectonics* 18(1), 148-160.
- Searle, M.P. (1988). Structure of the Musandam culmination (Sultanate of Oman and United Arab Emirates) and the Straits of Hormuz syntaxis. *Journal of the Geological Society, London* 145, 831-845.
- Searle, M.P. (2007). Structural geometry, style and timing of deformation in the Hawasina Window, Al Jabal al Akhdar and Saih Hatat culminations, Oman Mountains. *GeoArabia* 12(2), 99-130.
- Searle, M.P., James, N.P., Calon, T.J., & Smewing, J.D. (1983). Sedimentological and structural evolution of the Arabian continental margin in the Musandam mountains and Dibba zone, United Arab Emirates. *Geological Society of America Bulletin* 94, 1381-1400.
- Searle, M.P., Cherry, A.G., Ali, M.Y., & Cooper, D.J.W. (2014). Tectonics of the Musandam Peninsula and northern Oman Mountains: From ophiolite obduction to continental collision. *GeoArabia* 19(2), 135-174.
- Searle, M.P. (2019). *Geology of the Oman Mountains, Eastern Arabia*. Springer, p. 478.
- Shackleton, R.M., Ries, A.C., Bird, P.R., Filbrandt, J.B., Lee, C.W., & Cunningham, C.C. (1990). The Batain mélange of NE Oman. In: Robertson, A.H.F., Searle, M.P., Ries, A.C. (Eds.), *The Geology and Tectonics of the Oman Region*. Geological Society of London, Special Publication, vol. 49, pp. 673-696.
- Stanger, G. (1985). Silicified serpentinite in the Semail nappe of Oman. *Lithos* 18, 13-22.
- Vermeesch, P. (2018). IsoplotR: A free and open toolbox for geochronology. *Geoscience Frontiers* 9(5), 1479-1493, doi: 10.1016/j.gsf.2018.04.001.
- Villey, M., de Gramont, X., & Le Métour, J. (1986a). Geological map of Seeb, sheet NF 40-3C, scale 1:100,000, with Explanatory notes: Directorate General of Minerals, Oman Ministry of Petroleum and Minerals.
- Villey, M., Le Métour, J., & de Gramont, X. (1986b). Geological map of Fanjah, sheet NF 40-3F, scale 1:100,000, with Explanatory notes: Directorate General of Minerals, Oman Ministry of Petroleum and Minerals.
- Weidle, C., Wiesenberg, L., Scharf, A., Agard, P., El-shatkawy, A., Krüger, F., & Meier, T. (2021). Architecture of the crust and lithosphere beneath the Semail Ophiolite from ambient noise tomography and Receiver Functions: insights on the tectonic evolution of eastern Arabia. *vEGU 2021-8321*, Vienna, Austria.
- Woodhead, J., & Petrus, J. (2019). Exploring the advantages and limitations of in situ U-Pb carbonate geochronology using speleothems. *Geochronology*, 1(1), 69-84.
- Woodhead, J., Reisz, R., Fox, D., Drysdale, R., Hellstrom, J., Maas, R., Cheng, H., & Edwards, R.L. (2010). Speleothem climate records from deep time? Exploring the potential with an example from the Permian. *Geology* 38, 455-458.

Wyns, R., Béchenec, F., Le Métour, J., & Roger, J. (1992). Geological map of Tiwi, sheet NF40-8B, scale 1:100,000, with Explanatory notes: Directorate General of Minerals, Oman Ministry of Petroleum and Minerals.

Zoback, M.L., & Zoback, M.D. (2007). Lithosphere stress and Deformation. In A. Watts, G. Schubert (Eds.), *Earthquake Seismology – Treatise on Geophysics*, 6, pp. 253-274, Amsterdam, Elsevier.

Oligocene/early Miocene major E/W-shortening and NW-oriented sinistral slip with associated wrench-fault assemblage in the Oman Mountains related to oblique Arabia-India convergence

Andreas Scharf^a, Frank Mattern^b, Robert Bolhar^c, Ivan Callegari^d, Paul Mattern^e, Uwe Ring^f

a Department of Earth Sciences, College of Science, Sultan Qaboos University, PC 123, Al-Khod, Muscat, Sultanate of Oman

b School of Geosciences, University of the Witwatersrand, Braamfontein, 2001 South Africa

c Department of Applied Geosciences, German University of Technology in Oman, PC 130, Halban, Sultanate of Oman

d Institute of Geological Sciences, Freie Universität Berlin, 12249 Berlin, Germany

e Department of Geological Sciences, Stockholm University, 10691 Stockholm, Sweden

Corresponding author: Andreas Scharf

E-mail: scharfa@squ.edu.om

Abstract

Field survey, satellite image interpretation, geological map interpretation, literature review, GPlates reconstruction and LA-ICP-MS U-Pb dating of synkinematic calcites demonstrate that ~E/W-shortening in eastern Oman was significant and related to oblique convergence of Arabia and India from 32.5 to 20 Ma. Approximately N/S-oriented compressive structures, WNW to NNW-striking sinistral faults and ~E/W-oriented normal faults characterize a major shear zone in the eastern Oman Mountains (Hajar Shear Zone, HSZ) and its wrench-fault assemblage within an area spanning ~250 km x ~50 km. More than 10,000 mostly NW-striking lineaments as deduced from satellite image interpretation and numerous faults/folds indicate that strain of the HSZ is widely distributed but concentrated along WNW to NNW-striking major faults/fault zones at the SW margin of the Saih Hatat Dome. These faults/fault zones represent reactivated basement faults. GPlates reconstructions reveal that N-drifting India rotated 8° counter-clockwise with respect to fixed Arabia from 32.5 to 20 Ma, leading to ~100-135 km E/W-convergence between both plates (minimum value). This convergence created the sinistral HSZ with a displacement of a few to several tens of kilometers. Independently from the GPlates time constraints, two U-Pb ages of synkinematic calcites, crystallized along faults during HSZ movement, yield compatible ages of 30.08 ± 0.47 and 22.31 ± 2.15 Ma (2 standard error). E/W-shortening also affected the northern Oman Mountains, creating the ~N/S-oriented Hagab Thrust in the Musandam Peninsula and the Jabal Hafit Anticline.

Plain Language Summary

Eastern Arabia was thrust by the well-known Semail Ophiolite and related deep-sea sedimentary rocks during the Late Cretaceous. Convergence was directed towards the SSW. Ongoing ~N/S shortening between Arabia and Eurasia resulted in respective deformation within the Oman Mountains. However, field evidence indicates that ~E/W-shortening affected the Oman Mountains, too. Detailed and comprehensive field survey, literature review, satellite image interpretation, map interpretation, GPlates reconstruction and absolute U-Pb dating of carbonates documents that E/W-shortening was significant in the Oman Mountains. E/W-shortening of 100-135 km was related to the counter-clockwise rotation of India with respect to Arabia at 32.5 to 20 Ma. In response to this shortening, a NW-striking sinistral shear zone with wrench-fault assemblage formed in the eastern Oman Mountains (i.e., N/S-compressive structures, E/W-extensional structures, WNW-striking sinistral Riedel faults, and SW-striking dextral anti-Riedel faults). This shear zone is the Hajar Shear Zone, which spans an area of 250 km by 50 km. Presumably NW-striking deeply rooted pre-existing faults facilitate shearing along the Hajar Shear Zone. E/W-shortening also affected the northern Oman Mountains and is responsible for deformation at the Hagab Thrust in Musandam and the Jabal Hafit Anticline at the Oman/UAE border.

Keywords

Post-obductional E/W-shortening; wrench-fault assemblage; reactivation of basement faults; strike-slip tectonics

1. Introduction

During the Late Cretaceous, northeastern Oman was overthrust from the NE by the iconic Semail Ophiolite, including tectonically underlying nappes of Neo-Tethyan sedimentary rocks (e.g., Glennie et al., 1974). N/S-shortening was recorded in the Oman Mountains during the Cenozoic due to the Arabia-Eurasia convergence (e.g., Fournier et al., 2006; Hansman et al., 2017; Levell et al., 2021). In addition, the Oman Mountains, especially their southeastern part, underwent post-mid-Eocene ~E/W-shortening (e.g., Mann et al., 1990; Wyns et al., 1992; Fournier et al., 2006). This study focuses on timing and cause of this shortening.

Numerous N/S-striking post-mid-Eocene compressional structures of the eastern Oman Mountains are documented in maps and other publications (Table 1). However, these structures have never been examined in detail with respect to a common genetic context. Furthermore, major ~N/S-striking compressional structures of Oligocene to early-mid-Miocene age also occur on the western flank of the northern Oman Mountains (prominent ~N/S-oriented Hagab Thrust in the Musandam Peninsula and the NNW/SSE-trending Jabal Hafit Anticline; Fig. 1; Table 1). Besides ~N/S-oriented compressional features, abundant relevant post-mid-Eocene sinistral ~NW-striking faults are common in the eastern Oman Mountains, too.

At a local scale, Mann et al. (1990) recognized open N-trending folds in the Rusayl Embayment (Fig. 1), affecting mid-Eocene rocks. They related these folds to exhumation and gravitational collapse of the nearby Saih Hatat and Jabal Akhdar domes (Fig. 1), causing extensional transport to the NW from Saih Hatat Dome and to the NE from the Jabal Akhdar Dome. The converging rock masses produced N-trending folds. For the Rusayl Embayment, this would be a suitable geometric explanation. However, similarly aged N-trending compressive structures also exist beyond the Rusayl Embayment (i.e., Hagab Thrust, Jabal Hafit, Qalhat Fault; Fig. 1), where the formation of such structures must have a different cause.

At a large regional scale, Fournier et al. (2006) identified two compressional events in the Oman Mountains, which started during the late Oligocene or early Miocene with E/W to NE/SW-directed shortening (Fig. 2). They did not identify the actual causes of the deformation but pointed out that the origin of E/W to NE/SW-shortening is “not entirely clear and could result from the interaction between the Arabian and Indian plates”. Gaina et al. (2015) suggested minor E/W-shortening between Arabia and India from 40 Ma to the present (their Fig. 7). The strike of NW-striking faults varies in the eastern Oman Mountains, ranging from WNW to NNW. For simplification, we will refer to them as “NW-striking”. Such faults are known from the Rusayl Embayment in the NW, the southern margin of the Saih Hatat Dome, the Salma Plateau, the inverted Abat Basin and the Jabal Ja’alan area in the SE (Figs. 2 and 3; Table 1).

Table 1. Documented N/S to NW/SE-oriented post-obductional compressive structures and sinistral NW-striking faults of the Oman Mountains with focus on the eastern Oman Mountains. Listed in appearance from the NW (Musandam Peninsula) to the SE (Jabal Ja’alan/Batain area).

	N/S to NW/SE compressive structures	Age	Reference
1	Hagab Thrust	Oligocene to early Miocene	Searle et al., 2014
2	Jabal Hafit Anticline	Late Oligocene to early-middle Miocene	Hansman & Ring,
3	Suneinah area	Late Oligocene to Middle Miocene?	Boote et al., 1990; Fournier et al., 2006
4	Rusayl Embayment	Post-mid-Eocene	Villey et al., 1986a Fournier et al., 2006 Kajima et al., 2012 Scharf et al., 2016
5	Rusayl Embayment-offshore Sea of Oman	Late Eocene	Levell et al., 2021
6	Jabal Nakhl	Cenozoic	Rabu et al., 1986
7	Muscat area	Post-mid-Eocene?	Fournier et al., 2006 Searle et al., 2019 Hansman et al., 2006
8	Fanja area	Cenozoic	Villey et al., 1986b

	N/S to NW/SE compressive structures	Age	Reference
9	Saih Hatat Dome	Cenozoic	Coffield (1990)
10	Eastern Saih Hatat	Cenozoic	Le Métour et al., 1991
11	Qalhat Fault and nearby other faults	Post-mid-Eocene, Miocene	Miller et al., 2002 Wyns et al., 2021
12	Inversion of Abat Basin	Miocene	Fournier et al., 2002 Wyns et al., 1992
13	Near Jabal Ja'alan	Post-mid-Eocene	Fournier et al., 2002 Roger et al., 1991
14	Jabal Ja'alan	Post-mid-Eocene	Filbrandt et al., 1991
	NW-striking sinistral faults	Age	Reference
1	Rusayl Embayment (transpressive)	Post-mid-Eocene	Scharf et al., 2016
2	Rusayl Embayment (transtensional)	Post-mid-Eocene	Mattern et al., 2016
3	Wadi Mansah Fault Zone (transtensional)	Post-mid-Eocene	Bailey et al., 2019 Scharf et al., 2019a
4	Wadi Amdeh Fault	Unknown	Mattern et al., 2020
5	Issmaiya Fault Zone (transtensional)	Post-mid-Eocene	Callegari et al., 2019
6	Coastal Parallel Shear Zone (transpressional)	Post-mid-Eocene	Moraetis et al., 2019
7	Ja'alan Fault (transpressional)	Post-mid-Eocene	Filbrandt et al., 1991 Roger et al., 1991

It is surprising that the above-mentioned structures have never been scrutinized in detail in a mutual causal context. Likewise, some ~N/S-oriented compressive structures and ~NW-oriented sinistral faults are documented and were mapped in detail or occur along prominent roadcuts but have been largely neglected by geoscientific attention. We shed light on these known structures, which extend across the entire Oman Mountains (~700 km in length; Fig. 1).

This study aims to review previously documented structures and combine available knowledge (Table 1) with other mainly ~N/S-compressional and sinistral NW-striking structures in the field (Table 2) between the eastern Batinah Coastal Plain in the west to the Batain area in the East (Figs. 1-3). A focus will be placed on whether these structures are (1) of the same age, (2) belong to the same deformation plan, (3) can be linked with structures in the northern Oman Mountains, (4) evaluate possible geodynamic causes, including unrecognized plate tectonic process. To achieve above goals, existing literature was reviewed, existing geological maps were (re)interpreted, a comprehensive satellite image analysis and extensive field mapping was carried out, LA-ICP-MS U-Pb dating of synkinematic calcites was conducted, and plate configurations were reconstructed using the GPlates software.

2. Geological setting

Eastern Arabia was affected by the Late Paleozoic Pangean Neo-Tethys rifting, forming ~NW-striking extensional basement faults (e.g., Béchenec et al., 1990;

Blendinger et al., 1990; Chauvet et al., 2009). Subsequent to rifting, Arabia remained largely a passive margin during the Permian to mid-Cretaceous (e.g., Glennie et al., 1974; Searle, 2007). This resulted in deposition of mostly shallow-marine, shelfal sedimentary rocks on the Arabian platform (Hajar Supergroup; e.g., Glennie et al., 1973, 1974; Searle, 2007). These rocks were overthrust by Neo-Tethys-derived allochthonous Hawasina-Basin and trench-facies rocks from the NE (~1-2 km in thickness) and the Semail Ophiolite during the Late Cretaceous (~10-15 km in thickness; e.g., Glennie et al., 1973, 1974; Béchenec et al., 1992; Nicolas et al., 2000; Blechschmidt et al., 2004; Searle, 2007), forming the Oman Mountains. At the base of the ophiolite, a metamorphic sole formed coeval with the formation of the ophiolite (Rioux et al., 2016).

Post-obductional successions in the Muscat-Seeb area (Figs. 3 and 4) consist of the <860-m-thick late Campanian to Maastrichtian Al-Khod (or Qahlah) Formation, containing alternating fluvial, coastal and deltaic shales, sandstones and conglomerates (e.g., Nolan et al., 1990; Abbasi et al., 2014; Pickford, 2017). The Al-Khod Formation is unconformably overlain by the 250-to-300-m-thick late Paleocene to early Eocene shallow-marine limestone of the Jafanyn Formation (e.g., Nolan et al., 1990; Mattern and Bernecker, 2019). The Jafanyn Formation is conformably overlain by the ~150-m-thick Rusayl Formation, consisting of marl, shallow marine limestone and sandstone of lower Eocene age (e.g., Nolan et al., 1990; Mattern et al., 2021). The Rusayl Formation is conformably topped by the Seeb Formation. The latter measures ~600 m in thickness, consists of middle to upper Eocene shallow-marine limestone (e.g., Nolan et al., 1990; Hersi & Al-Harthy, 2010). The Oligocene MAM or Ma'ahm Beds Formation, consisting of reefal limestone, rests unconformably on the Seeb Formation (Hersi and Al-Harthy, 2010). The thickness of this formation is not known, owing to the poor exposure but assumed by us to measure ~100 m. The latest Oligocene to probably Pliocene ~170-m-thick Barzaman Formation rests stratigraphically on top of the MAM Reefs Formation (Mattern et al., 2020b). The lithology of this formation is highly variable, ranging from conglomerates to sand- and claystones and limestones reflecting terrestrial and marine deposition, intense weathering and erosion of the Oman Mountains during arid to pluvial episodes (Mattern et al., 2020b). Further details on the geology and tectonics of the eastern Oman Mountains are provided in Scharf et al. (2021a, 2021b).

Immediately after and/or slightly coeval with the emplacement of the ophiolite, major exhumation and top-to-the-NE shearing occurred in the Saih Hatat Dome, and some gentle exhumation with top-to-the NE shearing in the Jabal Akhdar Dome (e.g., Nolan et al., 1990; Breton et al., 2004; Fournier et al., 2006; Saddiqi et al., 2006; Al-Wardi and Butler, 2007; Searle, 2007; Agard et al., 2010; Hansman et al., 2017, 2021; Grobe et al., 2018, 2019; Scharf et al., 2019b; Figs. 1 and 4). Further convergence of Arabia and Eurasia led to major doming of the Jabal Akhdar and some mild doming/surface uplift in the Saih Hatat during the late Eocene to Oligocene (~43-30 Ma; e.g., Hansman et al., 2017, 2018; Grobe et al., 2018, 2019; Corradetti et al., 2019). Convergence was NE/SW-directed (e.g., Fournier et al., 2006; Fig. 5).

Extensional tectonics associated with doming at the flanks resulted from gravitational collapse (e.g., Hanna, 1990; Mann et al., 1990; Mattern & Scharf, 2018; Scharf et al., 2019a). Extension at the northern margin of the two domes was facilitated along the Frontal Range Fault (Mattern & Scharf, 2018; Figs. 2-4). The area between the northern Jabal Akhdar and Saih Hatat domes in the Muscat-Seeb area was deformed during extension (Rusayl Embayment; Fig. 3). Extension in the Rusayl Embayment was NE/SW-directed during the latest Cretaceous to early Eocene (Tectonic Stage 1) and NE/SW and NW/SE-directed (Tectonic Stage 2A and 2B) during the late Lutetian to possibly Miocene (Fournier et al., 2006; Scharf et al., 2020b; Figs. 4 and 5).

The geology and tectonics of the Batain area differs from that of the Oman Mountains. The Batain area is characterized by mostly deep-sea sediments derived from the Batain Basin whose fill was thrust to the WNW onto Arabia during the course of the obduction of the Masirah Ophiolite at the Cretaceous/Cenozoic boundary (e.g., Mountain & Prell, 1990; Shackleton & Ries, 1990; Schreurs & Immenhauser, 1999; Fig. 1). Emplacement of the Masirah Ophiolite and Batain nappes followed deposition of the upper Maastrichtian flysch-type Fayah Formation on the oceanic lithosphere of the Batain Basin (Immenhauser, 1996).

After the emplacement of the Masirah Ophiolite, the Batain area underwent extensional and compressional deformation (Schreurs & Immenhauser, 1999). The earlier extension is characterized by NNE-SSW and E/W-orientated conjugated extensional faults within Cenozoic sedimentary rocks (Fig. 5). Extension is probably linked to Cenozoic reactivation of the Cretaceous Masirah Graben, which is located beneath the Batain area (Beauchamp et al., 1995; Fig. 1). Deformation in the Batain area may correlate with extension in the Gulf of Aden starting during the late Eocene (e.g., Hempton, 1987). Basanite/alkaline intrusions in the Batain area of late Eocene age may be associated with this extension (e.g., Peters et al., 2001).

Extension was followed by Miocene-Pliocene compression, which affected late Paleocene to early Miocene rocks (Schreurs & Immenhauser, 1999). A ~NE/SW to ~E/W-oriented shortening interval produced NW/SE to N/S-oriented open folds (Roger et al., 1991). The Miocene Tahwah and Sur formations are intensely folded near the Qalhat Fault (Wyns et al., 1992). In the footwall of the Qalhat Fault, the uppermost beds of the Miocene Sur and Salmiyah formations cut across lower beds of the same formations, forming an angular unconformity (Wyns et al., 1992). The Miocene Salmiyah Formation is folded within an open N/S-trending syncline (Wyns et al., 1992).

Uplift and inversion in the Jabal Ja'alan area is post-mid-Eocene in age (Fournier et al., 2006). Uplift is associated with N/S-trending asymmetric anticlines and occurred during E/W-compression (Filbrandt et al., 1990). All these field observations indicate that the area near the Qalhat Fault underwent ~E/W-shortening from the Miocene to the present.

The transition between the Oman Mountains and the Batain area is broadly localized along the Qalhat Fault (Filbrandt et al., 1990; Figs. 1, 2). This major ~N/S-striking fault has a long-lasting history and may have originated during Pan-African terrane accretion, similar to the Semail Gap Fault Zone at the eastern margin of the Jabal Akhdar Dome (Romine et al., 2004; Scharf et al., 2019a; Mattern & Scharf, 2019; Weidle et al., 2021; Fig. 2). During the Phanerozoic, the Qalhat Fault was likely reactivated several times in different ways (Fournier et al., 2006). During the early Cenozoic, the transtensional Qalhat Fault bounded the Abat Basin and the future Salma Plateau to the West, with the Salma Plateau being uplifted the Abat Basin inverted during the Miocene (e.g., Wyns et al., 1992; Fournier et al., 2006). Details on the stratigraphy of the Abat Basin and the Salma Plateau are provided in Fournier et al. (2006) and Figure 4. The rocks west of the Qalhat Fault (Tiwi Platform or Salma Plateau) mostly consist of late Paleocene to mid-Eocene shallow-marine limestone, now uplifted to ~2000 m of elevation. This area is still uplifting, as indicated by a historical earthquake at Qalhat and uplifted marine terraces (e.g., Wyns et al., 1992; Fournier et al., 2006; Mattern et al., 2018a; Moraetis et al., 2018; Ermertz et al., 2020; Hoffmann et al., 2020). In contrast, no or only little Quaternary tectonic activity has been reported from the Central Oman Mountains (Scharf et al., 2019a; Moraetis et al., 2020). Mid-Eocene to Oligocene shallow-marine rocks east of the Qalhat Fault are not currently being uplifted and represent the footwall of the Qalhat Fault (Wyns et al., 1992).

In the Northern Oman Mountains, the Oligocene to early Miocene Hagab Thrust is a prominent N/S-striking compressional feature, interpreted to be associated with the Arabia/Eurasia convergence (Searle et al., 2014), although the thrust is highly obliquely oriented relative to the WNW-ESE-striking convergence zone. Further to the South, at the Oman/UAE border, the sizable NNW/SSE-oriented anticline of Jabal Hafit occurs (Fig. 1). This anticline grew during the late Oligocene to early-middle Miocene and is related to WSW-directed shortening (Hansman & Ring, 2018).

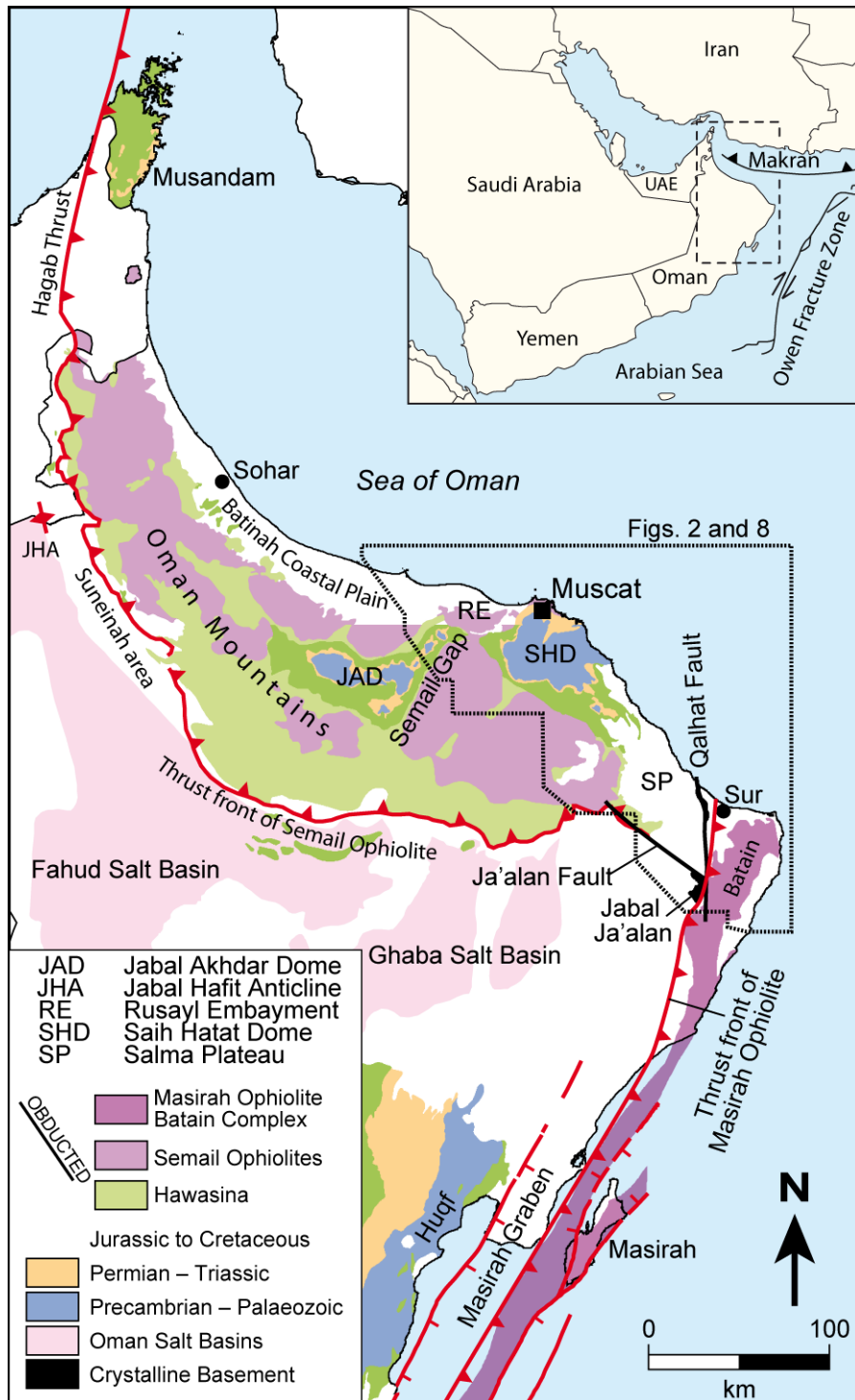


Figure 1. Geological map of the Oman Mountains after Schreurs and Immenhauser (1999) and Forbes et al. (2010). Black, dotted line indicates the outline of Figures 2 and 31. Overview image shows the larger study area with the Makran Subduction Zone and the Owen Fracture Zone, the present-day plate boundary between Arabia and India (Rodriguez et al. (2014).

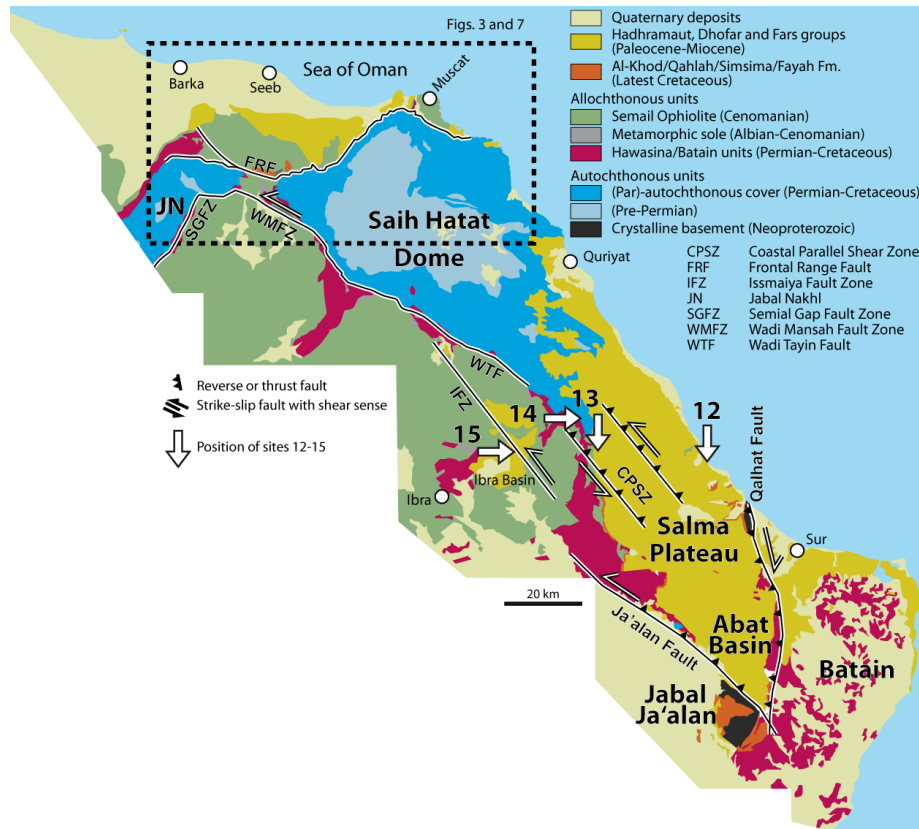


Figure 2. Geological map of the greater Saih Hatat to Batain area, simplified after Béchenec et al. (1986), Le Métour et al. (1986a, 1986b), Rabu et al. (1986), Villey et al. (1986a, 1986b), Roger et al. (1991), Wyns et al. (1992) and Peters et al. (2001, 2005). Box with black, dotted line outlines Figure 3. The Jabal Nakhl (JN) is the northern part of the Jabal Akhdar Dome.

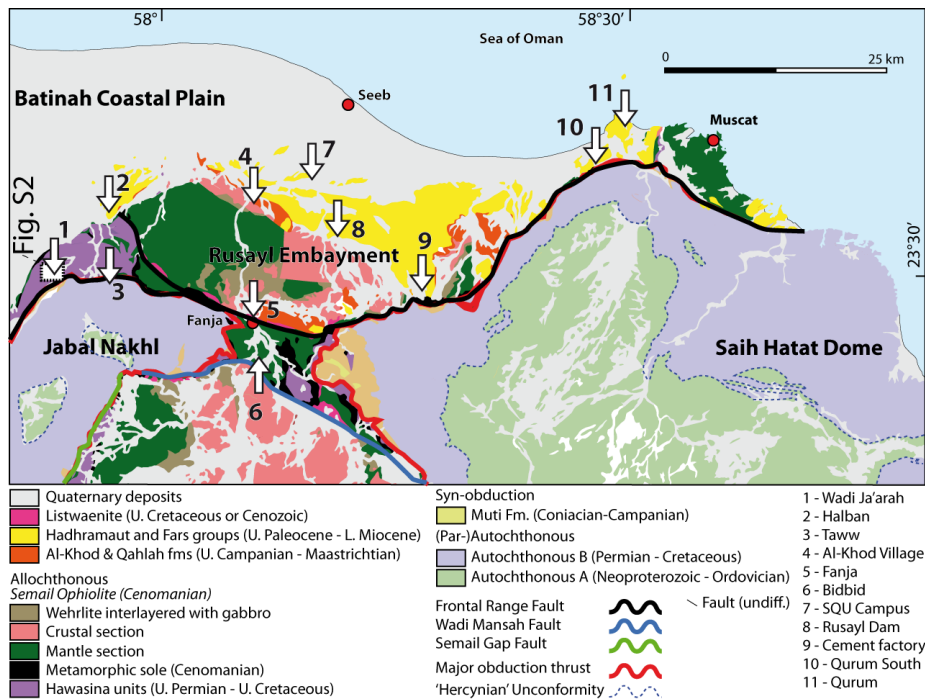


Figure 3. Geological map of the Muscat-Seeb area after Scharf et al. (2021c). Numbers 1-11 correspond to the sample sites of the structural measurements (Table 2; Supplementary Material S2).

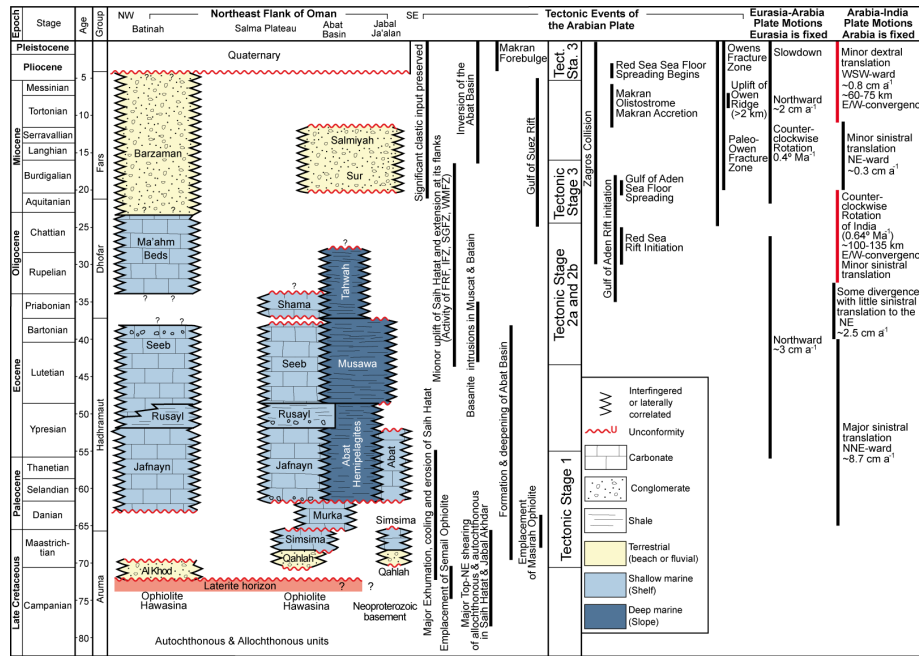


Figure 4. Simplified stratigraphic column of the post-obductional formations from the SE Batinah Coastal Plain to Jabal Ja'alan/Batain area, modified after Hansman et al. (2017) and Ninkabou et al. (2021). Stratigraphic column after Nolan et al. (1990), Fournier et al. (2006) and Mattern et al. (2020b). Age of major top-NE shearing (Grobe et al., 2018), emplacement of Semail Ophiolite (Searle, 2007), major exhumation and cooling of Saih Hatat (Hansman et al., 2017, 2021), minor uplift and extension of flank of Saih Hatat (Hansman et al., 2017; Scharf et al., 2020; FRF – Frontal Range Fault; IFZ – Issmaiyah Fault Zone; SGFZ – Semail Gap Fault Zone; WMFZ – Wadi Mansah Fault Zone), formation and deepening of Abat Basin (Fournier et al., 2006), Masirah Ophiolite (Schreurs & Immenhauser, 1999), Basinite intrusions (Gnos & Peters, 2003; Scharf et al., 2020), Tectonic stages 1-3 (Fournier et al., 2006; Fig. 2), Gulf of Aden (Leroy et al., 2013), Zagros collision (Fakhari et al., 2008; Gavillot et al., 2010; Agard et al., 2011; Mouthereau et al., 2012), Makran subduction and olistostrome (Platt et al., 1988; Schlüter et al., 2002; Burg et al., 2008), Owen Fracture Zone (Fournier et al., 2011; Rodriguez et al., 2014), Red Sea (Ghebream, 1998; Augustin et al., 2014), Makran Forebulge (Rodgers and Gunatilaka, 2002), Arabia-Eurasia plate motion (McQuarrie et al., 2003), Arabia-India plate motion (own data, based on GPlate, see section 4.4). Red bars indicate time for ~E/W-shortening in eastern Arabia.

Southeastern Oman Mountains		Batain area	
Time	Stress directions	Stress directions	Time
Tectonic Stage 1 Late Cretaceous to early Eocene extension Fournier et al. (2006)			Latest Maastrichtian to Paleocene Schreurs and Immenhauser (1999)
Tectonic Stage 2A Late Lutetian to Miocene extension - stage A			Late Eocene Conjugated sets of normal faults (NNE-SSW and E-W directed) Peters et al. (2001)
Tectonic Stage 2B Late Lutetian to Miocene extension - stage B Fournier et al. (2006) Scharf et al. (2020)			
Tectonic Stage 3 Late Oligocene to early Miocene shortening E-W to NE-SW			Early Miocene, Fournier et al. (2006) to late Miocene-Pliocene folding Schreurs and Immenhauser (1999)
Pliocene N-S shortening Fournier et al. (2006)			Post-mid-Eocene E/W-compression near Jabal Ja'alan Filbrandt et al. (1990)

Figure 5. Stress directions in the southeastern Oman Mountains and the Batain area. Time of Tectonic Stage 2 of Fournier et al. (2006) was adjusted using data of Scharf et al. (2020).

3. Methods

3.1. Kinematic analyses

Kinematic analyses of brittle fault planes in the field were performed, following Petit (1987) and Angelier (1994). All structural measurements are expressed as dip direction/dip angle for planar elements and plunge direction/plunge angle for linear features.

3.2. Remote sensing data interpretation

Satellite images to identify sub-vertical linear structures were analyzed. These structures were digitalized using the geographical information system (GIS). Linear features on a satellite image are commonly polygenetic planar elements (fractures, faults, strike-parallel features of resistant strata etc.). For simplification, we term such features on the satellite image as “lineaments“, although they are planar elements. The entire study area (~250 km by 50 km) was analyzed using world satellite imageries at different scales. Linear objects are interpreted as straight segments of valleys or geomorphological alignments related to brittle deformation of rock masses.

The interpretation of remote sensing data, combined with published geological maps of the study area (Béchenec et al., 1986; Villey et al., 1986a, 1986b; Le Métour et al., 1986b; Rabu et al., 1986; Wyns et al., 1992; Roger et al., 1991;

Peters et al., 2001, 2005) provided the basis for a brittle deformation model of our study area. More than 10,000 lineaments have been analyzed. The length of these linear features ranges between 100 m and 20 km. The results are summarized with respective rose diagrams for different sectors and for the entire working area, using the GIS extension tool of Jenness (2014).

Comparison of the linear features with geological maps confirms displacement at several places. Remote sensing data interpretation was conducted to see whether the linear features represent geological structures. The interpretation was carried out using the GIS tools (PolarPlots v.1.0.253 of Jenness, 2014) for ArcMap (v. 10.2, Esri ®) for the analysis of satellite imageries for northeastern Oman. The imagery features provided by Esri are WV03_VNIR satellite imagery with resolution of 0.31 m, accuracy of 10.2%, and source Digital Globe.

3.3. LA-SF-ICP-MS U-Pb dating

U-Th-Pb analyses were carried out in the Earthlab at the University of the Witwatersrand. The analytical protocol is similar to Ring and Bolhar (2020) (Supplementary Material S1).

Graphic presentation and calculation of lower intercept ages on a Tera-Wasserburg diagram were carried out using the software ISOPLOT-R (Vermeesch, 2018). Uncertainties of individual and mean/regressed ages are 2 SE (standard error, absolute). Intercept ages were based on individual dates and internal errors (not propagated). Propagated errors on U/Pb ratios can be estimated to be 1.25 times the internal errors for a similar analytical setup as adopted here (Woodhead & Petrus, 2019). Depth-resolution within each analysis is enabled by using a primary carbonate standard (WC-1; Roberts et al., 2017), coupled with downhole-fractionation correction; this further allowed to identify (and exclude) regions of high common Pb, and also to separate time intervals with distinctly variable U/Pb during ablations, sometimes resulting in more than one date for each spot (Woodhead & Petrus, 2019), reflecting age heterogeneity or variable common Pb within the carbonate.

LA-ICPMS data for standards are reported in tables S2 and S3. Sixty-six analyses of Duff Brown carbonate (ID-MC-ICP-MS age: 64.04 ± 0.67 ; 60.5 ± 4.6 ; 66.3 ± 3.9 Ma; 2 SE) produce a lower intercept age of 66.16 ± 0.5 Ma (MSWD=13; n=66), in excellent agreement with published values (Hill et al., 2016). Fifty-five analyses of the Richard's Spur speleothem provide an age of 299.96 ± 2.36 Ma (MSWD=3; n=55). This age is higher than the accepted ID-TIMS age of 289.2 ± 0.7 Ma (Woodhead et al., 2010) by 3.4 % (relative to accepted value). U-Pb ages for carbonates can be older for LA-based datasets when compared to isotope dilution (ID)-based datasets, possibly reflecting inadequate correction of common Pb in the gas blank (Woodhead & Petrus, 2019), or systematic differences in ablation behavior between carbonates types (speleothems versus micritic carbonates; Nuriel et al., 2017). One in-house standard ("Rio calcite") provides an accurate age of 56.25 ± 0.20 Ma (MSWD=4.7, n=39; C. Lana pers. Comm.). Two unknown samples yield an age of 30.08 ± 0.47 and 22.31 ± 2.15 Ma

(Table S4). Values of MSWD (2.4 and 5.3) are comparable to, or slightly higher than, the range quoted for U-Pb LA-ICP-MS carbonate ages of 2-4 (Woodhead and Petrus, 2019). Three other samples collected from the thrust at site 7a did not produce ages due to low U concentrations and very limited dispersion (Table S5).

3.4. GPlates reconstruction

The relative motions of Arabia and India during the Cenozoic were analyzed by the software GPlates (www.gplates.org). GPlates is based on a large database, including coastlines and seafloor magnetic anomalies (Matthews et al., 2011, 2016; Müller et al., 2016). In our study, Arabia is considered fixed while the relative translation and rotation of India was observed, allowing for estimation of changing distances between India and the eastern margin of Arabia through time.

4. Results

4.1. Field observations

The Oman Mountains from the eastern Batinah Coastal Plain to the Sur area (Fig. 1), encompass several Eocene to Miocene NW-striking sinistral transtensional and tranpressional faults, including (1) the “Tertiary Ridge” of Al-Khod Village (Scharf et al., 2016), (2) the Sunub Fault Zone (Mattern et al., 2018c), (3) the Wadi Mansah Fault Zone (Bailey et al., 2019; Scharf et al., 2019a), (4) the Issmaiya Fault Zone (Callegari et al., 2020), (5) the Ja’alan Fault (Filbrandt et al., 1990; Rogers et al., 1991), and (6) the Coastal Parallel Shear Zone (Wyns et al., 1992; Moraetis et al., 2018).

Eleven field sites in the Muscat-Seeb area were investigated, exhibiting ~N/S-striking compressional features and/or NW-striking sinistral faults (Figs. 2 and 3). Sites 1, 2, 3, 6, 10 and 11 are within and sites 4, 5, 7, 8 and 9 are outside the Rusayl Embayment (Fig. 3). Two NW-striking sinistral faults and one N-striking fold were studied at and near the Salma Plateau (Fig. 2; site 12-14). A NW strike-slip fault, E/W normal fault, N/S folds and thrusts were investigated in the Ibra Basin (site 15). The structures and their locations are shown in figures 1-3 and summarized in tables 2 and S1. Detailed outcrop descriptions are documented in the Supplementary Material (S2).

Table 2. Summary of field observations. More field details are presented in Table S1 and section S2. Sites are depicted in the Figures 2 and 3 and listed from the NW to the SE.

Sites	Location	Latitude	Longitude	Structure	Orientation
1	Wadi Ja’arah	23°29 04	57°55 00	Sinistral shear zone	WNW-striking
2	Halban	23°33 17	57°58 21	Open syncline Dextral fault	Sub-horizontal fol SW-striking
3	Taww	23°29 19	57°58 14	Sinistral shear zone	E/W-striking
4	Al-Khod Village	23°33 49	58°07 09	Reverse Fault	266/67

Sites	Location	Latitude	Longitude	Structure	Orientation
5	Fanja	23°27 28	58°07 00	Strike-slip shear zone	007/84
6	Bidbid	23°24 50	58°07 02	Sinistral shear zones	WNW to NW-striking
7a	SQU Campus	23°35 24	58°09 40	Synsedimentary thrust	083/27
7b	SQU Campus	23°35 16	58°10 33	Sinistral fault	052/77
8	Rusayl Dam	23°31 54	58°12 07	Open folds	Gently plunging folds
9	Cement factory	23°28 45	58°17 57	Open syncline	Gently plunging folds
10	Qurum South	23°36 00	58°28 58	Open anticline	Gently plunging folds
11	Qurum	23°37 00	58°30 36	Thrust Open anticline	270/30 Sub-horizontal folds
12	Tiwi	22°46 56	59°16 55	Sinistral positive flower structure	244/77
13	Salma Plateau	22°49 30	59°00 59	Sinistral faults Open anticline	026/65 and 037/50 Gently plunging folds
14	Wadi Al Khabbah	22°50 19	58°58 54	Sinistral fault	WNW-striking
15	Ibra Basin	22°04 42	58°44 48	Strike-slip fault Thrusts Normal fault Open anticline and syncline	NW-striking N/S-striking E/W-striking Sub-horizontal folds

4.2. Remote sensing analysis

Linear elements of the study area are projected on a satellite image, based on Remote Sensing data analysis (Fig. 6). Approximately 10,000 linear features were identified within the eastern Oman Mountains and the Batain area (Fig. 6). The investigated area was divided into eight sub-areas following a regional tectonic subdivision (Fig. 6; 1 – Jabal Nakhl; 2 – Rusayl Embayment; 3 – Fanja Saddle; 4 – Saih Hatat Dome; 5 – Salma Plateau; 6 – Wadi Mansah Fault Zone/ Wadi Tayin Fault/ Issmaiya Fault Zone/ Ja'alan Fault; 7 – Qalhat Fault; 8 – Batain area). All sub-areas reveal a similar lineament orientation pattern. Most of the lineaments trend WNW to NW (Fig. 6). Some of the lineaments are E/W and NE/SW-oriented (~055-235°). The latter orientation is more common in the Batain area.

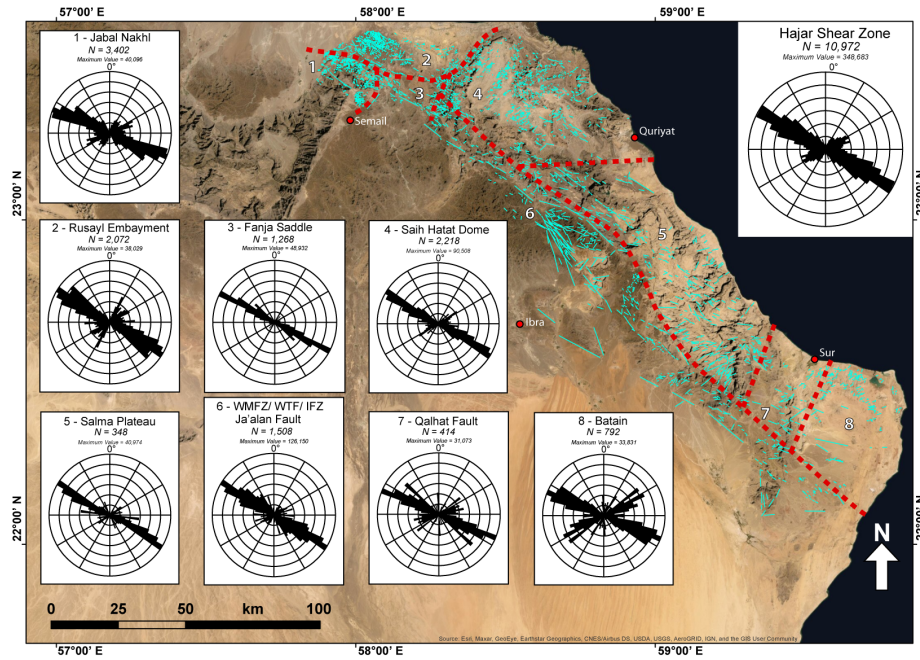


Figure 6. Satellite image analyses of the study area from west of the Rusayl Embayment to the Batain area. The study area is divided into eight sub-areas to potentially reveal local/regional variations in orientation of the lineamentary features (areas 1-8, separated by the red dashed lines). The orientations of the lineaments (light blue lines) from the satellite image are plotted in the rose diagrams (Jenness, 2014), with a bin size of 5°. All measurements are plotted in the rose diagram at the upper right. N=number of measured linear features; Maximum Values is the total length (in meters) of all measured lineaments.

4.3 Map analysis

This section summarizes previously mapped ~N/S-oriented compressive structures, ~E/W-oriented normal faults and ~NW-striking sinistral faults within eastern Oman (Figs. 7 and 8; Table 1). These structures affect mostly Paleocene/mid-Eocene sedimentary rocks but also some Miocene rocks, especially near the Qalhat Fault. Besides the mappable features, Wyns et al. (1992) measured sub-horizontal stylolite axes within Cenozoic carbonates, including those of the Oligocene Shama Formation near the Qalhat Fault. Stylolite axes are oriented ENE-WSE and interpret as axes of maximum compression during the Miocene (Wyns et al., 1992).

4.3.1. Folds

N/S to NW/SE-oriented folds within the post-obductional formation in the Muscat-Seeb area and the Permian rocks of the Saih Hatat Dome have been reported by Le Métour et al. (1986a), Villey et al. (1986a, 1986b), Mann et

al. (1990), Miller et al. (2002), Kajima et al. (2012a, 2021b, 2021c), Scharf et al. (2016), Searle et al. (2019), Hansman et al. (2021) and Levell et al. (2021), and are summarized in Table 1. Traces of fold axes are shown in Figure 7. The respective folds deform stratigraphic units up to the mid-Eocene limestone of the Seeb Formation. Mapped folds are open to tight and display sub-vertical fold axial planes. Fold axes plunge gently towards the north to NW or are sub-horizontally. The interlimb angle of individual folds within the Rusayl Embayment varies. Towards the South, the same fold elements (synclines/anticlines) are tighter than in the North, where the folds open (Mann et al., 1990). Interlimb angles are homogeneous along individual folds outside the Rusayl Embayment.

Ninkabou et al. (2021) and Levell et al. (2021) presented seismic and well data from offshore northeastern Oman. A pre-late Eocene NNE-trending major fold has been spotted by Levell et al. (2021). This fold occurs in the NNE-ward projected extension of the Jabal Akhdar/Jabal Nakhl. Further ~N/S-trending folds extend from the Rusayl Embayment into the Sea of Oman and near Muscat. Rabu et al. (1986) and Coffield et al. (1990) mapped several Cenozoic ~N/S to NNW/SSE-trending faults in the Fanja area between the Jabal Akhdar and Saih Hatat domes as well as along the Frontal Range Fault and the Wadi Mansah Fault (Fig. 7).

Approximately N/S-oriented open to tight folds have been mapped within Paleocene to Miocene formations near Quriyat, in the Salma Plateau and Batain area (Le Métour et al., 1986a, 1986b; Roger et al., 1991; Wyns et al. 1992; Peters et al., 2001). Further ~N/S-oriented open asymmetric folds and monoclines deformed Maastrichtian to Eocene rocks at Jabal Ja'alan (Filbrandt et al., 1990). The traces of some of these folds are depicted in Figure 8.

4.3.2 Faults

Fournier et al. (2006) mapped sets of conjugate strike-slip faults within the Jafnayn Formation in the Muscat area (Figs. 7 and 8). Dextral and sinistral faults strike NE/SW and E/W, respectively (Fournier et al., 2006). The computed maximum horizontal stress trends ENE/WSW (between N54°E and N85°E; Fournier et al., 2006).

A segment of the Paleogene rocks, including the Jafnayn, Rusayl and Seeb formations at the “Tertiary Ridge” at Al Khod Village represents a WNW-striking transpressive sinistral shear zone with ~N/S-oriented compressive structures (folds and reverse faults) and ~E/W-striking normal faults (Scharf et al., 2016). The horizontal shorting direction was ENE/WSW (Scharf et al., 2016).

In the Sunub area of the Rusayl Embayment and near the Frontal Range Fault, the well-exposed WNW-striking sinistral transtensional Sunub Shear Zone associated with ~E/W-striking normal faults exists. It has been interpreted as a negative flower structure with a shale dike (Mattern et al., 2018c).

The southwestern margin of the Saih Hatat Dome and the Fanja area is char-

acterized by the Wadi Mansah Fault Zone (Bailey et al., 2019; Scharf et al., 2019a). This major extensional shear zone has a throw of 7 km and a sinistral shear component. It has been interpreted as active during doming of the Jabal Akhdar and Saih Hatat domes during the late Eocene to Miocene (Scharf et al., 2019a). The southeastern extend of the Wadi Mansah Fault Zone is parallel to the margin of the Saih Hatat Dome and merges with the extensional Wadi Tayin Fault of Searle (2007). The latter has a throw of ~2 km (Searle, 2007). Numerous ~WNW-striking faults in the Fanja area affected autochthonous and allochthonous rocks (Stanger, 1985).

Within the Semail Ophiolite, parallelly orientated to the Wadi Mansah Fault Zone and near the Wadi Tayin Fault, a further sinistral transtensional fault zone is present – the Issmaïya Fault Zone (Callegari et al., 2020). This ~NW-striking shear zone is ~30 km long and ~3 km wide. Activity along this fault zone occurred first during the Maastrichtian to early Eocene and then following the mid-Eocene (Callegari et al., 2020).

The Salma Plateau, including mid-Eocene limestones, has been affected by numerous faults of the NW-striking sinistral transpressive Coastal Parallel Shear Zone (Wyns et al., 1992; Moraetis et al., 2018). Sinistral slip was determined by Roger et al. (1991) and Wyns et al. (1992).

In the southeastern prolongation of the Issmaïya Fault Zone, the NW-striking Ja'alan Fault is exposed (Roger et al., 1991; Wyns et al., 1992; Fig. 8). This fault is a present-day major reverse fault with a sinistral component (Filbrandt et al., 1990; Wyns et al., 1992). The throw amounts to a few kilometers. The Ja'alan Fault marks the southwestern limit of the Salma Plateau (Fig. 2).

The ~N/S-striking Qalhat Fault is located near Sur and defines the eastern margin of the Salma Plateau (Fig. 2). The throw along the major fault amounts to a few to several kilometers, where the Neoproterozoic crystalline basement was thrust onto Oligocene/Miocene sedimentary rocks (Wyns et al., 1992). Adjacent to the Qalhat Fault are several ~N/S-oriented folds (Roger et al., 2001). The rocks east of the Qalhat Fault were not uplifted, while the same Cenozoic rocks to the West have been uplifted to an elevation of >2000 m.

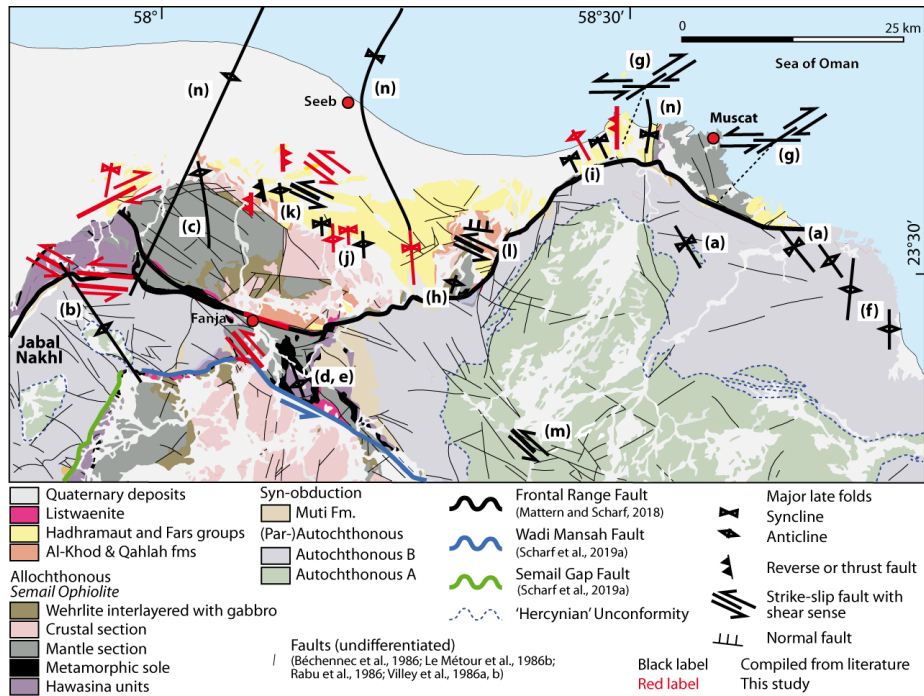


Figure 7. Structural map of the Muscat-Seeb area of Figure 4. Most of the black folds/faults are of post-mid-Eocene age; (a) – Le Métour et al. (1986a, 1986b); (b) – Rabu et al. (1986); (c) – Villey et al. (1986a); (d) – Villey et al. (1986b); (e) – Coffield (1990); (f) – Miller et al. (2002); (g) – Fournier et al. (2006); (h) – Kajima et al. (2012a); (i) – Kajima et al. (2012b); (j) – Kajima et al. (2012c); (k) – Scharf et al. (2016); (l) – Mattern et al. (2018c); (m) – Mattern et al. (2020a); (n) – Levell et al. (2021). Thin black lines represent undifferentiated faults, taken from Béchennec et al. (1986), Villey et al. (1986a, 1986b), Le Métour et al. (1986b) and Rabu et al. (1986). The age of these faults is unknown. Note that the large NNE-oriented anticline as continuation of the Jabal Akhdar/Jabal Nakhl is late Eocene in age, based on seismic data (Levell et al., 2021).

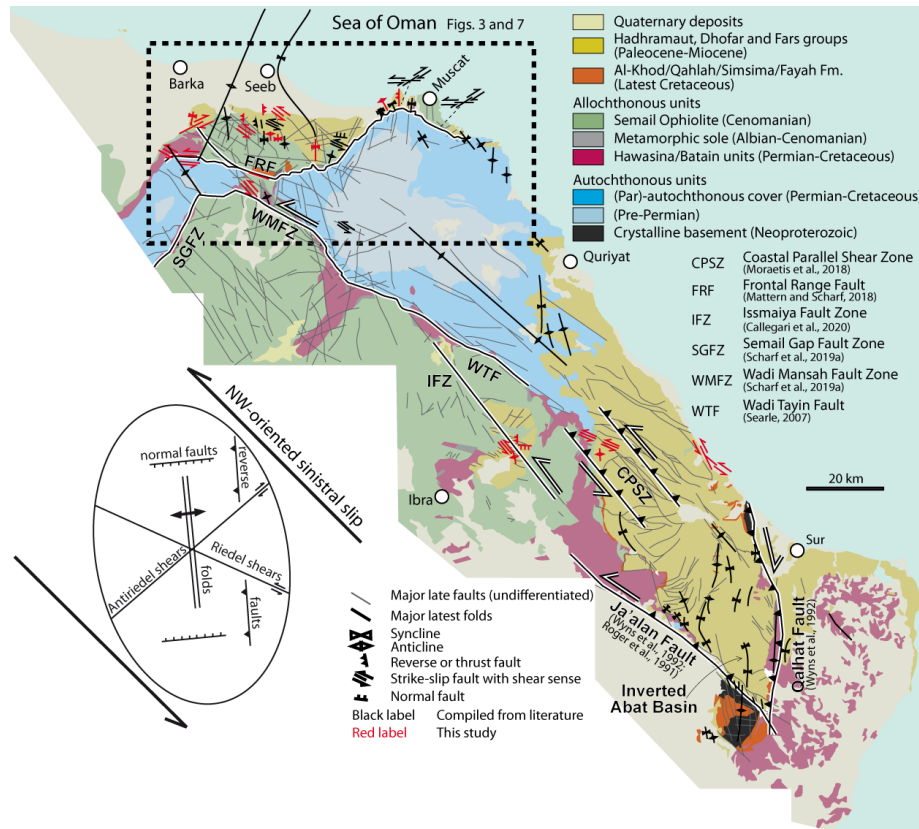


Figure 8. Structural map of eastern Oman, depicting post-mid-Eocene structures. Compiled after Béchenec et al. (1986), Villey et al. (1986a, 1986b), Le Métour et al. (1986a, 1986b), Rabu et al. (1986), Wyns et al. (1992), Roger et al. (1991), Peters et al. (2001, 2005), Moraetis et al. (2018), Callegari et al. (2020) and Levell et al. (2021). The age of the undifferentiated faults is unknown. The Harding Strain Ellipse (Harding, 1974) indicates a wrench-fault assemblage geometry for NW-striking sinistral slip. Note that most mapped structures conform to this geometry!

4.4. U-Pb dating of carbonates

Synkinematic carbonates from faults were analyzed with the U-Pb in-situ LA-ICPMS method (e.g., Woodhead & Petrus, 2019; Carminati et al., 2020; Ring & Bolhar, 2020; Roberts et al., 2020). Out of five carbonate samples only two synkinematic carbonates produced reliable and precise U-Pb LA-ICPMS ages (sample Baz 2 and HAB 1). Analytical data are presented in Figure 9 and reported in tables 3 and S2. Sample Baz 2 was collected from a sinistral fault from the Sultan Qaboos University Campus (site 7b) and yields an U-Pb age of 22.31 ± 2.15 Ma (2 SE). Sample HAB 1 consists of synkinematic calcite from a dextral fault of Halban (site 2), yielding an U-Pb age of 30.08 ± 0.47 Ma (2

SE).

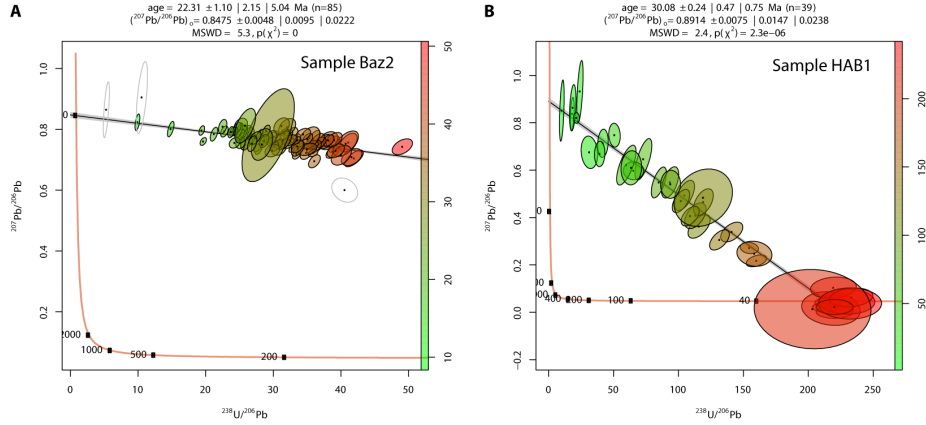


Figure 9. Tera-Wasserburg disagrams showing U-Pb age data (error ellipse=2 SE) for sample Baz 2 and HAB1 (A and B). Gray areas around discordia represent 2 SE uncertainty of linear regression. Analytical precision (age, initial $^{207}\text{Pb}/^{206}\text{Pb}$) is indicated as analytical uncertainty (first value, 1 sigma), “studentized 100(1-)% confidence interval for t using the appropriate number of degrees of freedom” (second value) and “approximate 100(1-)% confidence interval for t with over-dispersion, calculated as $z=y/\text{MSWD}$ ” (value 3). MSDW=mean squared weighted deviations, n=numbers of spot analyses. The U-Pb data ellipses are color-coded according to their $^{238}\text{U}/^{206}\text{Pb}$ value, displayed in the individual color scales at the right margin of the diagrams. Data points plotting to the left of the concordia were excluded from age regression; some outliers were also excluded, which plotted off the main regression line, without altering the original age estimate, but improving precision and MSWD values. Graphic presentation and age calculation utilized IsolpotR (Vermeesch, 2018).

Table 3. Sample details with U-Pb age results

Sample	Lat	Long	Lithology/structure
Baz 2	23°35'16"	58°10'33"	Carbonates and siliciclastics of the Barzaman Fm. / Calcified sinistral strike-slip fault
HAB 1	23°33'17"	57°58'21"	Carbonates of the Jafnayn Fm. / Calcified dextral strike-slip fault with calcified

4.5 GPlate reconstructions

Relative plate motions induce corresponding regional strain into plates near the plate boundary (Ledouzey, 1986; Heidbach et al., 2007; Zoback & Zoback, 2007). Eastern Oman is located near the present-day Arabia-India plate boundary, i.e., near the Owen Fracture Zone (Fournier et al., 2008; DeMets et al., 2010; Fig. 1).

The ~N/S to NW/SE-oriented Eocene to Miocene compressive structures deformed sedimentary rocks likely due to ~E/W to NE/SW-directed shortening. A suitable geodynamic cause for this shortening is the convergence history between the Arabian and Indian plates as suggested by Fournier et al. (2006) and Gaina et al. (2015). The latter authors suggested minor E/W-shortening between the Arabian and Indian plates from 40 Ma to the present (their Fig. 7). We analyzed the plate configurations of Arabia and India during the Cenozoic using the GPlates software to develop the causal relationship.

In all our reconstructions, Arabia is anchored (fixed). We describe the distance of India (near the present-day location of Karachi at 24°50 N/66°40 E) and the western tip of the 64 Ma isochron, as part of the Indian Plate, with respect to Arabia (East of Sur: 22°29 30 N/59°49 E; Figs. 10-12). We calculated/measured the E/W-component of distance of the two fix points between India and Arabia at different times (distance between Karachi and Sur, and distance between western tip of the 64 Ma isochron and Sur).

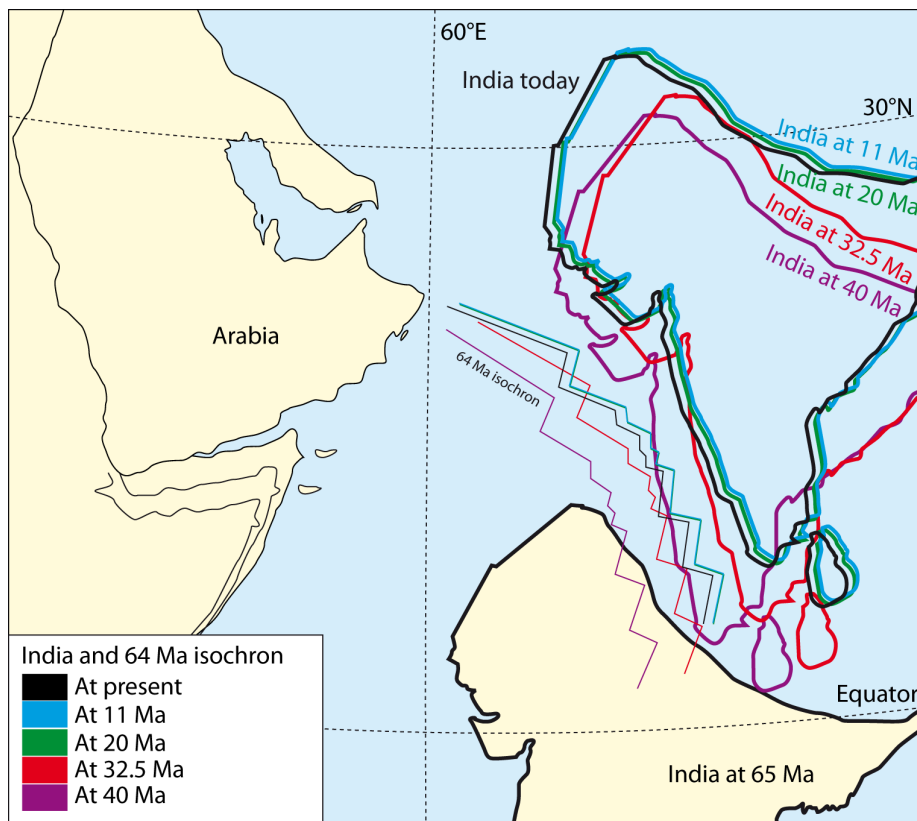


Figure 10. Cenozoic plate reconstruction between Arabia (fixed) and India, based on GPlates (version 2.2.0) with a 3D orthographic projection. Eurasia at the present stage is not depicted.

4.5.1 65 to 32.5 Ma

Left-lateral translation was the main relative motion between the Arabian and Indian plates between the beginning of the Cenozoic and ~40 Ma. At 65 and 40 Ma, the reference points at the Indian Plate were set at $3^{\circ}59'24''\text{N}/61^{\circ}10'12''\text{E}$ and $22^{\circ}29'30''\text{N}/59^{\circ}49'\text{E}$, respectively. Thus, India moved ~2165 km towards the NNE between 65 and 40 Ma (average velocity of 86.6 mm/a) with respect to fixed Arabia (Fig. 10).

Between 40 to 32.5 Ma, both plates underwent some divergence with left-lateral translation (~185 km translation of India towards the NE; ~24.67 mm/a; between 40 and 32.5 Ma; Fig. 10). The Indian reference point was set at $23^{\circ}13'48''\text{N}/68^{\circ}42'\text{E}$ at 32.5 Ma (Fig. 10). Thus, the relative motion between Arabia and India did not cause any shortening in Oman from 65 to 32.5 Ma.

4.5.2 32.5 Ma to present

Between ~32.5 and 20 Ma, both plates experienced ~100 to 135 km ~E/W-directed convergence owing to a minor ~northward motion and coeval anticlockwise rotation of India (8° ; $\sim 0.64^{\circ}/\text{Ma}$) with respect to Arabia (~228 km of rotation and translation of India to the NW; ~18.2 mm/a; between 32.5 and 20 Ma; Fig. 11). The Indian reference point was set at $24^{\circ}54'\text{N}/67^{\circ}21'\text{E}$ at 20 Ma (Fig. 11).

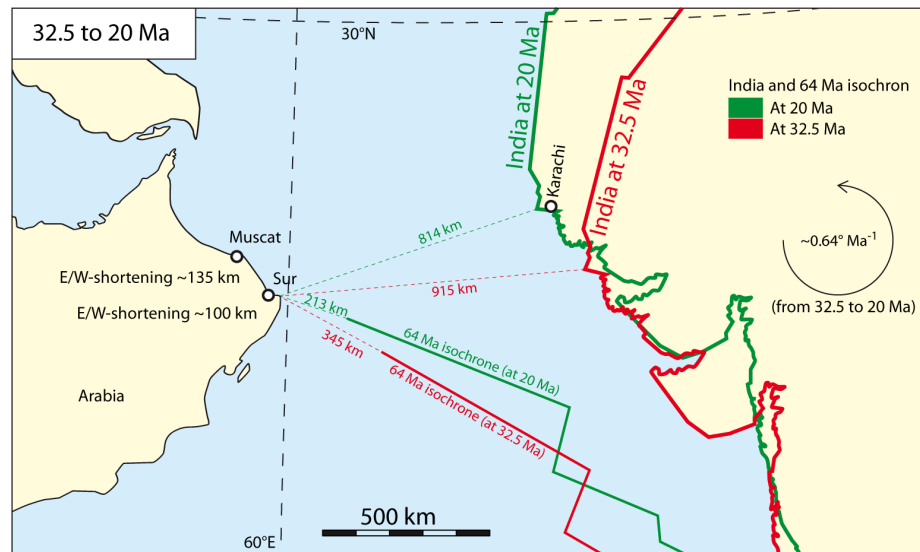


Figure 11. Plate reconstruction between Arabia and India between 32.5 and 20 Ma, using GPlates (version 2.2.0) with a 3D orthographic projection. Note that India rotated counterclockwise, resulting in oblique convergence between both plates! The component of E/W-shortening between both plates amounted to ~100-135 km.

After 20 Ma convergence stopped as counterclockwise rotation of India ceased, and both plates experienced minor left-lateral motion until 11 Ma with some divergence between both plates (~27 km translation of India toward the NE; ~2.7 mm/a; between 20 and 11 Ma). The Indian reference point was at 25°07'48" N/67°24'36" E at 11 Ma.

From ~11 Ma to the present, India translated relatively towards the WSW, resulting in right-lateral motion and ~ENE/WSW-convergence between Arabia and India (~83 km translation of India towards the WSW; ~7.5 mm/a; between 11 Ma and today; Fig. 12).

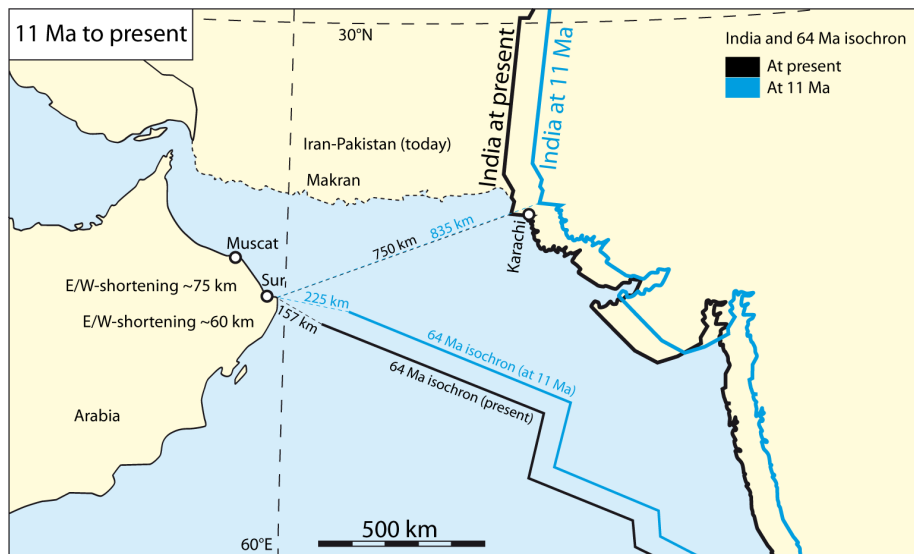


Figure 12. Plate reconstruction of Arabia and India between 11 Ma and today, using GPlates (version 2.2.0) with a 3D orthographic projection. Note that India translates towards the west-southwest, resulting in convergence and dextral motion at the plate boundary! The amount of E/W-shortening between both plates ranges between ~60 and ~75 km. Shortening/convergence is ongoing.

The time slots from ~32.5 to 20 Ma and from 11 Ma to the present indicate a relative ~E/W-directed convergence and shortening between the Arabian and Indian plates (Figs. 11 and 12). The E/W-directed shortening between the Arabian (near Sur) and Indian plates (near Karachi and the western end of the 64 Ma isochrone) amounted to ~100-135 km from ~32.5 to 20 Ma (Fig. 11) and ~60-75 km from 11 Ma to present-day (Fig. 12), resulting in convergence rates of ~10-12 mm/a and 5-7 mm/a, respectively.

5. Interpretation and discussion

5.1 Wrench-fault assemblage and satellite image analysis

Field analysis of 15 sites (Supplementary Material S2) and map interpretations

indicate that all formations/units (except the Quaternary deposits) in north-eastern Oman were affected by NW-striking sinistral faults, associated with ~WNW-striking sinistral Riedel faults, ~N/S to ~NW/SE-oriented compressive structures (i.e., folds, reverse faults, thrusts) and ~E/W-oriented normal faults. At Site 2 (Halban), a SW-striking dextral fault has been mapped. This dextral fault is interpreted as an anti-Riedel fault (antithetic to the main fault). All these structures combined indicate a wrench-fault assemblage of an overall NW-striking major sinistral shear zone (see Harding Strain Ellipse in Fig. 8).

Most of the >10,000 identified lineamentary features within the study area are WNW/ESE to NW/SE-oriented (Fig. 6). The orientation of the lineamentary features differs outside the study area (i.e., along the eastern margin of the Jabal Akhdar Dome and adjacent ophiolite rocks, with a mostly NNE/SSW-orientation; Scharf et al., 2019a). The general orientation of lineamentary features within different sub-areas of the study area does not change significantly (Fig. 6). Thus, most of the identified linear features formed during the same deformation/shearing event.

The WNW-oriented linear features are interpreted as sinistral Riedel faults with respect to the ~NW-striking main fault, while ~E/W-striking features are probably normal faults (see Harding Strain Ellipse of Fig. 8). The ~NE/SW-oriented lineaments are mostly found in the Batain area (Fig. 6). Only the Batain area was affected by ~WNW-directed obduction of the Masirah Ophiolite. Thus, we conclude that these features are related to the thrusting of the Masirah Ophiolite (i.e., these features present largely thrusts of the Masirah fold-and-thrust belt).

5.2 The Hajar Shear Zone

Wrench-fault assemblage (~NW-striking sinistral faults, ~N/S-oriented compressive structures, ~E/W-oriented extensional structures, ~WNW-striking sinistral fault – Riedel faults and ~SW-oriented dextral faults – anti-Riedel faults) and the WNW to NW-oriented lineamentary features are distributed over a wide area with a minimum length and width of ~250 km and ~50 km, respectively, from the eastern Batinah Coastal Plain to the Batain area (Fig. 8). This entire zone underwent NW-directed sinistral shear and E/W-shortening after the mid-Eocene. We reference this zone as “Hajar Shear Zone” (HSZ). Some parts along the HSZ are active, indicating ongoing ~E/W-shortening (e.g., seismicity near the Qalhat Fault and uplifting marine terraces; Fig. 1). Numerous faults, compressive and extensional structures are present within this area, indicating widely distributed strain. However, most of the sinistral shear is concentrated along major faults, probably because they reactivated older structures. These include a segment of the Frontal Range Fault near Fanja, the Wadi Mansah Fault Zone, possibly the Wadi Tayin Fault, the Issmaiya Fault Zone, the Coastal Parallel Shear Zone and the Ja’alan Fault (Fig. 8). In our model, we connect/link all these faults to one major sinistral fault zone, along which most of the shearing of the HSZ has been accommodated.

In the southeast, Quaternary deposits cover large parts of the Batain region, which makes it challenging to trace/map the continuation of the HSZ. The width of the HSZ could exceed 50 km because rocks to the SW of the Wadi Mansah/Issmaiya/Ja'alan faults display widely distributed WNW to NW-oriented sinistral faults, too (Fig. 8). However, most of this area consists of the Semail Ophiolite, where shearing is difficult to detect and date.

5.3. Time-constraining the deformation

5.3.1 Interval I

Ages of several structures within the HSZ have been constrained by different geological approaches to be Oligocene or younger. Most of the ~N/S-oriented structures (faults and folds) deformed late to mid-Eocene formations but also some Oligocene/Miocene formations in the Rusayl Embayment and Sur area. Thus, ~E/W-shortening must be younger than mid-Eocene.

Sinistral WNW to W-striking faults at Wadi Ja'arah, Taww and Fanja (sites 1, 2 and 5) cut all structures including top-to-the NE extensional structures (e.g., compare Al-Wardi and Butler, 2007; Grobe et al., 2018; Mattern and Scharf, 2018). Furthermore, sinistral strike-slip faults are vertical or sub-vertical and were not tilted during the main doming interval of the Jabal Akhdar, which lasted from the late Eocene to Oligocene (Hansman et al., 2017; compare Levell et al., 2021 for offshore folding). We suggest that these NW-striking sinistral faults are part of the HSZ with the ~E/W to WNW-striking sinistral faults representing Riedel faults (synthetic faults). Strike-slip faults at Taww post-date Jabal Akhdar doming and top-to-the-NNE extensional shearing and, thus, occurred during the Oligocene or later.

At Fanja, the strike-slip faults cut all extensional structures of the southern Fanja Half Graben. The first extensional interval at this half graben lasted from the latest Cretaceous to early Paleogene (Tectonic Stage 1 of Fournier et al., 2006) and the second interval was post-mid-Eocene (probably Oligocene; Tectonic Stage 2 of Fournier et al., 2006; Fig. 5). Therefore, strike-slip faults at Fanja are also Oligocene or younger in age.

The sinistral fault at the southwestern margin of the Saih Hatat Dome, at Wadi Al Khabbah (site 14; Fig. S22) displaces autochthonous Jurassic and Cretaceous rocks, which were tilted during the late Eocene to Oligocene doming of the Saih Hatat (Hansman et al., 2017). Thus, this WNW-striking fault must be Oligocene or younger, too.

A key outcrop is the syndepositional thrust at the Sultan Qaboos University Campus (site 7a; Fig. S13). This thrust occurs within the Upper Oligocene to Lower Miocene section of the Barzaman Formation (age based on foraminifera; Mattern et al., 2020b), attesting that ~E/W-directed shortening was active during the latest Oligocene to Early Miocene. This designated age agrees with computed paleostress information derived from fault slip data by Fournier et al. (2006), indicating that E/W-compression occurred during the

early Miocene.

A similar and slightly younger (Miocene) age for ~E/W-shortening has inferred by Fournier et al. (2006) and Schreurs and Immenhauser (1999) for the Batain/Sur area (Fig. 5). Filbrandt et al. (1990) assigned a post-mid-Eocene age to ~E/W-shortening in the Jabal Ja'alan area. The inversion of the Abat Basin started during the late Burdigalian (compare Wyns et al., 1992).

GPlates reconstructions document ~E/W-shortening between Arabia and India. Interval I is related to the counterclockwise rotation of India between 32.5 and 20 Ma (Rupelian to Burdigalian; Cohen et al., 2013). This deformation created the HSZ and its wrench-fault assemblage. Owing to coeval counterclockwise rotation of India and northward motion of India, the direction of shortening also rotated counterclockwise from ~E/W to ~ENE/WSW. This rotation and the coeval northward movement of India resulted in non-coaxial deformation (simple shear) at northeastern Oman.

Furthermore, U-Pb dating of synkinematic calcite proves a latest Oligocene/earliest Miocene age for sinistral deformation in the Barzaman Formation (22.31 ± 2.15 Ma; site 7b; Fig. S14). The age of 22.31 Ma corresponds to the Aquitanian (Cohen et al., 2013). This age indicates that deformation ensued during deposition of the Barzaman Formation, consistent with the age of the synsedimentary thrust at site 7a (Fig. S13).

A further precise U-Pb age for carbonate was obtained from the Halban area (30.08 ± 0.47 Ma; site 2; Fig. S3-6). This early Oligocene age (Rupelian; Cohen et al., 2013) dates dextral motion along a ~SW-striking anti-Riedel Fault of the HSZ and within the Jafnayn and Rusayl formations.

The independently obtained age constraints for ~E/W-shortening from map interpretation, cross-cutting relationships, syndepositional thrusting, GPlates reconstruction and U-Pb dating of synkinematic carbonate, demonstrate shortening along the HSZ between 32.5 and 20 Ma and define our Interval I.

5.3.2 Interval II

GPlates reconstructions indicate that no E/W-shortening between the Arabian and Indian plates occurred between 20 to 11 Ma. Further convergence with an E/W-shortening component started at 11 Ma (early Tortonian, Cohen et al., 2013) and lasting until present-day associated with ~60-75 km of shortening (Interval II). This ongoing shortening interval may have reactivated the Qahlah Fault (recent seismicity), is responsible for activities at the transpressional Coastal Parallel Shear Zone, inverted the Abat Basin and uplifted marine terraces NW of the Qalhat Fault (Fig. 13). However, further structural work and dating are needed confirm the GPlates results.

5.4 Amount of deformation in eastern Arabia and the HSZ

According to GPlates reconstructions, the E/W-convergence between the Arabian and Indian plates amounts to ~100-135 km from 32.5-20 Ma. Thus, the

combined amount of shortening of all described structures from Musandam to the Batain area cannot exceed this amount, assuming that the pre-Oligocene and present-day coastline of eastern Oman were at the same position and of the same shape as today.

The amount of Oligocene to early Miocene westward translation along the Hagab Thrust measures >15 km (Searle, 1988). The Oligocene/early Miocene shortening along Jabal Hafit Anticline and the Suneinah area has not been quantified but is assumed by us to amount to a few tens of kilometers (compare Boote et al., 1990; Hansman & Ring, 2018).

The amount of sinistral shearing (lateral displacement during Interval I) along the HSZ and ~E/W-shortening is unknown, due to a lack of markers. Numerous small structures occur within the HSZ (folds, thrusts, reverse faults, normal faults and strike-slip faults), and these structures are widely distributed throughout our study area of ~250 km by ~50 km. Folds are mostly open and range in size from several meters to kilometers in wave length. Mapped faults have a displacement of a few kilometers. We acknowledge that not all structures within this large area were measured and mapped.

A conservative estimate for sinistral shearing and ~E/W-shortening within the HSZ amounts to a few to several tens of kilometers. Some unknown amount of sinistral shearing and ~E/W-shortening may have been absorbed (1) in the non-mapped areas of the HSZ (Batainah Coastal Plain and Batain area), (2) within the Arabian Plate, i.e., the Central and Northern Oman Mountains, (3) the Omani margin offshore Batain (compare Rodriguez et al., 2014; 2016), (4) the former plate boundary of Arabia and India and (5) within the Indian Plate.

The amount of ~ENE/WSE-oriented shortening within eastern Oman (Interval II) remains unknown due to a lack of markers. The amount of plate convergence between India and Arabia is ~85 km since 11 Ma, resulting in 60-75 km of E/W-shortening (Fig. 12). The amount of dextral motion between the Arabian and Indian plates for the last 11 Ma (~7.5 mm/a; based on GPlates) exceeds the reported present-day dextral motion at the Owen Fracture Zone of 3 ± 0.4 mm/a (Fournier et al., 2008; DeMets et al., 2010). Thus, other active faults/plastic deformation/uplift may have absorbed the difference in plate motion (i.e., ~4.5 mm/a). Potential “absorbing structures” are the Owen Ridge with an uplift of >2 km (Rodriguez et al., 2014), the active Qalhat Fault and the uplifting marine terraces of the coastal Salma Plateau (e.g., Wyns et al., 1992; Mattern et al., 2018a; Moraetis et al., 2018).

5.5. Tectonic implications

Eastern Arabia contains ~NW-striking basement faults, which formed during the Pangean/Neo-Tethys rifting. One of these faults or fault zones is below the HSZ at the southwestern margin of the Saih Hatat Dome. It is likely that this structure was reactivated during the Oligocene/early Miocene ~E/W-convergence between Arabia and India. Thus, the pre-existing basement structure plays a major role in the localization of the HSZ, especially the localization

and concentration of sinistral slip and absorption of \sim E/W-shortening-related strain along the aligned Wadi Mansah, Wadi Tayin, Issmaiya and Ja'alan faults (Figs. 2 and 13).

GPlates modeling of motion between the Arabian and India plates shows that India rotated counterclockwise from \sim 32.5 to 20 Ma by \sim 8° with coeval northward motion of India; Fig. 11). Consequently, the direction of shortening during this stage rotated counterclockwise, too, resulting in simple shear deformation in eastern Oman and activity along the HSZ (Interval I). The overall \sim E/W-convergence/shortening between the Arabian and Indian plates amounts to a minimum of \sim 100-135 km.

The eastern Arabian Plate was affected by this deformation, evident by the wrench-fault assemblage associated with the HSZ (Figs. 8 and 13A). The amount of sinistral slip along the HSZ, including its associated wrench-fault assemblage, is not well constrained but could amount to a few to several tens of kilometers. Thus, the easternmost tip of continental Arabia was located further to the east by a few to several tens of kilometers prior to the Oligocene than today (Fig. 13). This interpretation is supported by the outline of the present-day shelf break (i.e., \sim 200 m water depth). The shelf break of eastern Oman may have been more or less straight before the Oligocene (Fig. 13A) and must have changed during the Oligocene due to left-lateral shearing. Correspondingly, the present-day shelf break changes direction. It kinks or veers to the North in the Batain area (Fig. 13). Most of this directional change occurs in the realm of the HSZ (Fig. 13). A former pre-Oligocene straight shelf break implies that easternmost Oman was left-laterally sheared for a few to several tens of kilometers (Fig. 13). Factoring in this aspect E/W-shortening during Interval I must have amounted to more than the estimated \sim 100-135 km of E/W-convergence/shortening, because GPlates uses the present-day countour of the shelf break which is post-deformational.

In addition, the present-day Qalhat Fault strikes NNW at its northern end, while it is oriented \sim N/S to NNE/SSW further to the South at Jabal Ja'alan (Fig. 2). This directional change is gradual. The latter orientation is similar to that of other major faults within the Oman Mountains such as the Semail Gap Fault Zone (Fig. 8; Weidle et al., 2021). We suggest that during sinistral shearing, the former \sim N/S to NNE/SSW-oriented Qalhat Fault was passively rotated or dragged in a counter-clockwise way to a NNE-strike at its northern end. A consequence of shortening and left-lateral shearing is that the Saih Hatat and Jabal Akhdar domes may have been further apart from one another in map view prior to shearing. In addition, we conclude that the \sim N/S to NW/SE-striking compressive structures in the northern Oman Mountains (e.g., Hagab Thrust, Jabal Hafit Anticline) also formed during Oligocene/early Miocene Arabia/India-shortening. This interpretation is supported by the orientation and age of these structures. The \sim N/S-oriented compressive structures unlikely formed during the NNE/SSW-directed Arabia/Eurasia-convergence as previously interpreted (e.g., Boote et al., 1990; Searle et al., 2014), because this

convergence would have produced differently oriented compressional structures.

If Interval II is accepted as factual, the sinistral faults were not reactivated during Interval I because the direction of shortening (\sim ENE/WSW) is at a high angle to the orientation of the NW-striking HSZ. Shortening during Interval II rather produced conjugate strike-slip faults, which are indicative for pure shear deformation (e.g., Fournier et al., 2006). Thus, Interval II deformation likely overprinted elements of the wrench-fault assemblage of the HSZ such as the compressive structures at the Coastal Parallel Shear Zone, responsible for Neogene to Quaternary uplift of marine terraces between Quriyat and Sur, Neogene inversion of the Abat Basin and active tectonics at the Qalhat Fault (Fig. 13).

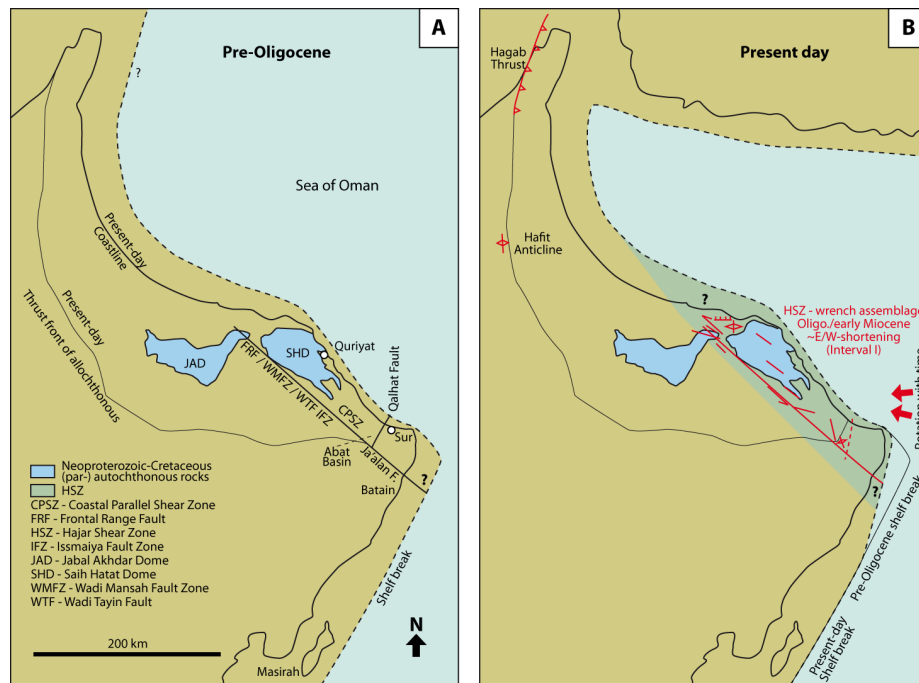


Figure 13. Outline of eastern Arabia before (A) and after (B) activity of the HSZ. Most likely, a pre-existing \sim NW-striking fault zone exists below the HSZ, especially were the aligned Wadi Mansah Fault Zone, Wadi Tayin Fault, Iss-maiya Fault Zone and Ja'alan Fault occur. This fault zone was reactivated during the Oligocene/early Miocene (Interval I). Outline of present-day shelf break (\sim 200 m water depth) using Google Earth. Left-lateal shearing along the HSZ with wrench-fault assemblage is widely distributed and passively rotated/dragged structures, such as the Qalhat Fault, the shelf break and the Saih Hatat Dome.

6. Conclusions

Structural field investigations, map analyses, satellite imagery analyses, syndepositional thrusting, GPlates reconstructions and absolute U-Pb dating of synkinematic calcite reveal that eastern Oman was affected by widely distributed NW-oriented sinistral motion within and along the Hajar Shear Zone, which is associated with a wrench-fault assemblage. Shearing affected an area of ~250 km by ~50 km, lasted from ~32.5 to 20 Ma (Rupelian to Burdigalian) and amounted to a few to several tens of kilometers displacement. Most shearing was absorbed along ~250 km long major fault zones from the Batinah Coastal Plain (Jabal Nakhl area), via the Fanja Saddle (Frontal Range Fault and Wadi Mansah Fault Zone), along the southwestern margin of the Saih Hatat Dome (Wadi Mansah Fault Zone, Wadi Tayin Fault, Issmaiya Fault Zone, Coastal Parallel Shear Zone, Ja'alan Fault) to the Batain area. It is likely that below these shear zones reactivated pre-existing faults exist, that may have formed during the Pangean Neo-Tethys rifting or earlier events.

Collected data indicates that pre-existing basement structures were likely reactivated during times of suitably oriented stress fields. Thus, such deep-seated structures are responsible for deformation/uplift at passive margins such as the one in eastern Oman.

The deformation pattern of the Hajar Shear Zone can be correlated with ~N/S-oriented compressional structures in the northern Oman Mountains (Hagab Thrust, Jabal Hafit Anticline). Thus, these structures formed during the ~E/W-directed Arabia/India-convergence and are not related to ~NNE/SSW-directed Arabia-Eurasia shortening. Convergence between Arabia and India is responsible for a minimum of ~100-130 km E/W-shortening in the Oman Mountains during the Oligocene and early Miocene.

The Oman Mountains were affected by largely coeval Oligocene/early Miocene convergence of Arabia-India (E/W) and Arabia-Eurasia (NNE/SSW). Previously, most mid-Cenozoic structures were believed to have formed in response to the Arabia/Eurasia-convergence. Our results document that many of these structures have developed due to the Arabia/India convergence. Thus, E/W-shortening in the Oman Mountains and eastern Arabia played a more important role than previously considered.

A further conclusion related to the ongoing ~WSW/ENE-convergence between Arabia and India is that respective deformation may have occurred at or near the Arabia-India plate boundary. Frequently reported earthquakes in the Sea of Oman and active tectonics/uplift in the Sur/Quriyat area may be due to this shortening.

Acknowledgements

Fieldwork was carried out from 2016-2021 with the continued support of the Sultan Qaboos University. We acknowledge the field assistance of Katharina Scharf and Gianluca Frijia. We furthermore thank Hamdan Al-Zidi and Bader Al-Waili (both Sultan Qaboos University) for preparation of rock samples for the U-Pb dating. R. Bolhar acknowledges financial support to establish the LA-SF-

ICP-MS facility at the School of Geosciences, University of the Witwatersrand, through a NRF-NEP grant (UID 105674). The Editor xxx and the two reviewers xxx and xxx greatly improved the manuscript.

References

- Abbasi, I.A., Hersi, O.S., & Al-Harthy, A. (2014). Late Cretaceous conglomerates of the Qalhah formation, north Oman. In: Rollinson, H.R., Searle, M.P., Abbasi, I.A., Al-Lazki, A.I., Al-Kindy, M.H. (Eds.), *Tectonic evolution of the Oman Mountains*. Geological Society, London, Special Publication, vol. 392(1), pp. 325-341, doi: 10.1144/SP392.17.
- Agard, P., Searle, M.P., Alsop, G., & Dubacq, B. (2010). Crustal stacking and expulsion tectonics during continental subduction: P-T deformation constraints from Oman. *Tectonics* 29, 1-19, doi: 10.1029/2010TC002669.
- Agard, P., Omrani, J., Jolivet, L., Whitechurch, H., Vrielynck, B., Spakman, W., Monié, P., Meyer, B., & Wortel, R. (2011). Zagros orogeny: a subduction-dominated process. *Geological Magazine* 148(5-6). 692-725.
- Al-Wardi, M., & Butler, R.W.H. (2007). Constrictional extensional tectonics in the northern Oman mountains, its role in culmination development and the exhumation of the subducted Arabian continental margin. In: Ries, A.C., Butler, R.W.H., Graham, R.H. (Eds.), *Deformation of the Continental Crust: The Legacy of Mike Coward*. Geological Society, London, Special Publications, vol. 272, pp. 187-202.
- Angelier, J. (1994). Fault slip analysis and paleostress reconstruction. In, P.L. Hancock (Ed.), *Continental Deformation*, pp. 53-100. Oxford, Pergamon Press.
- Augustin, N., Devey, C.W., van der Zwan, F.M., Feldens, P., Tominaga, M., Bantan, R.A., & Kwasnitschka, T. (2014). The rifting to spreading transition in the Red Sea. *Earth and Planetary Science Letters* 395, 217-239, doi: 10.1016/j.epsl.2014.03.047.
- Bailey, C.M., Hurtado, C., Scharf, A., & Mattern, F. (2019). Structural controls on listwaenite genesis in the Semail Ophiolite, Northern Oman. EGU 2019-5794, Vienna, Austria.
- Beauchamp, W.H., Ries, A.C., Coward, M.P., & Miles, J.A. (1995). Masirah Graben, Oman: A Hidden Cretaceous Rift Basin? *AAPG Bulletin* 79(6), 864-879.
- Beavington-Penney, S.J., Wright, V.P., & Racey, A. (2006). The Middle Eocene Seeb Formation of Oman: An Investigation of Acyclicity, Stratigraphic Completeness, and Accumulation Rates in Shallow Marine Carbonate Settings. *Journal of Sedimentary Research* 76(10), 1137-1161, doi: 10.2110/jsr.2006.109.
- Béchenec, F., Beurrier, M., Hutin, G., & Rabu, D. (1986). Geological map of Barka, sheet NF 40-3B, scale 1:100,000, Explanatory notes: Directorate General of Minerals, Oman Ministry of Petroleum and Minerals.

- Béchenec, F., Le Métour, J., Rabu, D., Bourdillon-de-Grissac, C., de Wever, P., Beurrier, M., & Villey, M. (1990). The Hawasina Nappes; Stratigraphy, paleogeography and structural evolution of a fragment of the South-Tethyan passive continental margin. In: Robertson, A.H.F., Searle, M.P., Ries, A.C. (Eds.), *The Geology and Tectonics of the Oman Region*. Geological Society London Special Publication, vol. 49, pp. 213-223.
- Béchenec, F., Roger, J., Le Métour, J., & Wyns, R. (1992). Geological map of Seeb, sheet NF 40-03, scale 1:250,000, with Explanatory Notes: Directorate General of Minerals, Oman Ministry of Petroleum and Minerals.
- Blechs Schmidt, I., Dumitrica, P., Matter, A., Krystyn, L., & Peters, T. (2004). Stratigraphic architecture of the northern Oman continental margin – Mesozoic Hamrat Duru Group Hawasina Complex, Oman. *GeoArabia* 9(2), 81-132.
- Blendinger, W., van Vliet, A.T., & Hughes Clarke, M.W. (1990). Uplifting, rifting and continental margin development during the Late Paleozoic in northern Oman. In: Robertson, A.H.F., Searle, M.P., Ries, A.C. (Eds.), *The Geology and Tectonics of the Oman Region*. Geological Society of London, Special Publication, vol. 49, pp. 27-37.
- Boote, D.R.D., Mou, D., & Waite, R.I. (1990). Structural evolution of the Suneinah Foreland, Central Oman Mountains. In: Robertson, A.H.F., Searle, M.P., Ries, A.C. (Eds.), *The Geology and Tectonics of the Oman Region*. Geological Society of London, Special Publication, vol. 49, pp. 397-418.
- Breton, J.-P., Béchenec, F., Le Métour, J., Moen-Maurel, L., & Razin, P. (2004). Eoalpine (Cretaceous) evolution of the Oman Tethyan continental margin: insights from a structural field study in Jabal Akhdar (Oman Mountains). *GeoArabia* 9(2), 41-58.
- Burg, J.P., Bernoulli, D., Smit, J., Dolati, A., & Bahroudi, A. (2008). A giant catastrophic mud-and-debris flow in the Miocene Makran. *Terra Nova* 20, 188-193, doi: 10.1111/j.1365-3221.2008.00804.x.
- Callegari, I., Braaten, A., Scharf, A., Mattern, F., Holzbecher, E., Al Kharusi, A., & Al Hajri, A. (2020). Evidence of postobductional, brittle and transtensional deformation: the lineamentary Issmaiya Fault Zone – insights from kinematic analyses and remote sensing data interpretation (Semail Ophiolite near Ibra, Oman Mts., Sultanate of Oman). EGU 2020-12472, Vienna, Austria.
- Carminati, E., Aldega, L., Smeraglia, L., Scharf, A., Mattern, F., Albert, R., & Gerdes, A. (2020). Tectonic Evolution of the Northern Oman Mountains, Parts of the Strait of Hormuz Syntaxis: New Structural and Paleothermal analyses and U-Pb Dating of Synkinematic Calcite. *Tectonics* 39, e2019TC005936, doi: 10.1029/2019TC005936.
- Chauvet, F., Dumont, T., & Basile, C. (2009). Structures and timing of Permian rifting in the central Oman Mountains (Saih Hatat). *Tectonophysics* 475, 563-574, doi: 10.1016/j.tecto.2009.07.008.

- Cohen, K.M., Finney, S.C., Gibbard, P.L., & Fan, J.-X. (2013) (updated 2016-04). The ICS International Chronostratigraphic Chart. *Episodes* 36, 199-204.
- Coffield, D.Q. (1990). Structures associated with nappe emplacement and culmination collapse in the Central Oman Mountains. In: Robertson, A.H.F., Searle, M.P., Ries, A.C. (Eds.), *The Geology and Tectonics of the Oman Region*. Geological Society of London, Special Publication, vol. 49, pp. 447-458.
- Corradetti, A., Spina, V., Tavani, S., Ringenbach, J.C., Sabbatino, M., Razin, P., Laurant, O., Brichau, S., & Mazzoli, S. (2019). Late-stage tectonic evolution of the Al-Hajar Mountains, Oman: new constraints from Palaeogene sedimentary units and low-temperature thermochronometry. *Geological Magazine*, 1-14, doi: 10.1017/S0016756819001250.
- DeMets, C., Gordon, R.G., & Argus, D.F. (2010). Geologically current plate motions. *Geophysical Journal International* 182, 1-80, doi: 10.1111/j.1365-246X.2009.04491.x.
- Ermertz, A.M., Kázmér, M., Adolphs, S.K., Falkenroth, M., & Hoffmann, G. (2019). Geoarchaeological evidence for the decline of the Medieval City of Qalhat, Oman. *Open Quaternary* 5(8), 1-14, doi: 10.5334/oq.56.
- Fakhari, M.D., Axen, G.J., Horton, B.K., Hassanzadeh, J., & Amini, A. (2008). Revised age of proximal deposits in the Zagros Foreland Basin and implications for Cenozoic evolution of the high Zagros. *Tectonophysics* 451, 170-185, doi: 10.1016/j.tecto.2007.11.064.
- Filbrandt, J.B., Nolan, S.C., & Ries, A.C. (1990). Late Cretaceous and early Tertiary evolution of Jabal Ja'alan and adjacent areas, NE Oman. In: Robertson, A.H.F., Searle, M.P., Ries, A.C. (Eds.), *The Geology and Tectonics of the Oman Region*. Geological Society of London, Special Publication, vol. 49, pp. 697-714.
- Forbes, G.A., Jansen, H.S.M., & Schreurs, J. (2010). *Lexicon of Oman subsurface stratigraphy. Reference guide to the stratigraphy of Oman's Hydrocarbon basins*. *GeoArabia*, Special Publication 5 by Gulf Petro Link, p. 373.
- Fournier, M., Lepvrier, C., Razin, P., & Jolivet, L. (2006). Late Cretaceous to Paleogene Post-obduction extension and subsequent Neogene compression in the Oman Mountains. *GeoArabia* 11(4), 17-40.
- Fournier, M., Chamot-Rooke, N., Petit, C., Fabbri, O., Huchon, P., Maillot, B., & Lepvrier, C. (2008). In situ evidence for dextral active motion at the Arabia-India plate boundary. *Nature geoscience* 1, 54-58, doi: 10.1038/ngeo.2007.24.
- Fournier, M., Chamot-Rooke, N., Rodriguez, M., Huchon, P., Petit, C., Beslier, M.O., & Zaragosi, S. (2011). Owen fracture zone: The Arabia-India plate boundary unveiled. *Earth and Planetary Science Letters* 302, 247-252, doi: 10.1016/j.epsl.2010.12.027.

- Gaina, C., van Hinsbergen, D.J.J., & Spakman, W. (2015). Tectonic interactions between India and Arabia since the Jurassic reconstructed from marine geophysics, ophiolite geology, and seismic tomography. *Tectonics* 34(5), 875-906, doi: 10.1002/2014TC003780.
- Gavillot, Y., Axen, G.J., Stockli, D.F., Horton, B.K., & Fakhari, M.D. (2010). Timing of thrust activity in the high Zagros fold-thrust belt, Iran, from (U-Th)/He thermochronometry. *Tectonics* 29, TC4025, doi: 10.1029/2009TC002484.
- Ghebreab, W. (1998). Tectonics of the red Sea region reassessed. *Earth-Science Reviews* 45(1-2), 1-44, doi: 10.1016/S0012-8252(98)00036-1.
- Glennie, K.W., Boeuf, M.G.A., Hughes Clarke, M.W., Moody-Stuart, M., Pilaar, W.F.H., & Reinhardt, B.M. (1973). Late Cretaceous nappes in Oman Mountains and their geological evolution. *American Association of Petroleum Geologists Bulletin* 57, 5-27.
- Glennie, K.W., Boeuf, M.G.A., Hughes Clarke, M.W., Moody-Stuart, M., Pilaar, W., & Reinhardt, B.M. (1974). Geology of the Oman Mountains. *Koninklijk Nederlands Geologisch en Mijnbouwkundig Genootschap, Transactions* 31(1), p. 423.
- Gnos, R., & Peters, T. (2003). Mantle xenolith-bearing Maastrichtian to Tertiary alkaline magmatism in Oman. *Geochemistry, Geophysics, Geosystems* 4(9), doi: 10.1029/2001GC000229.
- Grobe, A., Virgo, S., von Hagke, C., Urai, J.L., & Littke, R. (2018). Multiphase structural evolution of a continental margin during obduction orogeny: Insights from the Jebel Akhdar Dome, Oman Mountains. *Tectonics* 37(3), 888-913, doi: 10.1002/2016TC004442.
- Grobe, A., von Hagke, C., Littke, R., Dunkl, I., Wübbeler, F., Muechez, P., & Urai, J.L. (2019). Tectono-thermal evolution of Oman's Mesozoic passive continental margin under the obducting Semail Ophiolite: a case study of Jebel Akhdar, Oman. *Solid Earth* 10, 149-175, doi: 10.5194/se-10-149-2019.
- Hanna, S.S. (1990). The Alpine deformation of the central Oman Mountains. In: Robertson, A.H.F., Searle, M.P., Ries, A.C. (Eds.), *The Geology and Tectonics of the Oman Region*. Geological Society of London, Special Publication, vol. 49, pp. 341-359.
- Hansman, R.J., & Ring, U. (2018). Jabal Hafit anticline (UAE and Oman) formed by décollement folding followed by trishear fault-propagation folding. *Journal of Structural Geology* 117, 168-185, doi: 10.1016/j.jsg.2018.09.014.
- Hansman, R.J., Ring, U., Thomson, S.N., den Brock, B., & Stübner, K. (2017). Late Eocene uplift of the Al Hajar Mountains, Oman, supported by stratigraphic and low-temperature thermochronology. *Tectonics* 36(12), 3081-3109, doi: 10.1002/2017TC004672.

- Hansman, R.J., Albert, R., Gerdes, A., & Ring, U. (2018). Absolute ages of multiple generations of brittle structures by U-Pb dating of calcite. *Geology* 46(3), 207-210, doi: 10.1130/G39822.1.
- Hansman, R.J., Ring, U., Scharf, A., Glodny, J., & Wan, B. (2021). Structural architecture and Late Cretaceous exhumation history of the Saih Hatat Dome (Oman), a review based on existing data and semi-restorable cross-sections. *Earth-Science Review*, 103595, doi: 10.1016/j.earscrev.2021.103595.
- Harding, T.P. (1974). Petroleum traps associated with wrench faults. *AAPG bulletin* 58(7), 1290-1304.
- Heidbach, O., Reinecker, J., Tingay, M., Müller, B., Sperner, B., Fuchs, K., & Wenzel, F. (2007). Plate boundary forces are not enough: Second- and third-order stress patterns highlighted in the World Stress Map database. *Tectonics* 26, TC6014, doi: 10.1029/2007TC002133.
- Hempton, M.R. (1987). Constraints on Arabian Plate motion and extensional history of the Red Sea. *Tectonics* 6(6), 687-705.
- Hersi, O.S., & Al-Harhi, A. (2010). Lithofacies attributes of a Transgressive Carbonate System: The Middle Eocene Seeb Formation, Al Khoudh area, Muscat, Oman. *Sultan Qaboos University Journal for Science* 15, 41-54.
- Hill, C.A., Polyak, V.J., Asmerom, Y., & Provencio, P.P. (2016). Constraints on a Late Cretaceous uplift, denudation, and incision of the Grand Canyon region, southwestern Colorado Plateau, USA, from U-Pb dating of a lacustrine limestone. *Tectonics* 35, 896-906, doi: 10.1002/2016TC004166.
- Hoffmann, G., Schneider, B., Mechernich, S., Falkenroth, M., Dunai, T., & Preusser, F. (2020). Quaternary uplift along a passive continental margin (Oman, Indian Ocean). *Geomorphology* 350, 106870, doi: 10.1016/j.geomorph.2019.106870.
- Immenhauser, A. (1996). Cretaceous sedimentary rocks on the Masirah Ophiolite (Sultanate of Oman); evidence for an unusual bathymetric history. *Journal of the Geological Society of London* 153, 539-551.
- Jenness, J. (2014). Polar plots and circular statistics: Extension for ArcGIS. Jenness Enterprises.
- Kajima, M., & Ishii, G. (2012a). Geological map of Al Ansab, sheet NF 40-3C4/C, scale 1:25,000, with Explanatory notes: Directorate General of Minerals, Oman Ministry of Commerce and Industry.
- Kajima, M., Ishii, G., Otake, M., & Goto, M. (2012b). Geological map of Al Khuwayr, sheet NF 40-3C4/D, scale 1:25,000, with Explanatory notes: Directorate General of Minerals, Oman Ministry of Commerce and Industry.
- Kajima, M., Ishii, G., & Goto, M. (2012c). Geological map of Ar Rusayl, sheet NF 40-3C3/C, scale 1:25,000, with Explanatory notes: Directorate General of Minerals, Oman Ministry of Commerce and Industry.

- Le Métour, J., Villey, M., & de Gramont, X. (1986a). Geological map of Masqat, sheet NF 40-4A, scale 1:100,000, Explanatory notes: Directorate General of Minerals, Oman Ministry of Petroleum and Minerals.
- Le Métour, J., Villey, M., & de Gramont, X. (1986b). Geological map of Quryat, sheet NF 40-4D, scale 1:100,000, Explanatory notes: Directorate General of Minerals, Oman Ministry of Petroleum and Minerals.
- Leroy, S., Razin, P., Autin, J., Bache, F., d'Acremont, E., Watremez, L., Robinet, J., Baurion, C., Denèle, Y., Bellahsen, N., & Lucazeau, F. (2013). From rifting to oceanic spreading in the Gulf of Aden: A synthesis. In K. Al Hosni, F., Roure, R., Ellison, S. Lokier (Eds.), *Lithosphere Dynamics and Sedimentary Basins: The Arabian Plate and Analogues*, pp. 385-427. Berlin, Heidelberg: Springer Berlin Heidelberg, doi: 10.1007/978-3-642-30609-9_20.
- Levell, B., Searle, M., White, A., Kedar, L., Droste, H., & van Steenwinkel, M. (2021). Geological and seismic evidence for the tectonic evolution of the NE Oman continental margin and Gulf of Oman. *Geosphere* 17, doi: 10.1130/GEO02376.1.
- Mann, A., Hanna, S.S., & Nolan, S.C. (1990). The post-Campanian tectonic evolution of the Central Oman Mountains: Tertiary extension of the Eastern Arabian Margin. In: Robertson, A.H.F., Searle, M.P., Ries, A.C. (Eds.), *The Geology and Tectonics of the Oman Region*. Geological Society of London, Special Publication, vol. 49, pp. 285-305.
- Mattern, F., & Bernecker, M. (2019). A shallow marine clinoform system in limestones (Paleocene to Eocene Jafnayn Formation, Oman): geometry, microfacies, environment and processes. *Carbonates and Evaporites* 34, 101-113, doi: 10.1007/s13146-018-0444-z.
- Mattern, F., & Scharf, A. (2018). Postobductional extension along and within the Frontal Range of the Eastern Oman Mountains. *Journal of Asian Earth Sciences* 154, 369-385, doi: 10.1016/j.jseaes.2017.12.031.
- Mattern, F., & Scharf, A. (2019). Transition from the Hajir Formation to the Muaydin Formation: a facies change coinciding with extensional, syndepositional faulting (Ediacaran, Jabal Akhdar, Central Oman Mountains). *Journal of African Earth Sciences* 152, 237-244, doi: 10.1016/j.jafrearsci.2019.02.016.
- Mattern, F., Moraetis, D., Abbasi, I., Al-Shukaili, B., Scharf, A., Claereboudt, M., Looker, E., Al-Haddabi, N., & Pracejus, B. (2018a). Coastal dynamics of uplifted and emerged Late Pleistocene near-shore coral patch reefs at Fins (eastern coastal Oman, Gulf of Oman). *Journal of African Earth Sciences* 138, 192-200, doi: 10.1016/j.afrearsci.2017.11.018.
- Mattern, F., Scharf, A., & Al-Amri, S.H.K. (2018b). East-west directed Cenozoic compression in the Muscat area (NE Oman): timing and causes. 10th Gulf Seismic Forum, seismology and Earthquake Studies in the Arabian Plate Region, 19th-22th March 2018, Muscat, Oman.

- Mattern, F., Scharf, A., Al-Sarmi, M., Pracejus, B., Al-Hinaai, A., & Al-Mamari, A. (2018c). Compaction history of Upper Cretaceous shale and related tectonic framework, Arabian Plate, Eastern Oman Mountains. *Arabian Journal of Geosciences* 11(16), 444, doi: 10.1007/s12517-018-3781-2.
- Mattern, F., Scharf, A., Pu-Jun, W., Callegari, I., Abbasi, I., Al-Wahaibi, S., Pracejus, B., & Scharf, K. (2020a). Deformation of the Cambro-Ordovician Amdeh Formation (members 1 and 2): characteristics, origins and stratigraphic significance (Wadi Amdeh, Saih Hatat Dome, Oman Mountains). *Geosciences* 10, 48, doi: 10.3390/geosciences10020048.
- Mattern, F., Al-Sayigh, A., Farfour, M., Scharf, A., Al-Amri, S., & Al-Omairi, J. (2020b) Microfacies, Biostratigraphy, Depositional Environment, Seismic Refraction and Correlation of Coralline Limestones of the Barzaman Formation (Oligocene-Pliocene? Al-Khod, Muscat Area, Oman). *Sultan Qaboos University Journal for Science* 25(2), 85-99, doi: 10.24200/squjs.vol25iss2pp85-99.
- Mattern, F., Scharf, A., Al-Sarmi, M., Al-Sayigh, A., Al-Maktoumi, M., Al-Omairi, N., & Al-Rawahi, T. (2021). Lithostratigraphy, microfacies and paleogeography of the shallow marine Middle Limestone Member of the Lower Eocene Rusayl Formation, Oman: relationship to the Early Eocene Climatic Optimum, sea-level changes and regional uplift. *Journal of African Earth Sciences* 184, 104312, doi: 10.1016/j.jafrearsci.2021.104312.
- Matthews, K.J., Müller, R.D., Wessel, P., & Whittaker, J.M. (2011). The tectonic fabric of the ocean basins. *Journal of Geophysical Research*, doi: 10.1029/2011/JB008413.
- Matthews, K.J., Maloney, K.T., Zahirovic, S., Williams, S.E., Seton, M., & Müller, R.D. (2016). Global plate boundary evolution and kinematics since the late Paleozoic. *Global and Planetary Change*, doi: 10.1016/j.gloplacha.2016.10.002.
- McQuarrie, N., Stock, J.M., Verdel, C., & Wernicke, B.P. (2003). Cenozoic evolution of Neotethys and implications for the causes of plate motions. *Geophysical Research Letters* 30(20), 2036, doi: 10.1029/2003GL017992.
- Miller, J.M., Gray, D.R., & Gregory, R.T. (2002). Geometry and significance of internal windows and regional isoclinal folds in northeast Saih Hatat, Sultanate of Oman. *Journal of Structural Geology* 24, 359-386, doi: 10.1016/S0191-8141(01)00061-X.
- Moraetis, D., Mattern, F., Scharf, A., Frijia, G., Kusky, T.M., Yuan, Y., & Hussain, I.L. (2018). Neogene to Quaternary uplift history along the passive margin of the northeastern Arabian Peninsula eastern Hajar Mountains, Oman. *Quaternary Research* 90(2), 418-434, doi: 10.1017/qua.2018.51.
- Moraetis, D., Scharf, A., Mattern, F., Pavlopoulos, K., & Foreman, S. (2020). Quaternary thrusting in the Central Oman Mountains – novel observations and

causes: insights from OSL dating and kinematic fault analyses. *Geosciences* 10, 166, doi: 10.3390/geoscience10050166.

Mountain, G.S., & Prell, W.L. (1990). A multiphase plate tectonic history of the southeast continental margin of Oman. In: Robertson, A.H.F., Searle, M.P., Ries, A.C. (Eds.), *The Geology and Tectonics of the Oman Region*. Geological Society of London, Special Publication, vol. 49, pp. 725-743.

Mouthereau, F., Lacombe, O., & Vergés, J. (2012). Building the Zagros collisional Orogen: Timing, strain distribution and the dynamics of Arabia/Eurasia plate convergence. *Tectonophysics* 532-535, 27-60.

Müller, R.D., Seton, M., Zahirovic, S., Williams, S.E., Matthews, K.J., Wright, N.M., Shephard, G.E., Maloney, K.T., Barnett-Moore, N., Hosseinpour, M., Bower, D.J., & Cannon, J. (2016). Ocean Basin Evolution and Global-Scale Plate Reorganization Events Since Pangea Breakup. *Annual Review of Earth and Planetary Sciences* 44, pp. 107, doi: 10.1146/annurev-earth-060115-012211.

Nicolas, A., Boudier, F., Ildefonse, B., & Ball, E. (2000). Accretion of Oman and United Arab Emirates ophiolite – Discussion of a new structural map. *Marine Geophysical Researches* 21, 147-179.

Ninkabou, D., Agard, P., Nielsen, C., Smit, J., Gorini, C., Rodriguez, M., Haq, B., Chamot-Rooke, N., Weidle, C., & Ducassou, C. (2021). Structure of the Offshore Obducted Oman Margin: Emplacement of Semail Ophiolite and Role of Tectonic Inheritance. *Journal of Geophysical Research: Solid Earth* 126, e2020JB020187, doi: 10.1029/2020JB020187.

Nolan, S.C., Skelton, P.W., Clissold, B.P., & Smewing, J.D. (1990). Maastriichtian to Early Tertiary stratigraphy and paleogeography of the Central and Northern Oman Mountains: In: Robertson, A.H.F., Searle, M.P., Ries, A.C. (Eds.), *The Geology and Tectonics of the Oman Region*. Geological Society of London, Special Publication, vol. 49, pp. 307-325.

Nuriel, P., Weinberger, R., Kylander-clark, A.R.C., Hacker, B.R., & Craddock, J.P. (2017). The onset of the Dead Sea transform based on calcite age-strain analyses. *Geology* 45, 587-590.

Peters, T., Al Battashy, M., Bläsi, H., Hauser, M., Immenhauser, A., Moser, L., & Al Rajhi, A. (2001). Geological map of Sur and Al Ashkharah, sheets NF 40-8F and NF 40-12C, scale: 1:100,000, with Explanatory notes: Directorate General of Minerals, Oman Ministry of Commerce and Industry.

Peters, T., Blechschmidt, I., Krystyn, L., Dumitrica, P., Mercogli, I., El Amin, O., & Al Towaya, A. (2005). Geological map of Ibra with Explanatory notes, sheet NF 40-08A, scale 1:100,000. Directorate General of Minerals, Ministry of Commerce and Industry of Oman.

Petit, J.P. (1987). Criteria for the sense of movement on fault surfaces in brittle rocks. *Journal of Structural Geology* 9(5-6), 597-608, doi: 10.1016/0191-8141(87)90145-3.

- Pickford, M. (2017). Late Cretaceous *Lanistes* (Mollusca, Gastropoda) from Al-Khodh, Oman. *Al Hajar* 23, 15-27.
- Platt, J.P., Leggett, J.K., & Alam, S. (1988). Slip vectors and fault mechanics in the Makran accretionary wedge, Southwest Pakistan. *Journal of Geophysical Research* 93(4), 7955, doi; 10.1029/JB093iB07p07955.
- Rabu, D., Béchenec, F., Beurrier, M., & Hutin, G. (1986). Geological map of Nakhl, sheet NF40-3E, scale: 1:100,000, with Explanatory Notes: Directorate General of Minerals, Oman Ministry of Petroleum and Minerals.
- Ring, U., & Bolhar, R. (2020). Tilting, uplift, volcanism and disintegration of the Southern German block. *Tectonophysics* 228611, doi: 10.1016/j.tecto.2020.228611.
- Rioux, M., Garber, J., Bauer, A., Bowring, S., Searle, M.P., Kelemen, P., & Hacker, B. (2016). Synchronous formation of the metamorphic sole and igneous crust of the Semail ophiolite: New constraints on the tectonic evolution during ophiolite formation from high-precision U-Pb zircon geochronology. *Earth and Planetary Science Letters* 451, 185-195, doi: 10.1016/j.epsl.2016.06.051.
- Roberts, N. M., Rasbury, E. T., Parrish, R. R., Smith, C. J., Horstwood, M. S., & Condon, D. J. (2017). A calcite reference material for LA-ICP-MS U-Pb geochronology. *Geochemistry, Geophysics, Geosystems*, 18(7), 2807-2814.
- Roberts, N.M.W., Drost, K., Horstwood, M.S.A., Condon, D.J., Chew, D., Drake, H., Milodowski, A.E., McLean, N.M., Smye, A.J., Walker, R.J., Haslam, R., Hodson, K., Imber, J., Beaudoin, N., & Lee, J.K. (2020). Laser ablation inductively coupled plasma mass spectrometry (LA-ICP-MS) U-Pb carbonate geochronology: strategies, progress, and limitations. *Geochronology* 2, 33-61, doi: 10.5194/gchron-2-33-2020.
- Rodgers, D.W., & Gunatilaka, A. (2002). Bajada formation by monsoonal erosion of a subaerial forebulge, Sultanate of Oman. *Sedimentary Geology* 154(3-4), 127-146.
- Rodriguez, M., Chamot-Rooke, N., Huchon, P., Fournier, M., & Delescluse, M. (2014). The Owen ridge uplift in the Arabian Sea: Implications for the sedimentary record of Indian monsoon in late Miocene. *Earth and Planetary Science Letters* 394, 1-12, doi: 10.1016/j.epsl.2014.03.011.
- Rodriguez, M., Huchon, P., Chamot-Rooke, N., Fournier, M., Delescluse, M., & François, T. (2016). Tracking the paleogene India-Arabia plate boundary. *Marine and Petroleum Geology* 72, 336-358, doi: 10.1016/j.marpetgeo.2016.02.019.
- Roger, J. Béchenec, F., Janjou, D., Le Métour, J., Wyns, R., & Beurrier, M. (1991). Geological map of Ja'alan, sheet NF 40-08E, scale:100,000, with Explanatory Notes: Directorate General of Minerals, Oman Ministry of Petroleum and Minerals.

- Romine et al. (2004). North Oman Haima-Huqf Tectonostratigraphic Study, SRK Confidential Report to PDO, July 2004.
- Saddiqi, O., Michard, A., Goffé, B., Poupeau, G., & Oberhänsli, R. (2006). Fission-track thermochronology of the Oman Mountains continental widows, and current problems of tectonic interpretation. *Bulletin de la Société Géologique de France* 177(3), 127-134, doi: 10.2113/gssgfbull.177.3.127.
- Scharf, A., Mattern, F., & Al Sadi, S. (2016). Kinematics of Post-obduction Deformation of the Tertiary Ridge at Al-Khod Village (Muscat Area, Oman). *Sultan Qaboos University Journal for Science* 21(1), 26-40.
- Scharf, A., Mattern, F., Moraetis, D., Callegari, I., & Weidle, C. (2019a). Post-obduction Kinematic Evolution and Geomorphology of a Major Regional Structure – The Semail Gap Fault Zone (Oman Mountains). *Tectonics* 38(8), 2756-2778, doi: 10.1029/2019TC005588.
- Scharf, A., Mattern, F., & Pracejus, B. (2019b). Two new microscopic ductile kinematic indicators from the Oman Mountains. *Journal of Structural Geology* 119, 107-117, doi: 10.1016/j.jsg.2018.12.006.
- Scharf, A., Sudo, M., Pracejus, B., Mattern, F., Callegari, I., Bauer, W., & Scharf, K. (2020b). Late Lutetian (Eocene) mafic intrusion into shallow marine platform deposits north of the Oman Mountains (Rusayl Embayment) and its tectonic significance. *Journal of African Earth Sciences* 170, 103941, doi: 10.1016/j.jafrearsci.2020.103941.
- Scharf, A., Mattern, F., Al-Wardi, M., Frijia, G., Moraetis, D., Pracejus, B., Bauer, W., & Callegari, I. (2021a). Tectonostratigraphy of the eastern part of the Oman Mountains. *Geological Society, London, Memoirs*, M54(1), 11-47, doi: 10.1144/M54.2.
- Scharf, A., Mattern, F., Al-Wardi, M., Frijia, G., Moraetis, D., Pracejus, B., Bauer, W., & Callegari, I. (2021b). Tectonic evolution of the Oman Mountains. *Geological Society, London, Memoirs*, M54(1), 67-103, doi: 10.1144/M54.5.
- Scharf, A., Mattern, F., Al-Wardi, M., Frijia, G., Moraetis, D., Pracejus, B., Bauer, W., & Callegari, I. (2021c). Appendices to: The geology and tectonics of the Jabal Akhdar and Saih Hatat domes, Oman Mountains. *Geological Society, London, Memoirs*, M54(1), 113-115, doi: 10.1144/M54.7.
- Schlüter, H.U., Prexl, A., Gaedicke, C., Roeser, H., Reichert, C., Meyer, H., & von Daniels, C. (2002). The Makran accretionary wedge: Sediment thicknesses and ages and the origin of mud volcanoes. *Marine Geology* 185(3-4), 219-232, doi: 10.1016/S0025-3227(02)00192-5.
- Schreurs, G., & Immenhauser, A. (1999). West-northwest directed obduction of the Batain Group on the eastern Oman continental margin at the Cretaceous-Tertiary boundary. *Tectonics* 18(1), 148-160.
- Searle, M.P. (1988). Structure of the Musandam culmination (Sultanate of

- Oman and United Arab Emirates) and the Straits of Hormuz syntaxis. *Journal of the Geological Society*, London 145, 831-845.
- Searle, M.P. (2007). Structural geometry, style and timing of deformation in the Hawasina Window, Al Jabal al Akhdar and Saih Hatat culminations, Oman Mountains. *GeoArabia* 12(2), 99-130.
- Searle, M.P., James, N.P., Calon, T.J., & Smewing, J.D. (1983). Sedimentological and structural evolution of the Arabian continental margin in the Musandam mountains and Dibba zone, United Arab Emirates. *Geological Society of America Bulletin* 94, 1381-1400.
- Searle, M.P., Cherry, A.G., Ali, M.Y., & Cooper, D.J.W. (2014). Tectonics of the Musandam Peninsula and northern Oman Mountains: From ophiolite obduction to continental collision. *GeoArabia* 19(2), 135-174.
- Searle, M.P. (2019). *Geology of the Oman Mountains, Eastern Arabia*. Springer, p. 478.
- Shackleton, R.M., Ries, A.C., Bird, P.R., Filbrandt, J.B., Lee, C.W., & Cunningham, C.C. (1990). The Batain mélange of NE Oman. In: Robertson, A.H.F., Searle, M.P., Ries, A.C. (Eds.), *The Geology and Tectonics of the Oman Region*. Geological Society of London, Special Publication, vol. 49, pp. 673-696.
- Stanger, G. (1985). Silicified serpentinite in the Semail nappe of Oman. *Lithos* 18, 13-22.
- Vermeesch, P. (2018). IsoplotR: A free and open toolbox for geochronology. *Geoscience Frontiers* 9(5), 1479-1493, doi: 10.1016/j.gsf.2018.04.001.
- Villey, M., de Gramont, X., & Le Métour, J. (1986a). Geological map of Seeb, sheet NF 40-3C, scale 1:100,000, with Explanatory notes: Directorate General of Minerals, Oman Ministry of Petroleum and Minerals.
- Villey, M., Le Métour, J., & de Gramont, X. (1986b). Geological map of Fanjah, sheet NF 40-3F, scale 1:100,000, with Explanatory notes: Directorate General of Minerals, Oman Ministry of Petroleum and Minerals.
- Weidle, C., Wiesenberg, L., Scharf, A., Agard, P., El-shatkawy, A., Krüger, F., & Meier, T. (2021). Architecture of the crust and lithosphere beneath the Semail Ophiolite from ambient noise tomography and Receiver Functions: insights on the tectonic evolution of eastern Arabia. *vEGU 2021-8321*, Vienna, Austria.
- Woodhead, J., & Petrus, J. (2019). Exploring the advantages and limitations of in situ U–Pb carbonate geochronology using speleothems. *Geochronology*, 1(1), 69-84.
- Woodhead, J., Reisz, R., Fox, D., Drysdale, R., Hellstrom, J., Maas, R., Cheng, H., & Edwards, R.L. (2010). Speleothem climate records from deep time? Exploring the potential with an example from the Permian. *Geology* 38, 455-458.

Wyns, R., Béchenec, F., Le Métour, J., & Roger, J. (1992). Geological map of Tiwi, sheet NF40-8B, scale 1:100,000, with Explanatory notes: Directorate General of Minerals, Oman Ministry of Petroleum and Minerals.

Zoback, M.L., & Zoback, M.D. (2007). Lithosphere stress and Deformation. In A. Watts, G. Schubert (Eds.), *Earthquake Seismology – Treatise on Geophysics*, 6, pp. 253-274, Amsterdam, Elsevier.